STRUCTURAL AND FUNCTIONAL EFFECTS OF NON-STEROIDAL ANTI-INFLAMMATORY DRUGS ROFECOXIB AND VALDECOXIB ON DSPC MODEL MEMBRANES

A THESIS SUBMITTED TO
THE GRADUATE SCHOOL OF NATURAL AND APPLIED SCIENCES
OF
MIDDLE EAST TECHNICAL UNIVERSITY

BY

RICHARDAS RACHKAUSKAS

IN PARTIAL FULFILLMENT OF THE REQUIREMENTS
FOR
THE DEGREE OF MASTER OF SCIENCE
IN
BIOLOGY

AUGUST 2014

Approval of the Thesis:

STRUCTURAL AND FUNCTIONAL EFFECTS OF NON-STEROIDAL ANTI-INFLAMMATORY DRUGS ROFECOXIB AND VALDECOXIB ON DSPC MODEL MEMBRANES

submitted by **RICHARDAS RACHKAUSKAS** in partial fulfillment of the requirements for the degree of **Master of Science in Biology Department, Middle East Technical University** by,

Prof. Dr. Canan Özgen
Dean, Graduate School of **Natural and Applied Sciences** _____

Prof. Dr. Orhan Adalı
Head of Department, **Biology** _____

Assoc. Prof. Dr. Sreeparna Banerjee
Supervisor, **Biology Dept., METU** _____

Prof. Dr. Feride Severcan
Co-Supervisor, **Biology Dept., METU** _____

Examining Committee Members:

Assoc. Prof. Dr. Dilek Keskin
Engineering Sciences Dept., METU _____

Assoc. Prof. Dr. Sreeparna Banerjee
Biology Dept., METU _____

Prof. Dr. Feride Severcan
Biology Dept., METU _____

Assoc. Prof. Dr. Ayşen Tezcaner
Engineering Sciences Dept., METU _____

Dr. Aslı Sade Memişoğlu
Health Sciences Grad.School, Dokuz Eylül Univ. _____

Date: 19/08/2014

I hereby declare that all information in this document has been obtained and presented in accordance with academic rules and ethical conduct. I also declare that, as required by these rules and conduct, I have fully cited and referenced all material and results that are not original to this work.

Name, Last name: Richardas Rachkauskas
Signature:

ABSTRACT

STRUCTURAL AND FUNCTIONAL EFFECTS OF NON-STEROIDAL ANTI-INFLAMMATORY DRUGS ROFECOXIB AND VALDECOXIB ON DSPC MODEL MEMBRANES

Rachkauskas Richardas

M.Sc., Department of Biology

Supervisor: Assoc. Prof. Dr. Sreeparna Banerjee

Co-Supervisor: Prof. Dr. Feride Severcan

August 2014, 105 pages

Celecoxib (CLX), rofecoxib (RFX) and valdecoxib (VLX) belong to a family of Non-steroidal anti-inflammatory drugs (NSAIDs), which are selective COX-2 inhibitors. While these drugs are established analgesics, they also have a number of pleiotropic effects such as cancer chemoprevention, occasionally in a COX-2 independent manner. RFX and VLX were withdrawn from the market after clinical trials indicated that use of these drugs enhanced the risk of heart attack and stroke. CLX is currently FDA approved for pain management in rheumatoid arthritis. As these drugs are highly hydrophobic in nature, studies are underway on how the drugs can alter membrane properties such as fluidity, phase transition temperature and others. It has been shown that these drugs can affect lipid membrane properties such as fluidity and order and induce phase separation. Using differential scanning calorimetry (DSC) and Fourier transform infrared (FT-IR) spectroscopy, the current study compares the effects of

RFX and VLX on DSPC model membrane properties. Additionally, the effects of these drugs were compared with effects of CLX previously reported by our group. We have observed that VLX can alter the properties of DSPC model membranes in a manner very similar to CLX: it decreases the phase transition temperature (Tm) in a concentration-dependent manner and also has effects on the fluidity. FT-IR and DSC studies show that increasing drug concentration enhances some of these effects. Interestingly, RFX appears to have a different effect on membrane fluidity and no effect on Tm. The data show no difference in biophysical properties between the control DSPC membranes and RFX treated membranes at various concentrations. Given the fact that CLX and VLX have a common sulfonamide group while RFX lacks it and only has sulfone group, we suggest that the sulfonamide group may be responsible for specific interactions with the lipid bilayers altering the biophysical properties of model membranes. Additionally, some unique effects observed only with CLX are attributed to the presence of Fluorine functional group in the drug. The results provide us new insights into NSAID-lipid interactions which can help delineate further the effects of these drugs on cell membrane.

Keywords: FT-IR, DSC, NSAIDs, rofecoxib, valdecoxib, celecoxib, model membranes.

ÖZ

NONSTEROİD ANTİENFLAMATUAR İLAÇLAR ROFECOXIB VE VALDECOXIB'IN DSPC MODEL MEMBRANLARI ÜZERİNDEKİ YAPISAL VE FONKSİYONEL ETKİLERİ

Rachkauskas Richardas

Yüksek Lisans, Biyoloji Bölümü

Tez Yöneticisi: Doç. Dr. Sreeparna Banerjee

Ortak Tez Yöneticisi: Prof. Dr. Feride Severcan

Ağustos 2014, 105 sayfa

Selektif COX-2 inhibitörü olan celecoxib (CLX), rofecoxib (RFX) ve valdecoxib (VLX) nonsteroid antienflamatuar ilaçlar grubuna dahildir. Bu ilaçlar analjezik olarak kullanım görmelerinin yanında kanser kemoprevansiyon gibi pek çok pleyiotropik etkiye de sahiptir. Bu etki bazen COX-2 den bağımsızdır. Klinik denemelerin bu ilaçların kalp krizi ve inme geçirme riskini arttırdığını göstermesinden sonra RFX ve VLX klinik kullanımdan geri çekilmiştir. CLX in romatoid artrit de ağrı tedavisi ajanı olarak kullanımı FDA tarafından onaylanmıştır. Bu ilaçların yapısal olarak oldukça hidrofobik olmalarından dolayı membran yapısında örneğin akışkanlığında ya da faz geçiş sıcaklığı gibi diğer parametrelerde yaptığı değişikliklerle ilgili çalışmalar devam etmektedir. Bu ilaçların membran özellikleri üzerinde örneğin akışkanlığında, düzenliliğinde ve lipitlerdeki faz ayrımını indüklemede etkisi olduğu gösterilmiştir. Bu çalışma, RFX ve VLX' in DSPC model membran üzerindeki etkilerini ve ayrıca daha önce grubumuz tarafından yapılan CLX çalışmasının aynı etkisini diferansiyal

taramalı kalorimetri ve fourier dönüşümlü kızılötesi spektroskopisi yöntemlerini kullanarak karşılaştırmıştır. Çalışma sonucunda VLX'in DSPC model membran özelliklerini CLX'e benzer bir şekilde değiştirdiğini gözlemledik. VLX'in konsantrasyona bağlı olarak faz geçiş sıcaklığını (Tm) düşürmesi ve membran akışkanlığı üzerinde de etkisinin olması bu etkilerdendir. İlaç konsantrasyonunun bu etkileri arttırdığı fourier dönüşümlü kızılötesi spektroskopisi ve diferansiyal taramalı kalorimetri çalışmaları ile gösterilmiştir. İlginç şekilde RFX membran akışkanlığı üzerinde farklı etkiye ve faz geçiş sıcaklığı üzerinde de herhangi bir etkiye sahip değildir. Kontrol DSPC ve değişik konsantrasyonlarda VLX uygulanmış membran da herhengi bir biyofiziksel değişikliğin görülmediği gözlenmiştir. CLX ve VLX ortak sulfonamid grubuna sahipken RFX' de bunun yerine sulfon grubu vardır. Bu sulfonamid grubunun lipit çift katmanındaki spesifik etkileşiminin model membrandaki biyofiziksel değişikliklerden sorumlu olduğunu düşünmekteyiz. Ek olarak CLX'in bazı kendine has etkilerinin florin fonksiyonel grubundan kaynaklandığı düşünülmektedir. Bu sonuçlar, Nonsteroid antiinflamatuar ilaç-lipit etkileşiminde bize yeni bir bakış açısı sağlamıştır. Buda bize bu ilaçların daha başka etkilerini anlamakta yardımcı olmuştur.

Anahtar Kelimeler: Fourier dönüşümlü kızılötesi spektroskopisi, diferansiyal taramalı kalorimetri, nonsteroid antiinflamatuar ilaçlar, rofecoxib, valdecoxib, celecoxib, model membran.

To my grandmother and grandfather,

ACKNOWLEDGMENTS

I would like to sincerely thank my supervisor Assoc. Prof. Dr. Sreeparna Banerjee for her invaluable scientific expertise, excellent laboratory managing skills and creativity, which allowed this study to be born.

I would like to express my deepest gratitude to my co-supervisor Prof. Dr. Feride Severcan for her endless support and motivation during my years in METU, both undergraduate and graduate.

I am very happy that I had a chance to work at two labs at the same time. My thanks goes to members of labs B-59 and 146, who were always very supportive and fun: Aslı Sade, Aslı Erdoğ, Seda Tunçay, Shabnam Enayat, İsmail Çimen, Mümine Küçükdemir, Şeyma Ceyhan, Yanuar Limasale, Fatma Küçük, Aysun İnan, Nihal Şimşek Özek, Özlem Bozkurt, Tuğçe Başer, Ebru Aras, Rafik Gurbanov, Pınar Demir, Seza Ergün, Seher Gök.

I am also grateful to a lot of good friends I have in METU.

This thesis project was financially supported by Middle East Technical University Scientific Research Council project number BAP-07-02-2011-002.

TABLE OF CONTENTS

LIST OF TABLES

TABLES

LIST OF FIGURES

FIGURES

LIST OF ABBREVIATIONS

DSPC	1, 2-Distearoyl-sn-Glycero-3-Phosphocholine, 18:0 PC
CLX	Celecoxib
RFX	Rofecoxib
VLX	Valdecoxib
MLVs	Multilamellar vesicles
NSAIDs	Non-steroidal anti-inflammatory drugs
COX	Cyclooxygenase
PGHS	Prostaglandin H synthase
PGs	Prostaglandins
AA	Arachidonic acid
PBS	Phosphate buffered saline
DSC	Differential Scanning Calorimetry
FT-IR	Fourier Transform Infrared Spectroscopy
EE	Encapsulation Efficiency
PdI	The Polydispersity Index
SEM	Standard Error of the Mean
FDA	Food and Drug Administration

CHAPTER 1

INTRODUCTION

In this study, the interactions of several Non-steroidal anti-inflammatory drugs (NSAIDs) with 1,2-Distearoyl-sn-Glycero-3-Phosphocholine (DSPC) multilamellar vesicles (MLVs) were investigated at molecular level, using Fourier transform infrared spectroscopy (FT-IR), differential scanning calorimetry (DSC) and other techniques.

This chapter summarizes the available literature on lipid properties, biological and model membranes, NSAIDs and their pathways. The basic principles of Fourier transform infrared spectroscopy, differential scanning calorimetry and other techniques used in this study are explained as well.

1.1. Inflammation and Non-steroidal anti-inflammatory drugs

Chronic inflammation is known to have a significant effect in the promotion and progression of cancer and other diseases (Danese & Mantovani, 2010). Cyclooxygenases (COX) are key enzymes of the eicosanoid cascade which can convert arachidonic acid to prostaglandins, one of the important mediators of inflammation. An inducible isoform of COX (COX-2) is also overexpressed in the early stages of colon cancer (Shiff & Rigas, 1999). It is not surprising therefore, that non-steroidal anti-inflammatory drugs (NSAIDs) are associated with a reduced risk of colon cancer (Grösch, Maier, Schiffmann, Geisslinger, & Grosch, 2006).

1.1.1. Cyclooxygenases and inflammation

Cyclooxygenases (COX), also known as prostaglandin H synthases (PGHS), are enzymes localized at the nuclear or endoplasmic reticulum membrane of eukaryotic cells. These are the key enzymes of the eicosanoid cascade which can convert arachidonic acid (AA), a fatty acid distributed throughout the lipid bilayer, to prostaglandins (PGs) (Figure 1). Once cleaved by phospholipase enzymes, arachidonic acid is converted to PGH2 by a two-step mechanism. PGH2 is the root prostaglandin from which other prostaglandin isomers are produced by downstream synthases. These isomers, including thromboxane and PGD2, PGJ2, PGE2 and PGI2, are involved in various physiological processes, such as inflammation, fever, algesia, angiogenesis, platelet aggregation, ovulation, renal function, vasoconstriction and vasodilation (Funk, 2001).

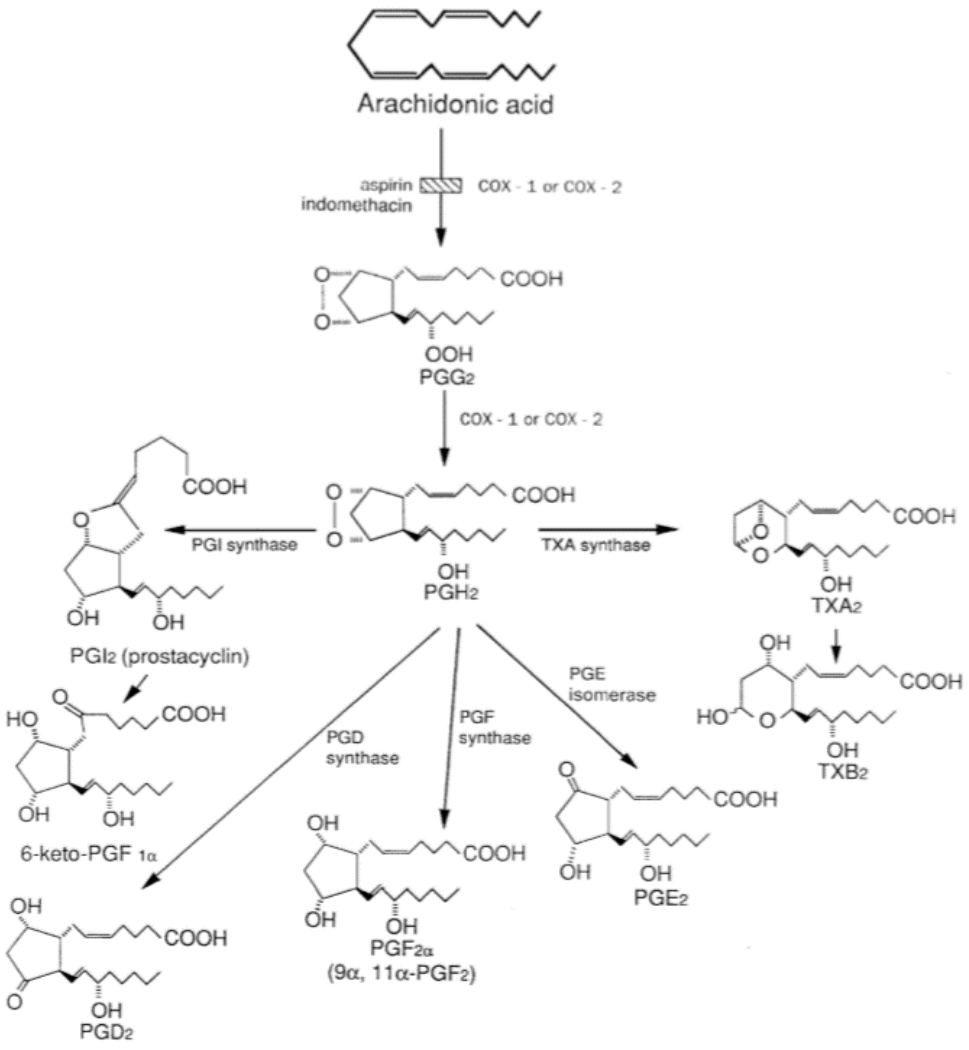

Figure 1. The arachidonic acid cascade (Vane, Bakhle, & Botting, 1998).

Cyclooxygenases have two isoforms, COX-1 and COX-2, which have different expression patterns in the tissues. COX-1 is expressed constitutively in most tissues and is responsible for a basal level of prostaglandin synthesis required for 'housekeeping' functions in the body such as gastrointestinal cytoprotection, renal functions and vascular homeostasis. COX-2 on the other hand, is not constitutively expressed in most tissues with the exception of kidney and brain (Funk, 2001). This isoform can be induced by a number of stimuli, such as bacterial lipopolysaccharide (LPS), interleukin-1 and 2, and tumor necrosis factor α (TNF-α), all of which are related to inflammation (Funk, 2001).The induction of COX-2 by inflammatory mediators led investigators to label this enzyme as pathological (Vane et al., 1998), especially since chronic inflammation is known to result in several diseases (Danese & Mantovani, 2010; Mantovani, Allavena, Sica, & Balkwill, 2008).

1.1.2. Non-steroidal anti-inflammatory drugs

Examples of Non-steroidal anti-inflammatory drugs (NSAIDs) include aspirin, ibuprofen, and indomethacin. They are widely prescribed in inflammatory diseases like osteoarthritis and rheumatoid arthritis, in order to relieve pain and other symptoms of inflammation. In 1971, Vane et al. showed that NSAIDs block prostaglandin synthesis by binding to both isoforms of COX and inhibiting conversion of AA to PGG2 (Vane, 1971). This happens by several known mechanisms. All "classical" NSAIDs, except aspirin, reversibly decrease COX activity by competing with the substrate AA for the active site of the enzyme. Aspirin, on the other hand, covalently and irreversibly modifies the active site by acetylation of Ser529. Because prostaglandins participate in a number of homeostatic functions, it is widely accepted that chronic inhibition of COX-1 leads to some undesirable side effects, such as gastritis, peptic ulcer and gastrointestinal bleeding, while that the anti-inflammatory activity of NSAIDs results from COX-2 inhibition (Goldenberg, 1999; Vane et al., 1998).

Unlike "classical" NSAIDs, celecoxib (CLX), rofecoxib (RFX) and valdecoxib (VLX) drugs belong to a family of NSAIDs which are selective COX-2 inhibitors. They were developed with a hypothesis that selective inhibition of COX-2 might retain the anti-inflammatory function of NSAIDs without affecting the important housekeeping

functions of COX-1 (FitzGerald, 2003). Indeed, selectively inhibiting activity of COX-2 enzyme in prostaglandin production pathway gave the advantage of reduced gastrointestinal bleeding compared to classical NSAIDs while relieving the symptoms of osteoarthritis and rheumatoid arthritis (Goldenberg, 1999; Penning et al., 1997). However, there is evidence that new generation NSAIDs may have side effects of their own, because COX-2 is constitutively expressed in some tissues, such as vascular endothelium, kidney, and brain (FitzGerald, 2003). Several studies have revealed an association of CLX, RFX and VLX use with increased incidence of cardiovascular risks (Bertagnolli et al., 2006; Hinz, Renner, & Brune, 2007). Moreover, VLX and RFX were withdrawn from market due to these concerns. Recently in a detailed study by Zhang et al., VLX appeared to have less adverse effects on the kidney and the heart compared to RFX, although renal risks were not ruled out (Zhang, Ding, & Song, 2006). In 2005, the return of RFX to the market was approved, stating that RFX's benefits outweighed the risks for some patients, however, the drug currently is still unavailable to the patients.

1.1.3. Molecular aspects of NSAIDs action

Most of the new generation NSAIDs are phenylsulfones or phenylsulfonamides, including the three drugs used in this study (Figure 2). The sulfone moiety binds to a pocket found in COX-2 but not COX-1. The selectivity of CLX for COX-2 comes from the smaller valine molecule in COX-2, giving access to this side pocket, which is also the site for the binding of all other selective inhibitors. On the other hand, the larger isoleucine in COX-1, blocks the access of the drug to this pocket.

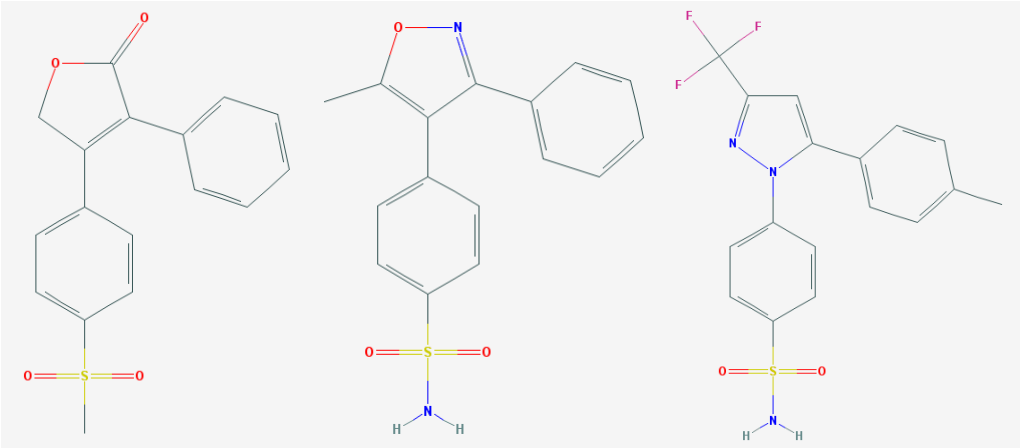

Figure 2. The chemical structures of the three drugs used by our research group. From left to right: rofecoxib, valdecoxib, celecoxib (source: The National Center for Biotechnology Information, PubChem).

Several studies indicate that COX-2 is involved in neurological disorders, like Alzheimer's disease, Parkinson's disease and ischemia, where COX-2 overexpression leads to neurotoxicity (Vries, 2006). Many aspects of the role of COX-2 in pathophysiology, however, remain unclear. Since COX-2 is overexpressed in the early adenoma stage of colon cancer, it is not surprising, that non-steroidal anti-inflammatory drugs are associated with a reduced risk of colon cancer (Grösch et al., 2006; Shiff & Rigas, 1999). The anticarcinogenic effects of CLX are not solely due to the inhibition of COX-2. COX-2 independent effects were observed in vitro (Grösch et al., 2006). Additionally targeted drug delivery systems for CLX, RFX and VLX (microspheres and liposomes) have been reported for cancer therapy, which may bypass the cardiovascular side effects of these drugs (Al-Saidan, Krishnaiah, Satyanarayana, & Rao, 2005; Deniz et al., 2010; Thakral, Ray, Bar-Shalom, Eriksson, & Majumdar, 2011). Finally, studies on membrane fluidity have been considered as a promising approach for cancer therapy since metastatic tumor cells have higher membrane fluidity compared to non-metastatic cells (Nakazawa & Iwaizumi, 1989).

1.1.4. Interaction of NSAIDs with Membranes

It is not clear how NSAIDs affect biological membranes, i.e. is it through a direct interaction with membrane bound enzymes or through interaction with cellular

membranes, which in turn alters the activity of these enzymes. Studies on the interaction of NSAIDs with membranes at a molecular level are very limited. Using small angle X-ray diffraction, Walter et al. showed that CLX is localized at the interfacial region of 1- palmitoyl-2-oleoyl-sn-glycero-3-phosphocholine (POPC) - cholesterol membranes, at a 1:10 drug to phospholipid mole ratio (9.1 mol% drug) (Walter et al., 2004). In other studies, fluorescence anisotropy technique revealed that CLX decreases membrane fluidity in a mouse neuroblastoma cell line N2a and Tomisato et al. reported that CLX causes a decrease in membrane fluidity in egg phosphatidylcholine model membranes using fluorescence polarization (Gamerdinger, Clement, & Behl, 2007; Tomisato et al., 2004). Using DSPC model membranes, our group has previously shown that CLX decreases the fluidity of the membrane and induces phase separation of the lipids (Sade, Banerjee, & Severcan, 2010). The current study focuses on interaction of the other two drugs (RFX and VLX) with DSPC in the lipid vesicles and comparing different aspects of this interaction.

1.2. Basic Theory of Biological and Model Membranes

Biomembranes are the dynamic borders of the cells, defining them and separating them from the environment. They also define and separate functional compartments and organelles within the cell, such as Endoplasmic Reticulum and others. All biological membranes are composed primarily of lipids and proteins, with some additional components, which may include short chains of carbohydrates (Hauser & Poupart, 2004). Membrane lipids are amphipathic. One part of the molecule, namely the long fatty acid chains, is hydrophobic and the other, which is the head group, is hydrophilic. The hydrophobic interactions with each other and the hydrophilic interactions with water result in spontaneous packing of lipid molecules into lipid bilayers in most scenarios. Membranes are mainly composed of three kinds of lipids; one of them is cholesterol and the other are two types of phospholipids: glycerophospholipids (phosphoglycerides) and sphingolipids (glycosylceramides). Glycerophospholipids consist of a glycerol backbone to which two fatty acids are attached in an ester linkage to the first and second carbons (sn-1 and sn-2 positions) and a phosphate group is attached through a phosphodiester linkage to the third carbon (sn-3 position) (Lewis & McElhaney, 2011). Sphingolipids have only one fatty acid attached to the backbone.

The phosphate group bound to an alcohol constitutes the highly polar head group of phospholipids. Phosphatidylcholine (PC) which has choline in its head group is one of the major phospholipids found in biological membranes (Figure 3). The fatty acids in phosphoglycerides can be any of a wide variety, each of which is specific for a kind of organism or a tissue. In general, glycerophospholipids contain a C16 or C18 saturated fatty acid at C-1 and a C18 to C20 unsaturated fatty acid at C-2.

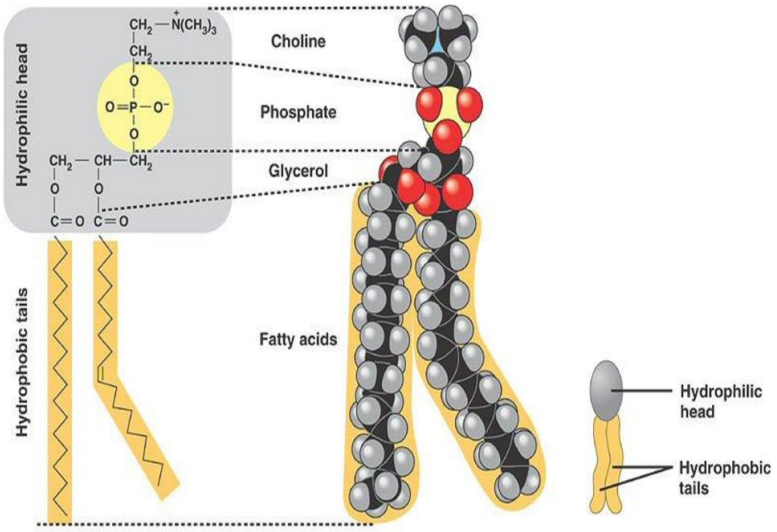

Figure 3. Structure of Phosphatidylcholine (source: http://meyerbio1b.wikispaces.com/%E2%80%A2Lipids).

1.2.1. Molecular Motions in Membranes

There are several types of motion of phospholipids that can occur in a membrane and they can be classified into intermolecular and intramolecular motions. Examples of intermolecular motions are rotation around the long molecular axis, translational diffusion within a leaflet of the bilayer and transverse diffusion (flip-flop) between the two leaflets of the bilayer. Intramolecular motions include torsional motions around single bonds and segmental motions like rotation of the acyl chains or the head groups (Jain, 1979). The basic types of intermolecular motions are shown in Figure 4-A.

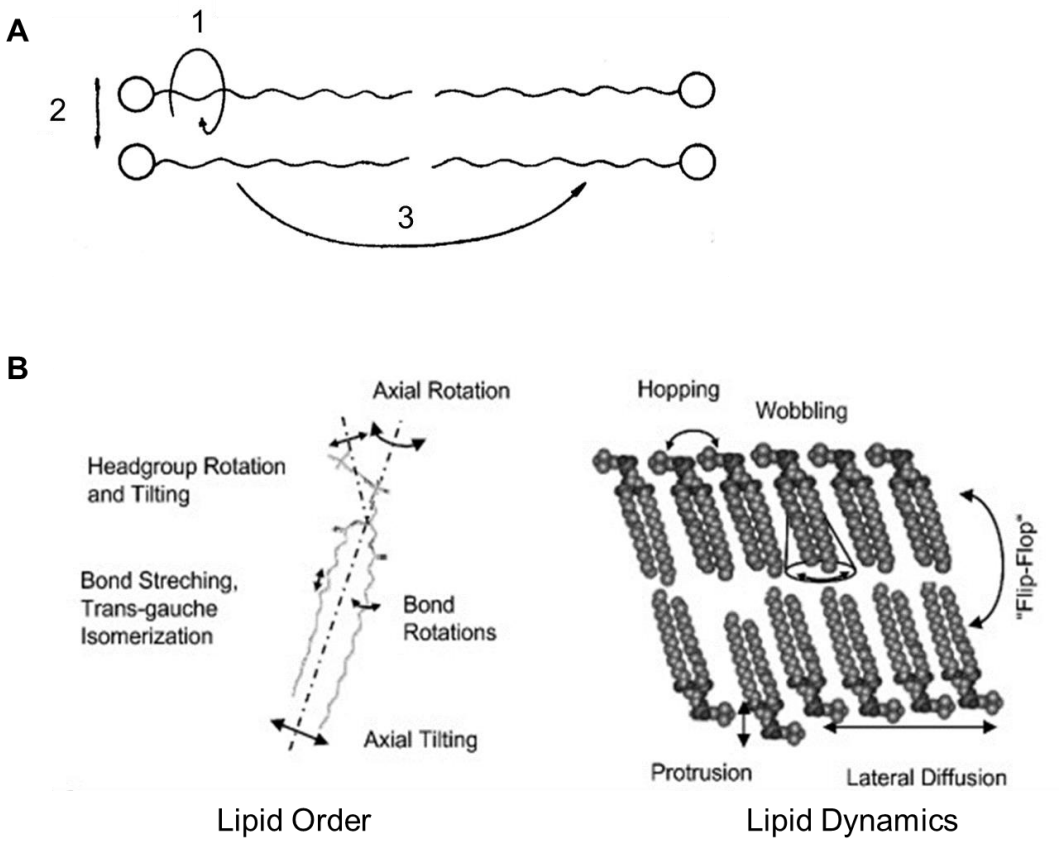

Figure 4. A. Molecular motions in membranes. (1) rotational motion, (2) lateral diffusion, (3) flip-flop (Jain, 1979). B. Differences between lipid order and lipid dynamics (lipid fluidity).

Rotational motion around the long axis of a lipid molecule occurs without disruption of intermolecular interactions. The lipid molecule has van der Waals interactions with the neighboring lipid chains and non-specific van der Waals interactions between the components of the membrane, the latter being able to induce lateral motion. Besides these weak forces, the polar head groups are only stabilized by surrounding water molecules and to some extend by electrostatic forces with nearby polar groups. Thus the molecules are free to move past each other in the plane of the membrane. This type of motion can induce phase separation in the bilayer. Transverse motion is a rare process since it requires interaction of head groups with the hydrophobic core of the membrane (Jain, 1979). Membrane asymmetry phenomenon may be a result of this motion. All of these types of intermolecular motions can account for the dynamics and fluidity of the lipid bilayer, while intramolecular motions affect the membrane order (Figure 4-B).

1.2.2. Structural Isomerizations in Membranes

There are two main conformational isomers of lipids in membrane called trans and gauche isomerizations of acyl chains. The trans-gauche isomerizations of acyl chains account for the flexibility of the chains and result from rotations around the C-C bonds. If the rotation is 120°, it leads to transient gauche isomer (or kink) formation (Figure 5). The all-trans conformation allows for the closest packing of the fatty acyl chains. If one or more gauche conformer is present, there are distortions produced in the shape and size of the acyl chains. Gauche conformers increase the cross-sectional area and decrease the length of the acyl chains by producing kinks in their structure (Jain, 1979).

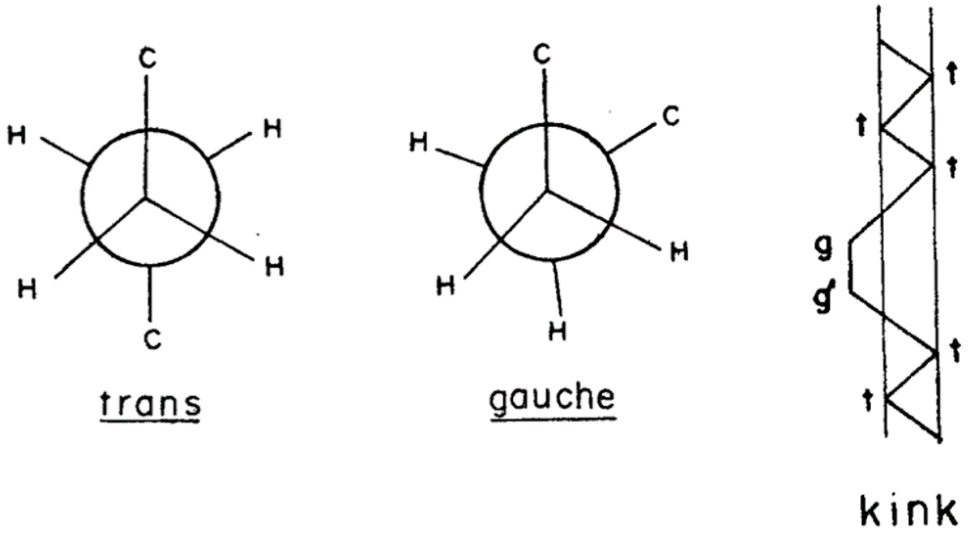

Figure 5. Trans-gauche isomerizations in acyl chains of phospholipids (Jain, 1979).

1.2.3. Phospholipid Assemblies in Solutions

The membrane lipids can exist in a variety of different kinds of organized structures, that is, they are highly polymorphic. The polymorphic form that predominates at particular conditions depends on the structure of the lipids, temperature, pressure, and pH. Depending on the properties of the solution and the types of lipid present in it, there can be several basic types of the structures lipids can form (Figure 6.). The most fundamental one is the lipid bilayer, the primary structure found in all living cells of all organisms. It is formed in aqueous environment when lipid polar head groups face the water molecules and interact with them, while the fatty acid chains are enclosed within the bilayer stabilizing it by hydrophobic interactions. Besides large lipid

bilayers of cell membranes and large organelles, lipids can form smaller vesicles. A vesicle is defined as a small organelle within a cell, consisting of fluid enclosed by a lipid bilayer membrane. Natural vesicles are formed, for example, during the processes of secretion (exocytosis), uptake (phagocytosis and endocytosis) and transport of materials within the cytoplasm.

Unlike biological membranes, in model membranes, large artificial lipid bilayers are not used as often. A lipid monolayer can be considered a special case formed on top of aqueous solution, and it sometimes used in preparation of custom and complex lipid bilayers. More abundant, however are micelles and artificial vesicles, known as liposomes, which are widely used in model membrane studies and as drug delivery systems (Figure 6).

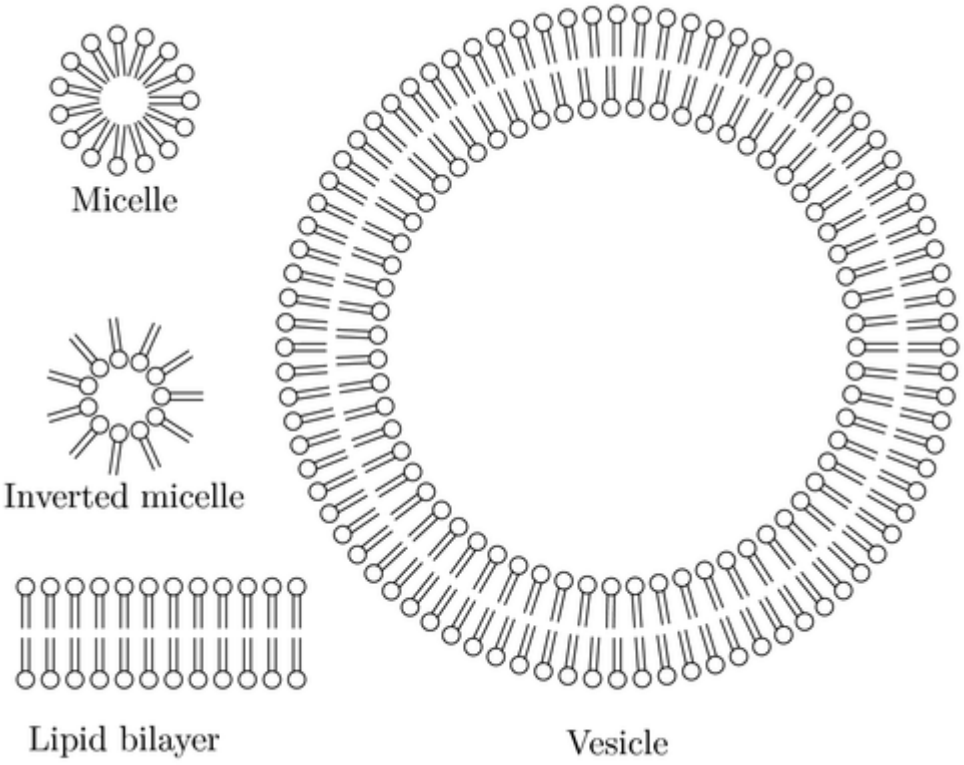

Figure 6. Types of phospholipid assemblies formed in various solutions (source: http://www.texample.net/tikz/examples/lipid-vesicle/).

Micelles are formed with phospholipid molecules having either short fatty acid chains or with a single fatty acid chain, while liposomes are formed with phospholipid molecules containing longer fatty acid chains. Liposomes are considered as artificial

vesicles that can be formed after suspending dry lipid material in an aqueous solution with mechanical agitation (Bangham, 1972). The types of liposomes are the multilamellar vesicles (MLVs), giant unilamellar vesicles (GUVs), large unilamellar vesicles (LUVs), small unilamellar vesicles (SUVs), multivesicular and oligovesicular vesicles (MVVs and OVVs), and the cochleate vesicles (Figure 7). MLVs, resulting from aqueous dispersions of most phospholipids have diameters between 20-5000 nm and contain multiple layers. Other types of vesicles require more complex preparation procedures. For example, on sonication or extrusion, MLVs disperse into unilamellar vesicles which are categorized into groups according their sizes (Figure 7). Vesicles of sizes under 100 nm are usually considered as SUVs and the larger ones are called LUVs and GUVs (Szoka & Papahadjopoulos, 1980). Phospholipids are the most commonly used lipids in liposomes. However, liposomes can also be prepared from single chain amphiphiles and lysophospholipids in the presence of equimolar cholesterol, which occupies the free place from the missing acyl chain.

Finally, yet another structure that lipids can form are inverted micelles and bilayers, which can be formed in non-polar solvents.

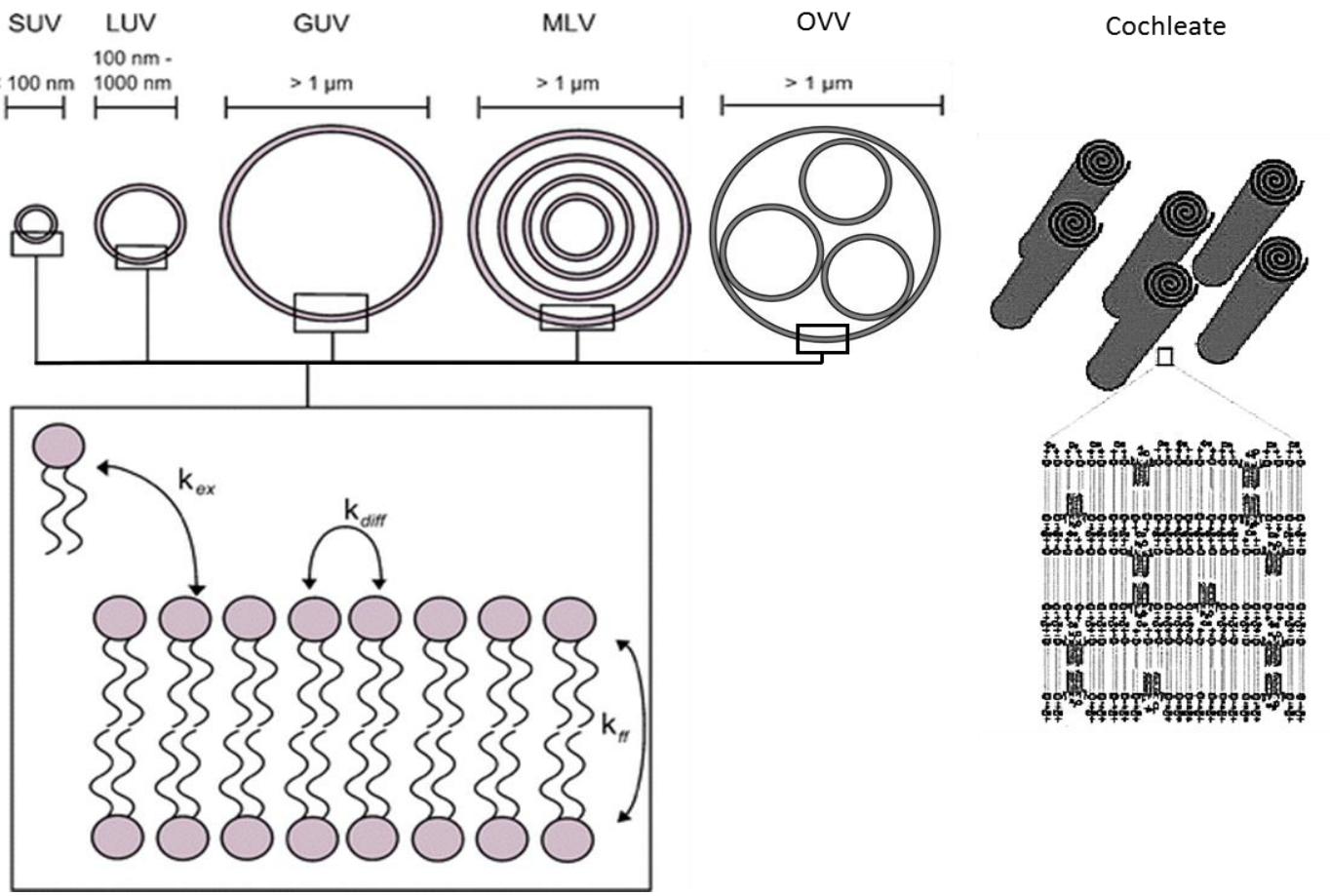

Figure 7. Types of artificial vesicles (liposomes) (Santangelo et al., 2000; Voskuhl & Ravoo, 2009; modified).

1.2.4. Liposomes as Model membranes

The extremely complex structure and function of biological membranes necessitates the use of model membranes of much less complexity. Liposomes are used as models for cells, to characterize the properties of bilayers or as a matrix for the reconstitution of membrane functions from isolated membrane components (Jain, 1988). Additionally, liposomes are also used as delivery systems for drugs (Drummond, Meyer, Hong, Kirpotin, & Papahadjopoulos, 1999) and DNA (Srinivasan & Burgess, 2009).

MLVs are the best model systems if physical properties and interactions between the molecules are of interest, because they are reasonably large, contain relatively higher amount of lipids and also are more stable. However, in permeability studies unilamellar vesicles are preferred (Bangham, 1972; Madden, 1997). This is mainly because unilamellar vesicles are more unstable and have smaller radius of curvature compared to MLVs. LUVs, SUVs and micelles are also preferred for drug delivery systems because they are smaller and more mobile, allowing them to penetrate into tissues. They also aggregate less with each other, preserving their size. Hydrophilic drugs can be encapsulated inside the aqueous compartment of the vesicles and hydrophobic drugs within the membrane.

MLVs can also encapsulate hydrophobic substances in their lipid layers and thus can be used to study interactions of those substances with lipids in model membranes. MLVs were proved to be useful systems in examining the physical and structural properties of phospholipids and became a favored model due to their simplicity and ease of preparation (Korkmaz & Severcan, 2005; Madden, 1997; Mannock, Lee, Lewis, & McElhaney, 2008).

1.2.5. Thermotropic Phase Transitions in Membranes

Membrane lipids can exist in a variety of the polymorphic forms. The one that predominates at particular conditions depends on the structure of the lipids, temperature, pressure, and pH. The behavior of lipid molecules in membranes is strongly influenced by temperature. Phospholipid bilayers exist in all-trans conformation at low temperatures because this conformation has the lowest free

energy. The probability of gauche conformations increases with increasing temperature. Because the van der Waals forces stabilizing the acyl chains in all-trans conformers require extensive overlap between neighboring chains, introducing a gauche conformer into a chain would force the neighboring chains to have a similar structure. Therefore if there is an external perturbation like temperature, a cooperative change in the packing of the bilayer would be induced. This is what happens in the case of gel to liquid-crystalline phase transition of membranes. The thermally induced transition of membranes from a relatively ordered, gel phase to a relatively disordered, fluid like state as a result of the cooperative melting of the fatty acyl chains is called gel to liquid-crystalline lipid phase transition (Melchior & Steim, 1976). When the membrane is undergoing phase transition, energy is absorbed by the system, without causing an increase in the temperature. Temperature at which this occurs is said to be the phase transition temperature (Tm).

The phase transitions of membranes can be monitored by a number of spectroscopic and calorimetric techniques. Each kind of phospholipid has a characteristic phase transition temperature, that is, transitions of pure phospholipids are sharp, symmetrical and first order processes. If comparing several phospholipids, it can be observed that the phase transition temperature is affected by the degree of unsaturation and the length of the fatty acyl chains. However, biological membranes are composed of more than one phospholipid type, and also have other components such as cholesterol, proteins and carbohydrates. Therefore, the transitions of biological membranes appear to be broad and asymmetric. In addition, since lipids undergo rapid lateral diffusion, fractional crystallization and hence lateral phase separation can be observed (Zhao, Feng, Kocherginsky, & Kostetski, 2007). Mixture of two or more kinds of lipids that differ in their structure and phase transition characteristics, often exhibit lateral phase separations within the plane of the membrane (Figure 13).

In addition to the main phase transition, there are two other transitions observed in lipid membranes, namely, subtransition and pretransition. The subtransition arises from changes in the hydration states of the head groups and the pretransition reflects changes in the tilt angle of the acyl chains (Casal & Mantsch, 1984). When combining all of these transition states, the molecular organization of phospholipids in the bilayer can be divided into four different states; crystalline gel (L_c), lamellar gel ($L_{\beta'}$), rippled

gel (P_β) and liquid crystalline (L_α) (Figure 8). Similar to the main phase transition, the temperatures for subtransition and pretransition are characteristic for each kind of phospholipid. It is known that, 1,2-Distearoyl-sn-Glycero-3-Phosphocholine (DSPC), used in this study (Figure 3), undergoes transitions at the temperatures shown in the diagram below (Chen, Sturtevant, & Gaffney, 1980; Mabrey & Sturtevant, 1976).

$$L_c \xrightarrow{T_s\,(21\,^\circ C)} L_\beta \xrightarrow{T_P\,(51\,^\circ C)} P_\beta \xrightarrow{T_m\,(54\,^\circ C)} L_\alpha$$

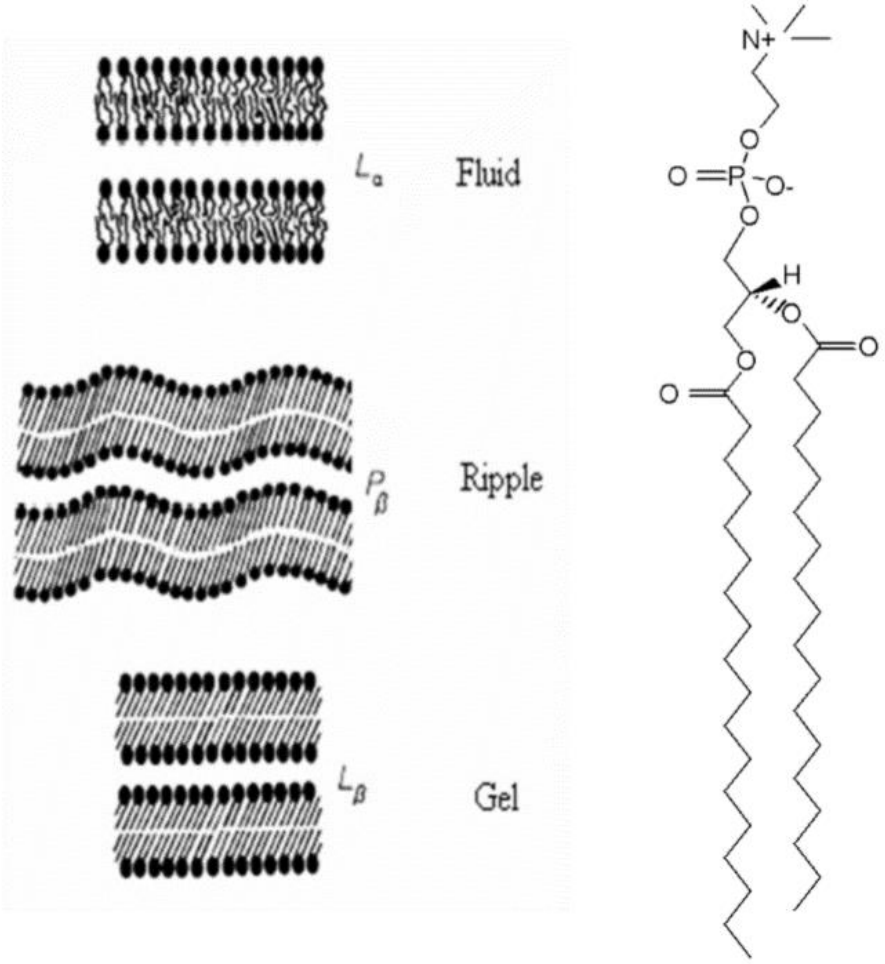

Figure 8. Different phases of phospholipids (left) and the structure of DSPC (right) (Stuart & Ando, 1997).

1.2.6. Lipid Interdigitation

An important property of some lipid bilayers is the ability to interdigitate, interlocking the acyl chains between the two monolayers. This usually happens in the gel phase and is known as interdigitated gel phase ($L_{\beta}I$).

There are multiple types of interdigitation (Figure 9). The type of interdigitation that forms is heavily dependent on the structure and symmetry of the hydrocarbon chains (Slater & Huang, 1988). Interdigitated lipid systems can also be separated into two categories: spontaneous and induced. In case of spontaneous interdigitation, lipids self-assemble into the interdigitated gel phase when fully hydrated under typical preparation procedures and at ambient pressure. The balance of properties that favor and disfavor interdigitation determines if a lipid can spontaneously interdigitate. These characteristics of lipids may often have opposing effect regarding their ability to interdigitate. Thus, there is no simple formula for determining which lipids will spontaneously interdigitate without relying on experimental data.

Induced interdigitation can be pressure-induced, chemically-induced or caused by covalent modifications of the phospholipids that normally do not interdigitate. For example, it has been reported that incorporating Fluorine moiety (similar to the one in CLX) group to the end of the fatty acids of certain phospholipids induced fully interdigitated lipid bilayers (Smith, Smith, Tanksley, & Dea, 2014).

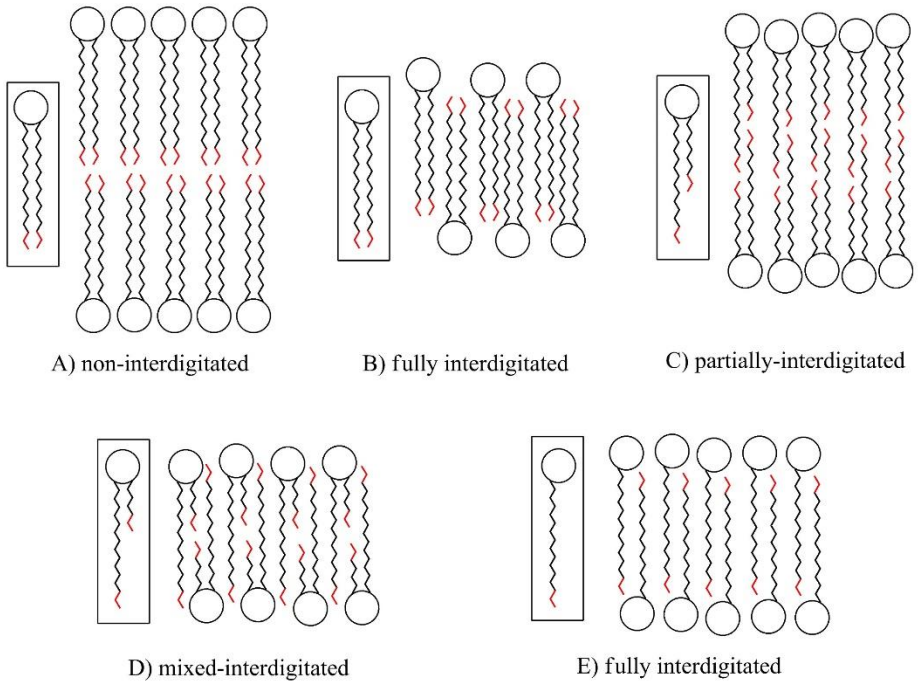

Figure 9. Types of interdigitated lipid bilayers (Smith & Dea, 2013).

As can be seen in Figure 9, the structural difference between the interdigitated and non-interdigitated lipid phases can be substantial. In the non-interdigitated membrane, both ends of the hydrocarbon chains meet in the membrane midplane (Figure 9-A). Two well-defined leaflets are formed and there is a thick hydrophobic core in-between them. In the fully-interdigitated membrane, the thickness of the membrane is greatly reduced and there is the loss of the midplane. This leads to an increase in the spacing between the polar lipid head groups making the ends of the lipid hydrocarbon chains more exposed to the aqueous interface (Slater & Huang, 1988). This difference is most obvious in the fully interdigitated membrane compared to the non-interdigitated one (Figure 9-B). In the partially-interdigitated system, the longer chain extends to the other side of the membrane and aligns with the opposing shorter chain (Figure 9-C). In the mixed-interdigitated membrane, the short hydrocarbon chains line up with each other and the full-length chain extends to the other side of the membrane (Figure 9-D). Lysophospholipids and sphingolipids can also form a fully interdigitated structure (Figure 9-E) (Hui & Huang, 1986).

1.2.7. Cholesterol in Biological Membranes

Cholesterol is the major sterol present in mammalian cell membranes. Usually a cholesterol to phospholipid ratio of 1:1 is favored in most biological membranes but 2:1 ratio is also observed under some circumstances. This ratio varies from 0.11 to 0.33 in plasma membranes and subcellular membranes (Demel & De Kruyff, 1976). The structure of cholesterol is shown in Figure 10.

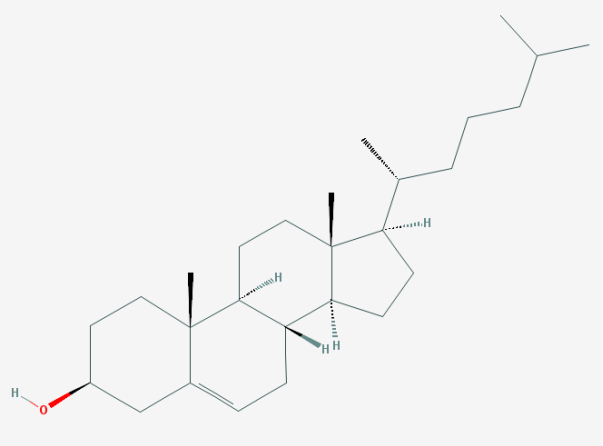

Figure 10. Structure of Cholesterol (source: The National Center for Biotechnology Information, PubChem).

The main part of cholesterol molecule is a steroid ring system, referred to as planar sterol nuclei. A hydroxyl group is found at C3 and a hydrophobic tail at C17. Despite the fact that, most of the molecule is hydrophobic, the hydroxyl group gives cholesterol an amphipathic character. Due to such structure, a specific orientation of cholesterol in the bilayer is observed. The polar hydroxyl group faces the aqueous solvent and the hydrophobic steroid rings are oriented parallel to the fatty acyl chains of phospholipids, which is shown in Figure 11. Studies with various techniques such as 31P NMR (Yeagle, Hutton, Huang, & Martin, 1975), X-ray diffraction (McIntosh, 1978) and infrared (Mannock et al., 2008) have excluded the possibility of an interaction between cholesterol the head groups of phospholipids. It has been accepted that the –OH group of cholesterol should be located close to the ester carbonyl group with H- bonding forming between these moieties as proposed by several investigators (Arsov & Quaroni, 2007; Yeagle et al., 1975).

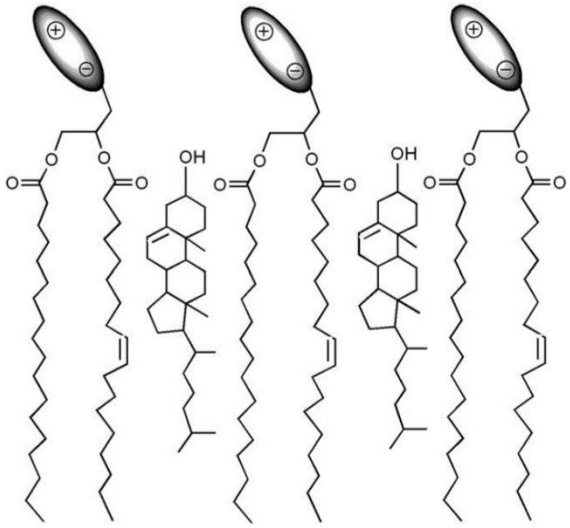

Figure 11. Localization of cholesterol in the phospholipid bilayer (Chen & Tripp, 2008).

Cholesterol, being the most abundant sterol in biological membranes, is believed to be a primary modulator of the characteristics of bilayers. The effect of cholesterol on the phase behavior, structure, permeability and dynamics of model and biological membranes has been heavily investigated by a variety of physical techniques. One of the best known effects of cholesterol is on the phase transition properties of phospholipid bilayers. Cholesterol decreases the Tm, enthalpy and the cooperativity of the Lβ/Lα phase transition in a concentration dependent manner, eliminating it totally at 50 mol%. It also eliminates the pretransition at a concentration around 6 mol% (McMullen, Lewis, & McElhaney, 1993). Cholesterol exerts opposing effects on the acyl chain conformation below and over the Tm of phospholipids. It disorders the membrane in the gel phase and orders it in liquid crystalline, thus also affecting the permeability and condensation of the membrane. With cholesterol incorporation, the permeability of the membrane increases in the gel phase and decreases in the liquid crystalline phase (Demel & De Kruyff, 1976; Yeagle, 1985). It is proposed that diffusion of small molecules through a membrane is enhanced by lipids in gauche conformation forming kinks, resulting in transient voids between the chains of phospholipids (Yeagle, 1985). With cholesterol suppressing the formation of gauche conformers in the liquid crystalline phase, the permeability is decreased in this phase and vice versa in the gel phase. Cholesterol also has a so called “condensing effect”

on the membrane in the liquid crystalline phase (Hung, Lee, Chen, & Huang, 2007; Levine & Wilkins, 1971). It is described as the reduction in the average cross-sectional area of phospholipids, which also leads to the decrease in the number of gauche conformers.

Because of all of these properties of cholesterol, researchers conclude that, cholesterol converts the L_α and L_β of the lipid membranes to a state intermediate between them, called the liquid ordered (L_o) phase (Vist & Davis, 1990). At cholesterol to total lipid concentration ratio lower than 0.5, and below the main transition temperature, L_o phase coexists with the L_β phase. At temperatures higher than the transition temperature, L_o phase coexists with L_α phase. However, at cholesterol to total lipid concentration ratio higher than 0.5, only L_o phase exists at all temperatures (Liu & Conboy, 2009; Tamai et al., 2008). The authors suggest that cholesterol is distributed in a regular pattern in the bilayer membrane which is favored energetically. This type of organization of cholesterol was reported previously and called the superlattice model (Somerharju, Virtanen, & Cheng, 1999). According to this model, different phospholipid classes tend to adopt regular, rather than random distributions. Since the head groups of PCs occupy a larger cross-sectional area than their acyl chains, a repulsive force occurs between them with the glycerol backbone gaining a tilted configuration in order to overcome this effect. If a molecule with a smaller hydrophilic group like cholesterol is incorporated into this system, the packing frustrations are relieved because of complementary structures of the two species. This decreases the tilt angle of the backbone leading to the hydration of the head groups by water molecules (Chen & Tripp, 2008; Demel & De Kruyff, 1976). Maximal effect is obtained when the two species organize into a regular, superlattice like distribution, forming the most energetically favorable conformation. According to this model there is only a limited number of allowed, critical concentrations for each component and a superlattice of a certain composition is in dynamic equilibrium with randomly arranged domains, as well as with superlattices with different compositions. Based on the superlattice model, some illustrations showing the possible distributions of DSPC/Cholesterol mixtures at different stoichiometric ratios are shown in Figure 12 (Tamai et al., 2008).

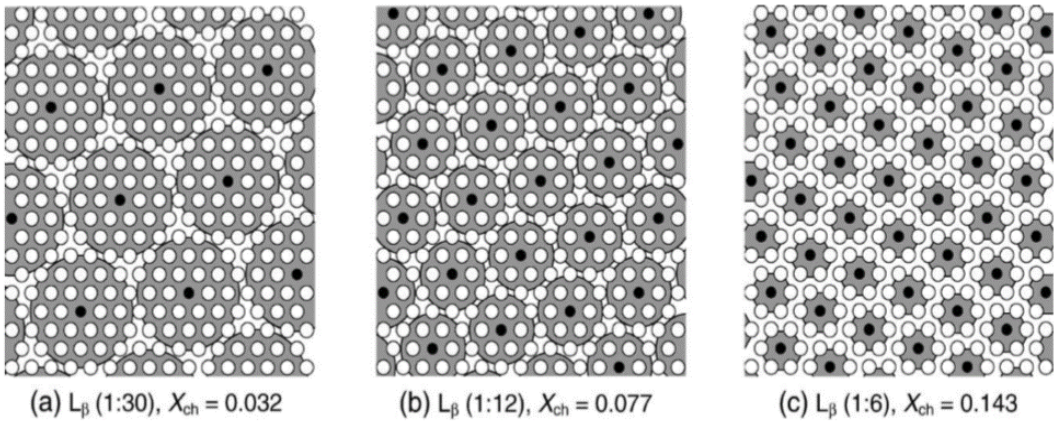

Figure 12. Schematic illustration for various types of regular distribution of cholesterol in binary bilayer membranes. Closed and open circles represent cholesterol and DSPC molecules, respectively. (Tamai et al., 2008).

The superlattice distribution model also helps us understand the composition of the lipid rafts. Lipid rafts are laterally segregated domains in biological membranes (Edidin, 2003; London, 2005). They were originally thought as long-lived domains of relatively large size, with low amounts of phospholipids but high amounts of sphingolipids and lipid-anchored proteins. They were suggested to exist in a L_o state, in contrast to the non-raft regions that are in a L_α state. Differences between these domains cause the differential segregation of proteins throughout the membrane. The existence of such domains has been accepted as a fact, but the exact composition, function and structure of the lipid rafts is still an area of ongoing research.

Cholesterol has showed controversial effects on membrane fluidity. In some studies, cholesterol was shown to increase fluidity in the gel phase and decrease fluidity in the liquid crystalline phase, similar to its effect on membrane order (Demel & De Kruyff, 1976; Kutchai, Chandler, & Zavoico, 1983). However, other studies claim that cholesterol either increases the fluidity in all phases or has no effect on the dynamics of the membranes (Ghosh, 1988; Lindblom, Johansson, & Arvidson, 1981; van Ginkel, van Langen, & Levine, 1989). These discrepancies may result from the misuse of the terms order, microviscosity and fluidity (Figure 4-B).

Studies also show that cholesterol can affect the bilayer thickness. A study by McIntosh et al. compares the effects of cholesterol on various PCs changing in the acyl

chain length from 12C to 18C, using X-ray diffraction technique (McIntosh, 1978). It revealed that, cholesterol increases the bilayer thickness of 12 Carbon and 16 Carbon PC bilayers, while decreasing it in 18 Carbon PC (DSPC) bilayers. This may occur due to the relative hydrophobic lengths of cholesterol and DSPC. The DSPC molecule should produce kinks near its methyl ends in order to fill the space caused by the shorter cholesterol molecule. In a study by McMullen et al., some other variations of the effect of cholesterol were observed when 18 Carbon and longer PCs were studied (McMullen et al., 1993). The hydrophobic mismatch theory was used to explain those effects. This theory states that, the hydrophobic thickness of PC bilayers decreases by approximately one-third at the gel to liquid-crystalline phase transition due to the introduction of gauche conformers. Thus, incorporation of an amphiphilic molecule, can affect the stability of the gel and liquid-crystalline phases according to the degree of mismatch between the effective hydrophobic length of the amphiphile and the phospholipid hydrocarbon chains. The smallest effect should be observed when the effective length of the molecule is equal to the mean of the length of the acyl chains. The effective length of the cholesterol molecule is ~17.5 Å which is close to the thickness of 17 Carbon PC bilayer and the hydrophobic length of DSPC is ~22.4 Å. Thus the differing effects of cholesterol on longer chain PCs can be explained.

Because alterations of membrane thickness affect conformation of membrane-embedded proteins, the function of several membrane-spanning and membrane-associated enzymes is altered by cholesterol as well (Li et al., 2004; Maxfield & Tabas, 2005).

1.2.8. Cholesterol-like properties of NSAIDs in lipid bilayers

Because of similarities in structure and possibly positioning within the lipid bilayer, some NSAIDs have been shown to have cholesterol-like effects on membranes. Drugs like CLX increase the order in liquid membranes by aligning the long fatty acid acyl chains of phospholipids more perpendicular to the plane of the membrane, which in turn results in a thicker and more rigid membrane.

In recent studies, CLX was reported to alter γ-secretase activity, resulting in enhanced production of amyloid-β 42 (Kukar et al., 2005). CLX shares some similarities in

activity with cholesterol in that both exert inhibitory effects on sarco(endo)plasmic Ca^{2+}-ATPases (SERCA) (Johnson, Hsu, Lin, Song, & Chen, 2002; Li et al., 2004). It has also been shown that, several selective diaryl heterocycle COX inhibitors and fibrates mimic cholesterol effects concerning biological membranes and the function of membrane-spanning proteins, in particular the activity of β- and γ-secretase (Gamerdinger et al., 2007). Finally, Sade et al. showed that the effects of CLX on lipid order and fluidity were similar to that of cholesterol (Sade et al., 2010). Unfortunately, less of such studies are available on RFX and VLX.

One of the most important properties of drugs and other substances incorporating into bilayers, such as hormones or coenzymes is the ability to induce phase separation and domain formation in the vesicles. The basic domain separation is explained in Figure 13. Similarly, addition of a compound might induce chemical-rich and poor domains formation. This has been observed with melatonin (Severcan et al., 2005), progesterone (Korkmaz & Severcan, 2005), vitamin D_2 (Kazanci, Toyran, Haris, & Severcan, 2001), and CLX as well (Sade et al., 2010).

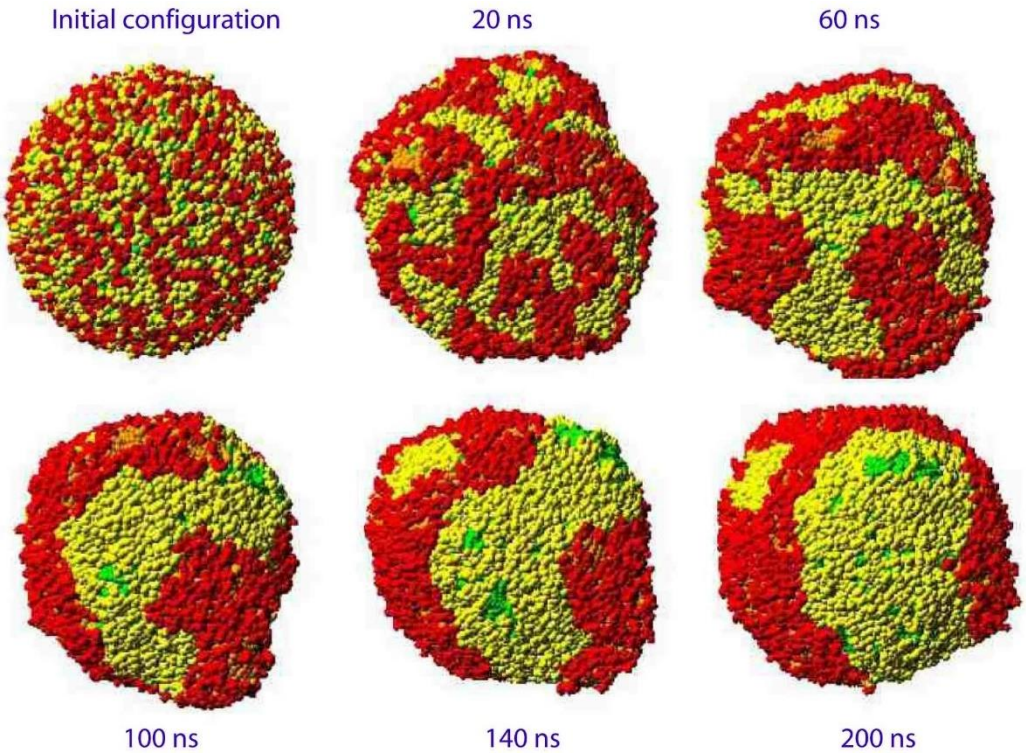

Figure 13. Visual representation of lipid domain formation. The initial configuration of the vesicle membrane corresponds to a random mixture of the two lipid species. After 200 ns, the lipids form one large "red" domain as well as one large and one small "yellow" domain (Illya, Lipowsky, & Shillcock, 2006).

1.3. Electromagnetic Radiation and Optical Spectroscopy

The interaction between electromagnetic radiation and matter is the main research interest of spectroscopy. A spectrum is defined as a plot of absorbance versus the wavelength of the electromagnetic radiation. Spectra are used to identify the chemical components of a sample. They can also be used to either measure the amount of a material or to detect the certain amount of a material in a sample. According to the frequency (wavenumber), electromagnetic radiation is classified into seven groups: radio waves, microwaves, infrared radiation, visible light, ultraviolet radiation, X-rays and gamma rays (Figure 14).

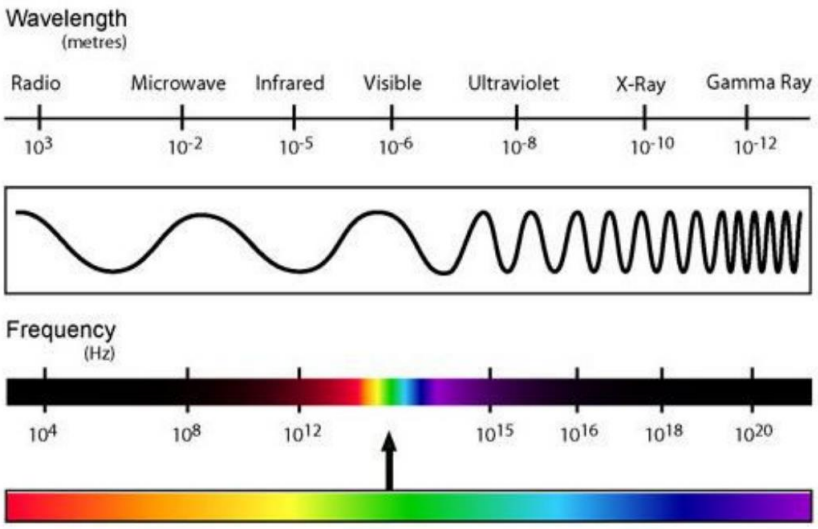

Figure 14. The electromagnetic spectrum.

Electromagnetic radiation has three main types of interaction with the matter: it can be scattered (its direction of propagation changes upon encountering molecule), absorbed (its energy is transferred to the molecule) or emitted (energy is released by the molecule). The probability of the occurrence of each process is a property of the particular molecule encountered. If the energy of the light is absorbed, the molecule is said to be excited. A molecule or part of a molecule that can be excited by absorption is called a chromophore. An excited molecule can possess any one of the discrete set amounts (quanta) of energy, known as the energy levels of the molecule. A typical energy-level diagram describing these energy levels is presented in Figure 15. The

major energy levels are determined by the possible spatial distributions of the electrons and are called electronic energy levels. The vibrational levels superimpose on them and indicate the various modes of vibration of various covalent bonds of the molecule. The lowest electronic level is called the ground state and all others are excited states. The absorption of energy is most likely to occur only if the amount absorbed corresponds to the difference between energy levels. The process when molecules change energy levels is called a transition. Mechanically, a transition between electronic energy levels represents the energy required to move an electron from one orbit to another (Freifelder, 1983).

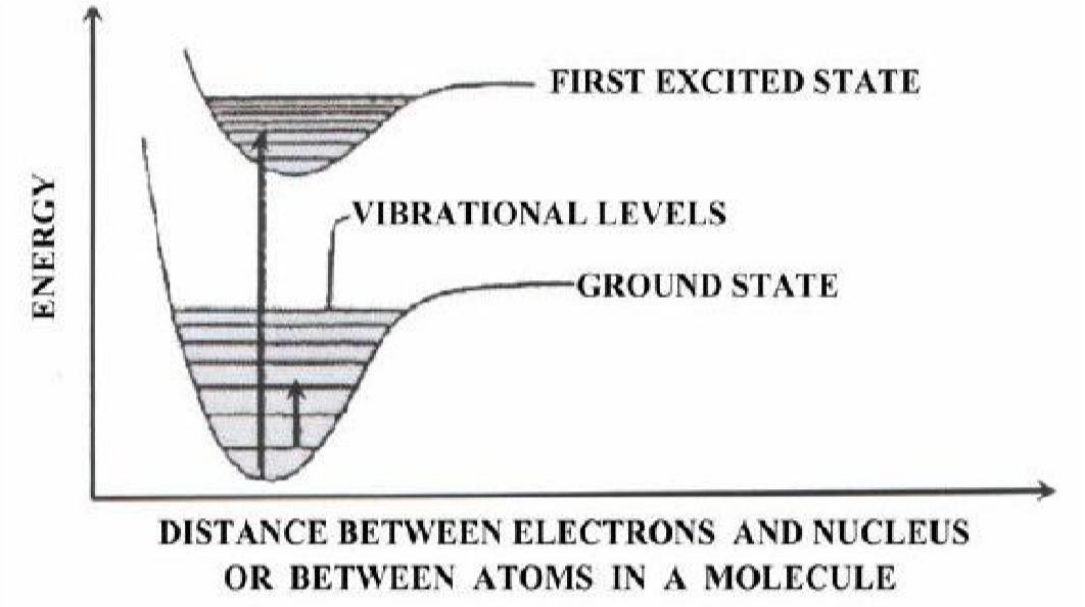

Figure 15. Typical energy-level diagram showing the ground state and the first excited state. Vibrational levels are shown as thin horizontal lines. A possible electronic transition between the ground state and the fourth vibrational level of the first excited state is indicated by the long arrow. A vibrational transition within the ground state is indicated by the short arrow (Freifelder, 1983).

The total energy of a molecule is given by the sum of energies of every different motion that the molecule has. Then, the formula of total energy is:

$$E_{TOTAL} = E_{transition} + E_{rotation} + E_{vibration} + E_{electronic} + E_{electron\ spin\ orientation} + E_{nuclear\ spin\ orientation}$$

Each energy type in the equation represents the appropriate energy as indicated by its subscript. In a solution, molecules can translate, rotate and vibrate. The energies associated with each of these are quantized (Campbell & Dwek, 1984). $E_{rotation}$, $E_{vibration}$ and $E_{electronic}$ are associated with the microwave, infrared and ultraviolet-visible region of the electromagnetic spectrum, respectively (Campbell & Dwek, 1984).

Spectroscopic studies involve irradiation of a sample with some type of electromagnetic radiation, measurement of the scattering, absorption, or emission in terms of some parameters, and the interpretation of these measured parameters to give useful information.

1.3.1. Infrared Spectroscopy

Transitions between vibrational levels of a molecule in the ground state occur as a result of the absorption of light in the infrared (IR) region, between 103 and 105 nm. Infrared region is divided into three sub regions: the far infrared (400-0 cm^{-1}), the mid-infrared (4000-400 cm^{-1}) and the near infrared (14285-4000 cm^{-1}). Most infrared applications involve the mid-infrared region (Stuart & Ando, 1997). A molecule will most likely absorb infrared radiation of the same frequency as the oscillating electric field which results from the vibration of the atoms in the molecule (Freifelder, 1983). A selection rule of IR spectroscopy states that a molecule can only show infrared absorptions if the electric dipole moment of the molecule changes during the vibration. A dipole occurs when there is charge separation across a bond and this dipole changes when the bond stretches or bends. So, stretching and bending are two basic molecular motions in infrared spectroscopy. A stretch is a movement along the line between the atoms so that the interatomic distance is either increasing or decreasing. A bend is a change in the bond angle which can occur either in the plane of the molecule or out of plane (Stuart & Ando, 1997). Stretching vibrations and several types of bending vibrations are shown in Figure 16.

One can obtain an infrared spectrum by passing infrared radiation through a sample and determining what fraction of the incident radiation is absorbed at a particular energy. The result is a highly complex absorption spectrum, which is the plot of

absorption as a function of wavenumber (ν) expressed in terms of cm^{-1}. The infrared spectra are generated by the vibrational motions (e.g., bond stretching, bond bending, etc.) of various functional groups (e.g., methyl, carbonyl, phosphate, etc.) with each peak of the spectrum assigned with a unique type of either of them. The modes of vibration of each group are very sensitive to changes in chemical structure, conformation, and environment. This feature allows infrared researchers to perform valuable comparative analyses not available with ultraviolet and visible light spectroscopy (Freifelder, 1983).

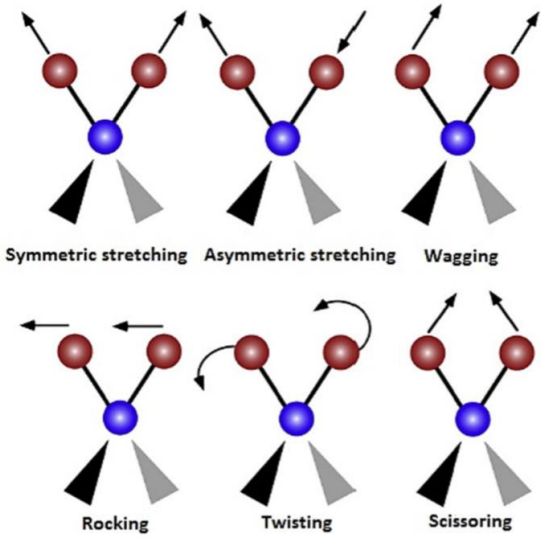

Figure 16. The vibrational modes associated to a molecular dipole moment change detectable in an IR absorption spectrum (Marcelli, Cricenti, Kwiatek, & Petibois, 2012).

1.3.2. Fourier Transform Infrared Spectroscopy (FT-IR)

The basis of Fourier-transform infrared (FT-IR) spectroscopy is the interference of radiation between two beams yielding an interferogram, which is a signal produced as a function of the change of path length between the two beams (Stuart & Ando, 1997). The main components of an FT-IR spectrometer are shown schematically in Figure 17.

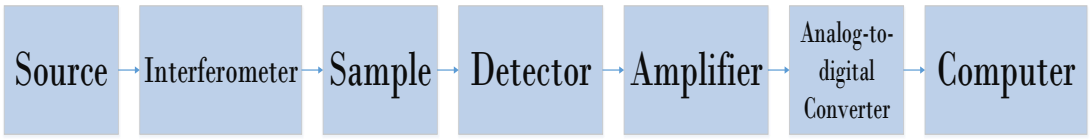

Figure 17. Basic components of an FT-IR spectrometer.

The radiation emerging from the source is passed through an interferometer, and then goes to the sample, which absorbs all the wavelengths characteristic of its spectrum. Next comes the detector which reports variation in energy versus time for all wavelengths, at the same time. For rapid-scanning interferometers liquid nitrogen cooled mercury cadmium telluride (MCT) detectors are used. For slower scanning types of interferometer, pyroelectric detectors (e.g. a deuterated triglycine sulfate (DTGS) detector element) can be used. This multiplexing of the infrared signals and the high optical throughput of the interferometer, result in higher signal-to-noise values for interferometric infrared spectrometers compared to dispersive instruments. After amplification of the signal by a filter, eliminating high-frequency contributions, the data is converted to digital form by a converter and transferred to the computer, which performs a mathematical function called Fourier-transformation, which allows us to convert an intensity versus time spectrum into an intensity versus frequency spectrum.

1.3.3. Infrared Spectroscopy in Membrane Research

The critical property of FT-IR spectroscopy is the ability to assign a band in the infrared spectra to a functional group or a bond in a molecule. The changes in the spectral characteristics of these bands can be directly linked to the corresponding molecular properties. This approach in vibrational spectroscopy is referred to as group frequencies (Stuart & Ando, 1997). The main spectral parameters include band shapes, peak heights, bandwidths, frequency shifts, and integrated intensities of the vibrational bands (Chapman & Hayward, 1985). Band frequency is affected by the nature of the atoms in a chemical bond, their conformation and immediate molecular environment, these properties being collectively referred to as molecular order. On the other hand, bandwidth is related to the dynamics of the molecule. Therefore, IR spectra provide

information on both the chemical structure of the molecule and on its conformation and dynamics.

Valuable structural information about lipids, which are the main components of membranes can be obtained using FT-IR spectroscopy. The infrared spectra of phospholipids can be divided into the spectral regions that originate from the molecular vibrations of the hydrocarbon tail, the interface region and the head group (Casal, Cameron, Smith, & Mantsch, 1980; Casal & Mantsch, 1984; Chapman & Hayward, 1985; Severcan et al., 2005). The hydrocarbon tail has the most intense vibrations in the infrared spectra of lipid systems. These acyl chain C-H stretching vibrations give rise to bands in the 3100-2800 cm^{-1} region. The most useful infrared bands for probing the glycerol-acyl chain interface of ester lipids are the ester carbonyl stretching modes (C=O stretching) which give rise to strong infrared bands in the spectral region 1750-1700 cm^{-1}. Vibrational modes of the moieties found in the head group of membrane lipids give rise to a number of characteristic infrared bands, which in case of phospholipids, originate from the vibrations of the phosphate moiety. There are two strong bands around 1230 and 1085 cm^{-1} due to the P=O double bond stretching (PO_2^- antisymmetric and symmetric stretch, respectively).

One of the most studied physical properties of membrane lipids is their thermotropic phase behavior. The remarkable structural rearrangements of phospholipids during the gel to liquid crystalline phase transition can be studied by the infrared spectra of phospholipids (Casal et al., 1980). Also, FT-IR spectroscopy can be used to study the interactions of membrane lipids with a variety of small molecules such as drugs, environmental chemicals and organic solvents. These agents exert their effects by various means, such as by passing through the membrane, by interacting with membrane proteins or with the membrane itself; therefore investigating their mechanism of action is important in a number of disciplines (Jain, 1979). The important course of action during the interpretation of the phase transitions and membrane interactions is to correlate the changes in the spectroscopic parameters with the changes that are known to occur in the structure of the lipids during those processes.

1.3.4. Dynamic Light Scattering

Light scattering is the deflection of a ray from a straight path, for example by irregularities in the propagation medium, particles, or in the interface between two media. Deviations from the law of reflection that happen due to irregularities on a surface are also usually considered to be a form of scattering. Most objects are visible due to the light scattering from their surfaces, making this phenomenon the primary mechanism of physical observation. Scattering of light depends on the wavelength or frequency of the light being scattered.

There are several experimental techniques based on the scattering effect of light. Static light scattering studies the time-average intensity of scattered light, while dynamic light scattering studies the fluctuations in light intensity. Both techniques are mainly used to characterize colloids and polymers.

Using dynamic light scattering one can determine the size distribution profile of either small particles in a suspension or polymers in a solution (Figure 18). It can also be used to probe the behavior of complex fluids such as concentrated polymer solutions.

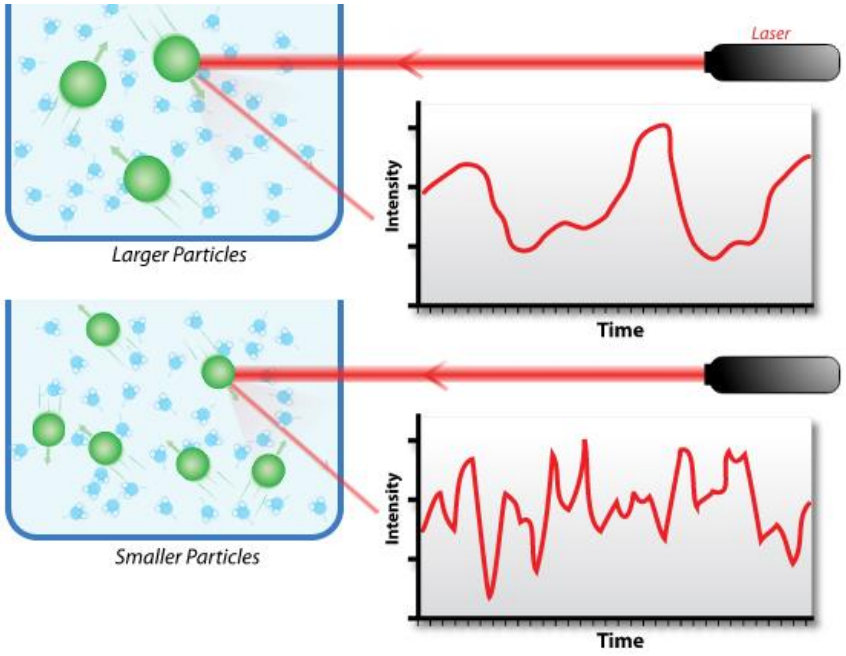

Figure 18. Dynamic light scattering of two samples: Larger particles on the top and smaller particles on the bottom (source: http://en.wikipedia.org/wiki/File:DLS.svg).

When light hits small particles, the light scatters in all directions (Rayleigh scattering) as long as the particles are small enough compared to the wavelength (below 250 nm). Using a laser as a light source results in monochromatic and coherent light. In this scenario the scattering intensity fluctuates over time due to the Brownian motion of the small molecules and the resulting changing distance between the scattering particles.

1.3.5. Turbidity Technique

Turbidity technique can be considered a form of light scattering. Scattering is usually detected at an angle θ to the incident wave, but it may also be detected by the reduction in the transmitted light at θ=0 which is called turbidity (Campbell & Dwek, 1984). Thus, turbidity is the decrease by scattering of the transmitted light, and thus is equal to the scattering over all angles. The main advantage of light scattering is minimal perturbation during experiments. A standard spectrophotometer is often easily adapted to measure light scattering (Chong & Colbow, 1976).

Turbidity is generally used in protein denaturation studies, but it is also useful in studying thermotropic phase transitions of membranes, and the effects of additives on the size, structure, aggregation and fusion processes of lipid vesicles (Chong & Colbow, 1976; Eker, Durmus, Akinoglu, & Severcan, 1999).

1.4. Differential Scanning Calorimetry (DSC)

DSC is a simple thermal analysis method used to describe physical and chemical changes as a function of temperature. The DSC instrument has two cells: one for reference and one for sample. Both of them are heated at identical rates. The temperatures of both reference and sample that does not undergo a phase transition increase linearly and the temperature difference between them is zero. However, when the sample undergoes a thermal transition, this produces a temperature differential between the sample and the reference. It is important to choose reference that does not undergo phase transition in the studied temperature interval. During sample phase transition, the system supplies more heat either to the sample or to the reference in

order to keep the temperatures of the two cells equal. This excess specific or differential heat is then recorded as a function of temperature. If the sample does not undergo a thermal event, the output should be a straight, horizontal baseline, but if a transition occurs, the recorder pen is deflected from the baseline. The direction of the deflection depends on whether the event is endothermic (upwards) or exothermic (downwards), and the magnitude of the deflection depends on the magnitude of the differential heating rate (McElhaney, 1982).

The DSC curve is analyzed to determine the transition temperature, Tm, and the calorimetric enthalpy of transition, ΔH_{cal}. Lipid bilayer gel to liquid-crystalline phase transition of a pure phospholipid is a first order transition, thus Tm is where the excess specific heat reaches its maximum value. The value of the calorimetric enthalpy (ΔH_{cal}) for the phase transition is determined by peak area integration (McElhaney, 1982).

DSC is used to study the effect of composition, hydration state, pH, and addition of chemicals on the phase-transition profile of biological membranes and pharmaceuticals, to characterize complex processes, such as protein denaturation and to perform specific heat measurements in the glass-transition of polymers. Despite being a classic method, DSC has been applied to biological systems relatively recently. This technique is very useful for the routine measurement of gel to liquid-crystalline phase transitions in model and biological membranes. The current high-sensitivity DSC instruments require only relatively dilute suspensions of material permitting accurate control of the pH and ionic composition of the aqueous phase. Unlike many other techniques, DSC does not require the introduction of foreign probe molecules into the system under investigation. Moreover, this technique is the only one that provides a direct and accurate measurement of the thermodynamic parameters of the lipid phase transition (McElhaney, 1982).

1.5. Scope and Aim of this study

Using DSPC model membranes, our group has previously shown that CLX decreases the fluidity of the membrane and induces phase separation of the lipids (Sade et al., 2010). Additional studies carried out in our laboratory have shown that the properties

of lipid vesicles are changed significantly in the presence of CLX. Vesicles showed increased aggregation properties, which complicated the handling of the liposomes during procedures such as extrusion, and also increases the diameter of vesicles (R.R., S.B. F.S., unpublished data). Interestingly, the same studies showed that RFX did not alter the membrane properties in the way CLX did. To understand the mechanism behind these differences in the biophysical properties of the membranes, FT-IR and DSC studies were conducted on model membranes in the presence or absence of RFX. To further understand these differences, VLX, which has a structure very similar to CLX was chosen for comparison in this study. These three drugs are from the same family of selective COX-2 inhibitors, and have some similarities in their structure and functional properties. However, all three of them also have unique functional groups (Figure 2). RFX is the only sulfone among the three. VLX and CLX are sulfonamides, but CLX has also additional F_3 moiety. Thus if a drug shows unique interaction, which the other two do not, it can be suggested that a certain unique part of the molecule is responsible for it. We have hypothesized that similarities in FT-IR or DSC data could stem from similarities in the structure of the drug, its positioning and interactions with model membranes.

CHAPTER 2

MATERIALS AND METHODS

2.1. Materials

18:0 PC (1,2-Distearoyl-sn-Glycero-3-Phosphocholine: DSPC) was purchased from Avanti Polar Lipids (Alabaster, Alabama, USA) and stored at –20°C. Celecoxib and rofecoxib were purchased from Yick-Vic Chemicals & Pharmaceuticals (Hong Kong, China) and certified to be 98% pure by HPLC. Valdecoxib was purchased from Cayman Europe (Tallinn, Estonia). All other chemicals were of analytical grade and purchased from Merck (Darmstadt, Germany).

2.2. Preparation of Phosphate Buffered Saline (PBS)

Phosphate buffered saline (PBS) 0.1 M, pH 7.4 was prepared by weighing 8 g sodium chloride (NaCl), 0.27 g potassium dihydrogen phosphate (KH_2PO_4), 1.78 g disodium hydrogen phosphate 2-hydrate ($Na_2HPO_4.2H_2O$) and mixing in 500 mL of distilled water. The pH of the solution was adjusted to 7.4 by adding hydrogen chloride (HCl) and the final volume was completed to 1 L by adding distilled water. The prepared buffer was autoclaved and stored at room temperature.

2.3. Preparation of DPSC, RFX and VLX stock solutions

RFX stock solution was prepared by dissolving 10 mg of RFX powder in 1 mL of pure chloroform. VLX stock solution was prepared by dissolving 10 mg of VLX powder in

1 mL of pure ethanol. DSPC stock solution was prepared by dissolving 100 mg of DSPC in 1 mL of pure chloroform.

2.4. Preparation of Model Membranes

For all experiments, multilamellar vesicles (MLVs) were prepared according to the procedure reported previously (Bangham et al., 1965; Korkmaz & Severcan, 2005). DSPC was added from the stock solution prepared in chloroform to the sample Eppendorf tubes and excess chloroform was evaporated by using a gentle stream of nitrogen. A dried lipid film was obtained by subjecting the samples to vacuum drying for 3 hours, using the HETO-spin vac system (HETO, Allerod, Denmark). The lipid films were then hydrated by adding certain volume of 0.1-M phosphate-buffered saline (PBS) buffer (pH 7.4). MLVs were formed by vortexing the mixture at 70–75°C, which is above the Tm of DSPC (∼55°C) for 30 minutes.

The amount of DSPC used for MLV preparation and the volume of PBS used in the hydration procedure changed according to the experiment. Thus, 4 mg DSPC and 100 µl PBS was used for DSC, Size analysis and Encapsulation efficiency studies, 10 mg and 70 µl PBS for FT-IR, 0.4 mg and 1.5 ml for Turbidity measurements.

To prepare drug-containing liposomes, the required amount of RFX or VLX (1, 3, 6, 9, 12, 18 mol %) from a stock solution (in chloroform for RFX, in ethanol for VLX) was first added to sample tubes before DSPC addition. In case of VLX, excess ethanol was evaporated by using a gentle stream of nitrogen, then the needed amount of DSPC was added to the tubes from the stock solution in chloroform. This was done to prevent ethanol and chloroform mixing with each other, which may alter lipid solubility and phase separation properties. MLVs were then prepared as described above.

2.5. FT-IR measurements

For FT-IR measurements, 20 µL of sample suspensions in PBS buffer (0.1 M, pH 7.4) were placed between CaF_2 windows with a cell thickness of 12 µm and immediately placed in the sample holder of the FT-IR equipment. Spectra were recorded on a Perkin-Elmer Spectrum One FT-IR spectrometer (Perkin-Elmer Inc., Norwalk, Connecticut, USA) equipped with a deuterated triglycine sulfate (DTGS) detector. Interferograms were averaged for 50 scans at 2 cm^{-1} resolution. To see the effect of

temperature, the samples were collected between 30 and 75°C and incubated at each temperature for 5 minutes before data acquisition. The temperature was controlled by a recently calibrated Graseby Specac (Kent, UK) digital temperature-controller unit. To see the effect of drug concentration (between 3 and 18 mol %), the samples were scanned at 45 and 65 °C, temperatures which were decided according to the DSC measurements, for correct monitoring of the gel and liquid crystalline phases. The experiments were repeated six times, for statistical analyses. The spectra were analyzed by using Spectrum v5.0.1 software (Perkin-Elmer). In order to provide a better resolution of the infrared bands, 0.1-M PBS buffer (pH 7.4) bands were subtracted by flattening the band located around 2,125 cm^{-1}. The band positions were measured according to the center of weight, and bandwidth was measured at 0.80× peak height position and confirmed by measurements from the first derivative.

2.5.1. Infrared spectral regions used in this study

In this study, four absorption bands were primarily taken into consideration (Figure 19). Two of them are the strong bands at 2920 cm^{-1} and 2850 cm^{-1} of the infrared spectrum that correspond to the CH_2 antisymmetric and CH_2 symmetric stretching modes of the acyl chains of the phospholipid membranes, respectively. The phase transition behavior and the order-disorder state of membrane systems can be studied by the frequency analyses of these bands (Korkmaz & Severcan, 2005; Severcan et al., 2005). The frequency of the CH_2 stretching bands of acyl chains depend on the average trans/gauche isomerization in the systems and shifts to higher wavenumbers correspond to an increase in the number of gauche conformers (Casal & Mantsch, 1984; Severcan et al., 2005; Severcan, 1997; Toyran & Severcan, 2003). In addition, variations in the bandwidth of these groups are sensitive to mobility of the lipids, thus give information about the dynamics of the membrane. An increase in the bandwidth is an indication of an increase in the dynamics of the membrane (Casal et al., 1980; Korkmaz & Severcan, 2005; Lopez-Garcia, Micol, Villalain, & Gomez-Fernandez, 1993; Severcan et al., 2005; Toyran & Severcan, 2003).

The third infrared band used is the carbonyl absorption band at 1735 cm^{-1} arising from the stretching vibrations of ester carbonyl groups of phospholipids. This band is conformationally sensitive to the level of hydration at the membrane interface and is

influenced by hydrogen bonding (Korkmaz & Severcan, 2005; Severcan et al., 2005). The more hydrated the carbonyl group, the lower the frequency.

The fourth absorption band is the PO_2^- antisymmetric stretching band, located at 1220-1240 cm^{-1}. Information about the hydration state of the polar head groups of the phospholipids can be monitored by the analysis of the frequency of this band (Korkmaz & Severcan, 2005; Lopez-Garcia et al., 1993; Severcan et al., 2005).

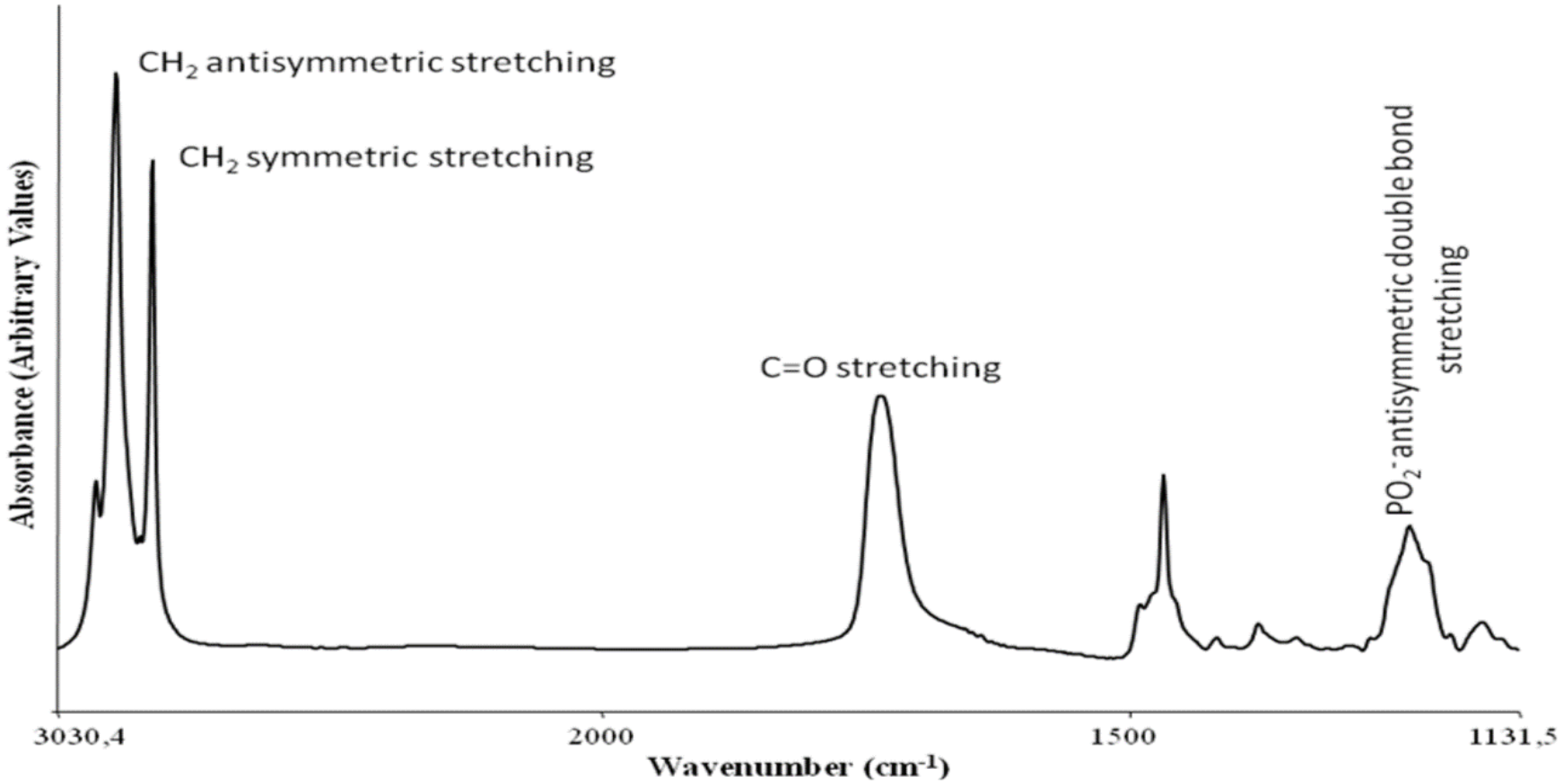

Figure 19. The main infrared bands of FT-IR spectrum of DSPC model membranes (Sade et al., 2010).

2.5.2. Spectral Analysis

The spectra were analyzed using Spectrum v5.0.1 software (Perkin-Elmer Inc., Norwalk, CT, USA). The O-H stretching bands due to water, appear in the regions of 3400-3200 cm^{-1} and 1800-1500 cm^{-1}, however, these regions overlap with the region of C-H and C=O stretching bands, respectively. Therefore, PBS buffer without drugs and lipids was scanned at different temperatures and it was subtracted from the spectra of liposomes at corresponding temperatures. The subtraction process was done manually by flattening the band located around 2125 cm^{-1}. Moreover, molecules in the air interfere with the spectra of samples. To prevent this interference, the spectrum of the air was recorded and subtracted automatically from the spectra of samples by the software program.

2.6. DSC experiments

The DSC experiments were carried out in a Universal TA DSC Q 100 (TA Instruments Inc., New Castle, Delaware, USA). The samples were encapsulated in hermetically sealed standard aluminum DSC pans. An empty pan was used as a reference to exclude the calorimetric effect of the pan. The samples were scanned over a temperature range of 20–75°C at a heating rate of 1°C/min, as reported previously (Severcan, Sahin, & Kazanci, 2005). Transition temperatures and changes in the transition enthalpies (ΔH_{cal}) were calculated by integrating the area under the peak, using the TA Universal Analysis v4.1D program (TA Instruments).

2.6.1. Thermogram Analyses

In the DSC thermograms of pure lipids, each lipid has its own transition temperature and enthalpy change. DSPC has a main phase transition temperature of ~55 °C and a transition enthalpy of 9.8 cal/g. The pretransition temperature of DSPC is ~51 °C (Mabrey & Sturtevant, 1976; T. P W McMullen & McElhaney, 1997; Tamai et al., 2008). On the DSC thermogram, the main phase transition of a lipid appears as a sharp peak and occurs within a very narrow temperature interval. Therefore, thermally induced phase transition occurs abruptly. Figure 20 shows the DSC thermogram of DSPC liposomes. The maximum point of the peak was taken as the main phase transition temperature of the lipid. The transition enthalpies were calculated by

integrating the area under the peak, using TA Universal Analysis v4.1D program (TA Instruments Inc., New Castle, DE, USA).

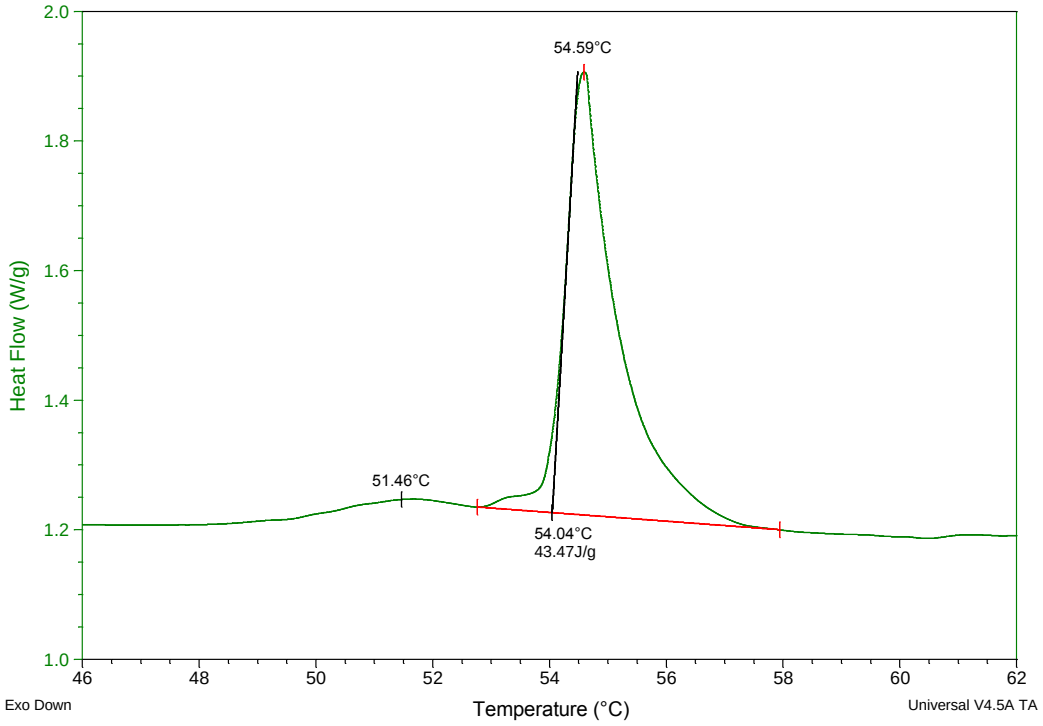

Figure 20. DSC thermogram of DSPC MLVs. The small peak shows pretransition, the sharp peak shows main phase transition. The peak maximums and transition enthalpy are indicated.

Enthalpy changes reflect the changes in the packing properties of the acyl chains. An increase in ΔH_{cal} is observed with increasing chain lengths of saturated phosphatidylcholines. Since the acyl chains of longer chain PCs are more tightly packed, they resist trans to gauche isomerization and thus more heat will be required to melt these PCs (McElhaney, 1982). The decreases in the enthalpy are also attributed to the presence of a perturbing agent within the cooperativity region (C1- C8) of membranes (Zhao et al., 2007).

2.7. Turbidity

Turbidity studies were carried out by using a Varian- Cary 300 UV/Visible spectrophotometer (Varian Inc., Melbourne, Australia), as reported before (Severcan

et al., 2000). Clear plastic cuvettes (LP Italiana, Milan, Italy) of 1 cm in path length were used. Reference cuvettes were filled with PBS buffer to automatically account for background absorbance of the buffer. Turbidity measurements were performed at 440 nm to minimize any light-scattering effect (Severcan et al., 2000). Absorbance values were recorded as a function of temperature between 35 °C and 70 °C.

2.8. Encapsulation efficiency

To ensure the presence of the drug in our model membrane preparations, an encapsulation method developed initially for CLX was adapted for this study (Deniz et al., 2010). MLVs were prepared as described above and dried completely under vacuum using a HETO spin vac system and redissolved in methanol for RFX and ethanol for VLX-containing liposomes. These solvents were chosen because of the optimal solubility of the drugs. After vortexing, the absorbance was measured in a scanning UV–visible spectrophotometer (Hitachi U-2800A) at 282 nm for RFX and 203 nm for VLX, corresponding to the wavelength of maximum absorption (λ_{max}) of the drugs. These λ_{max} values were obtained by scanning the absorbance of both drugs between 200 and 900 nm in their respective solvents. The calibration curves (Appendix A) were constructed for RFX in methanol and VLX in ethanol and were used to quantify RFX and VLX in the liposomal preparations by Beer-Lambert's law and then to calculate the percentage EE. The following formula was used (Deniz et al., 2010):

$$EE\ (\%) = \frac{mg\ of\ drug\ in\ MLVs}{mg\ of\ drug\ initially\ added} \times 100$$

2.9. Size measurement

To confirm the preparation of MLVs the size analysis was necessary, and the same dynamic light scattering method was used as with the CLX study (Deniz et al., 2010). The particle size distributions and the Polydispersity Index (PdI) of MLVs were determined by Zeta sizer (Malvern Mastersizer 2000; Malvern Instruments, METU Central Laboratory).

2.10. Statistical analyses

Statistical analyses of the data were performed using Graphpad Prism v5 software (GraphPad Software, Inc., La Jolla, California, USA), which was also used to draw diagrams and bar charts. After performing Normality Test, non-parametrical analysis was chosen for all of the data. Specific analysis for each experiment is indicated in the Figure legends. Unless otherwise mentioned, the mean of at least six experiments was plotted together with the standard error of the mean. Statistical significance was assessed by using a two-tailed P-value calculated with the Mann – Whitney nonparametric test. Significant difference was statistically considered at the level of $P \leq 0.05$.

CHAPTER 3

RESULTS

In this study, the lipid-phase behavior in response to increasing concentrations of RFX and VLX was monitored with DSC (Korkmaz & Severcan, 2005; Severcan et al., 2005). FT-IR spectroscopy was then used to determine the changes in membrane structure and dynamics by analyzing the frequency and bandwidth of different vibrational modes, which represent the acyl chains, head group, and interfacial region of lipid molecules (Biruss, Dietl, & Valenta, 2007; Casal & Mantsch, 1984; Severcan et al., 2005). Additionally, MLV characterization data such as EE and size analysis provided good insights on the quality of our experiments.

3.1. Characterization of RFX and VLX loaded MLVs

3.1.1. Size Analysis

The particle size distribution was analyzed by laser diffraction principle and hydrodynamic diameter of the particles in solution was calculated utilizing Mie theory by the Malvern Mastersizer2000 software. The representative images of size distribution of MLV particles in PBS solution are given in Figure 21.

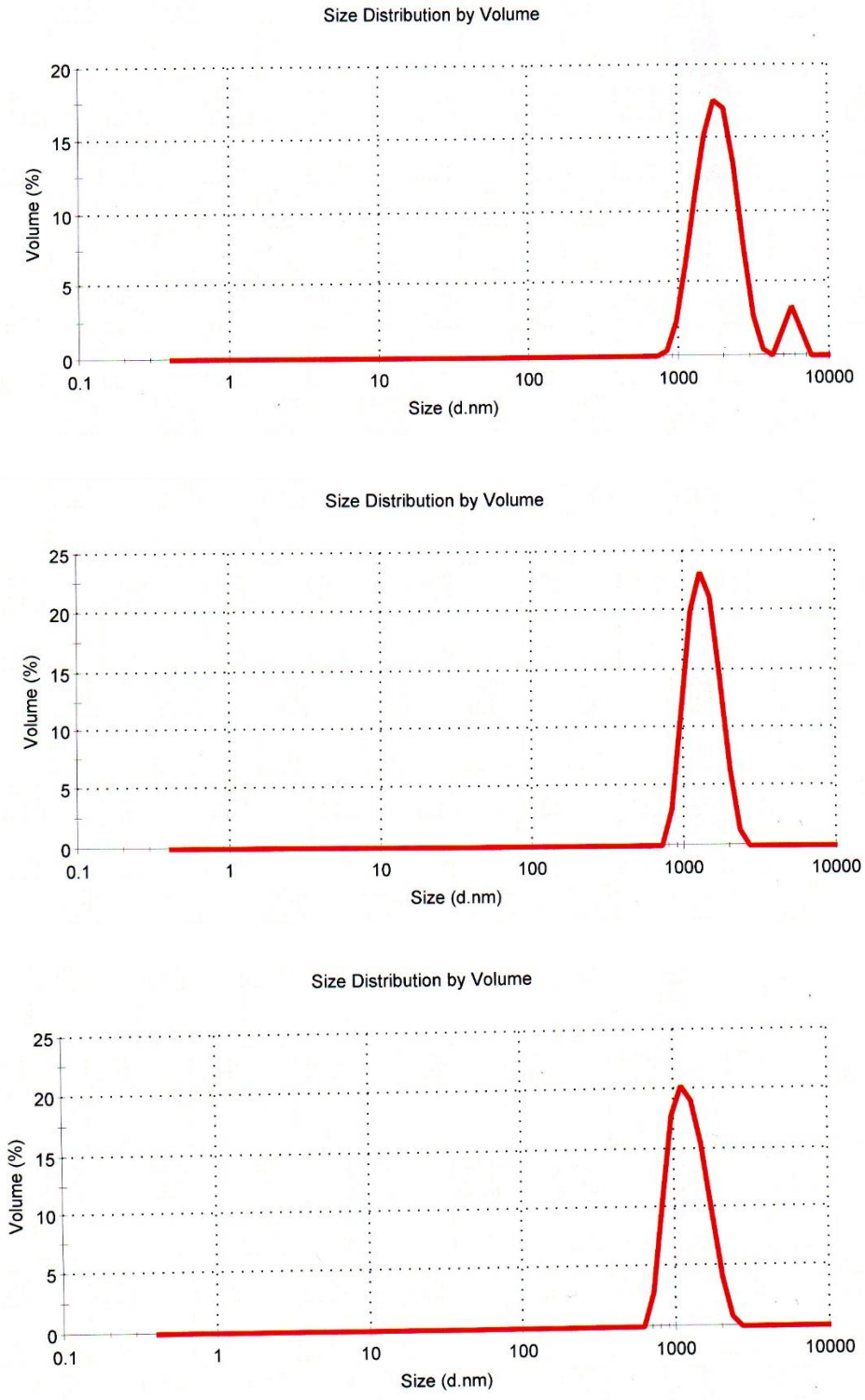

Figure 21. Representative particle size distribution analysis results for (A) DSPC only, (B) RFX MLVs, (C) VLX MLVs.

The average hydrodynamic diameter (Zavg) corresponds to the diameter of a spherical particle with same translational diffusion coefficient as the particle being analyzed; therefore it is not a direct measurement of the actual particle size. Average size derived from this parameter was found close to 1000 nm for the particles confirming them as MLVs. Polydispersion index (PdI) represents the size range the most particles fall into, and smaller PdI represents less size distribution. Zavg, PdI and the main peak nm value for MLVs with RFX, VLX and no drug are given in Table 1.

Table 1. Particle size of liposomes in absence and presence of RFX and VLX.

Liposome formulation	**Z_{avg} (nm)**	**PdI**	**Diameter peak (nm)**
DSPC only	2074	0.231	1823
DSPC + 18 mol % RFX	1666	0.308	1359
DSPC + 18 mol % VLX	1826	0.369	1235

It can be seen that the addition of drugs slightly decreases average particle size, but also increases dispersion index. This might indicate that MLVs aggregate less when drugs are added.

3.1.2. Encapsulation Efficiency

Calibration curves of RFX and VLX used for calculations are shown in Appendix A.

Average EE of MLVs is shown in Table 2. All MLV formulations successfully encapsulated more than 90 % of the drugs. Slight overestimation of encapsulation was observed due to high rates of evaporation of ethanol and methanol during the experimental procedure, which lead to some values being more than 100 %.

Table 2. Average drug Encapsulation Efficiency of MLV formulations containing RFX and VLX drugs.

Drug concentration (mol %)	Average EE (%)
RFX (18%)	93.16 ± 5.87
RFX (9%)	107 ± 5.30
RFX (6%)	103.4 ± 2.94
RFX (3%)	100.2 ± 3.64
VLX (18%)	97.93 ± 6.95
VLX (9%)	93.07 ± 7.71
VLX (6%)	95.91 ± 4.01
VLX (3%)	104.7 ± 6.36

3.2. DSC analysis of VLX and RFX containing DSPC model membranes

Figures 22 and 23 show thermograms of DSPC MLVs obtained using DSC. The thermogram for pure DSPC liposomes shows two endothermic peaks corresponding to the pre- and main phase transitions. Peaks representing main transition from gel to liquid crystalline phase were used to determine the Tm. MLVs containing RFX drug showed no significant change in Tm or lipid phase transition profile when the drug concentration was increased (Figure 22). Additionally, the small pretransition peak and the transition itself were unaffected by RFX. However, the changes observed in the VLX containing MLVs were highly reminiscent of the changes observed in CLX containing MLVs as reported by Sade et al. (2010). The Tm value was seen to be decreasing with increasing VLX concentration as shown in Figure 23. The pretransition peak appeared to be eliminated by the presence of VLX. The bar diagrams shown in Figure 24 show that the Tm change was significant in VLX containing vesicles, but not with RFX. Additionally, Tables 3 and 4 show the main phase-transition temperatures (Tm), and transition enthalpy changes for different

concentrations of drugs. Transition enthalpy (ΔH_{cal}) reflects the acyl chain-packing properties (McElhaney, 1982) and thus is a parameter of membrane stability. It can be seen from the tables that both drugs have varying effects on acyl chain packing depending on the concentration, however, transition enthalpy values are still found close to the pure DSPC value reported in the literature, which is 9.8 cal/g (Lewis & McElhaney, 2011).

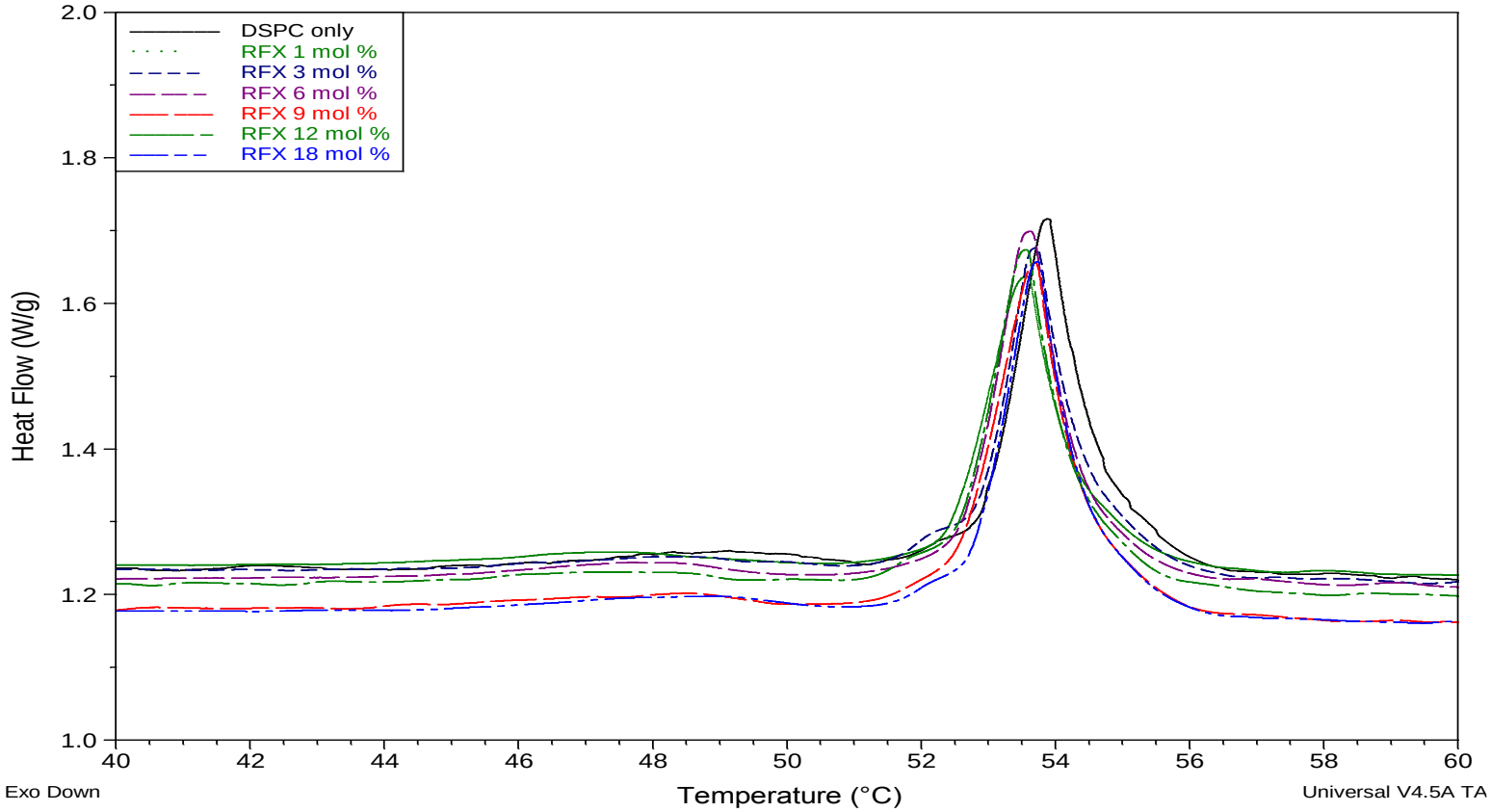

Figure 22. DSC thermogram of DSPC MLVs in the absence and presence of different concentrations of RFX.

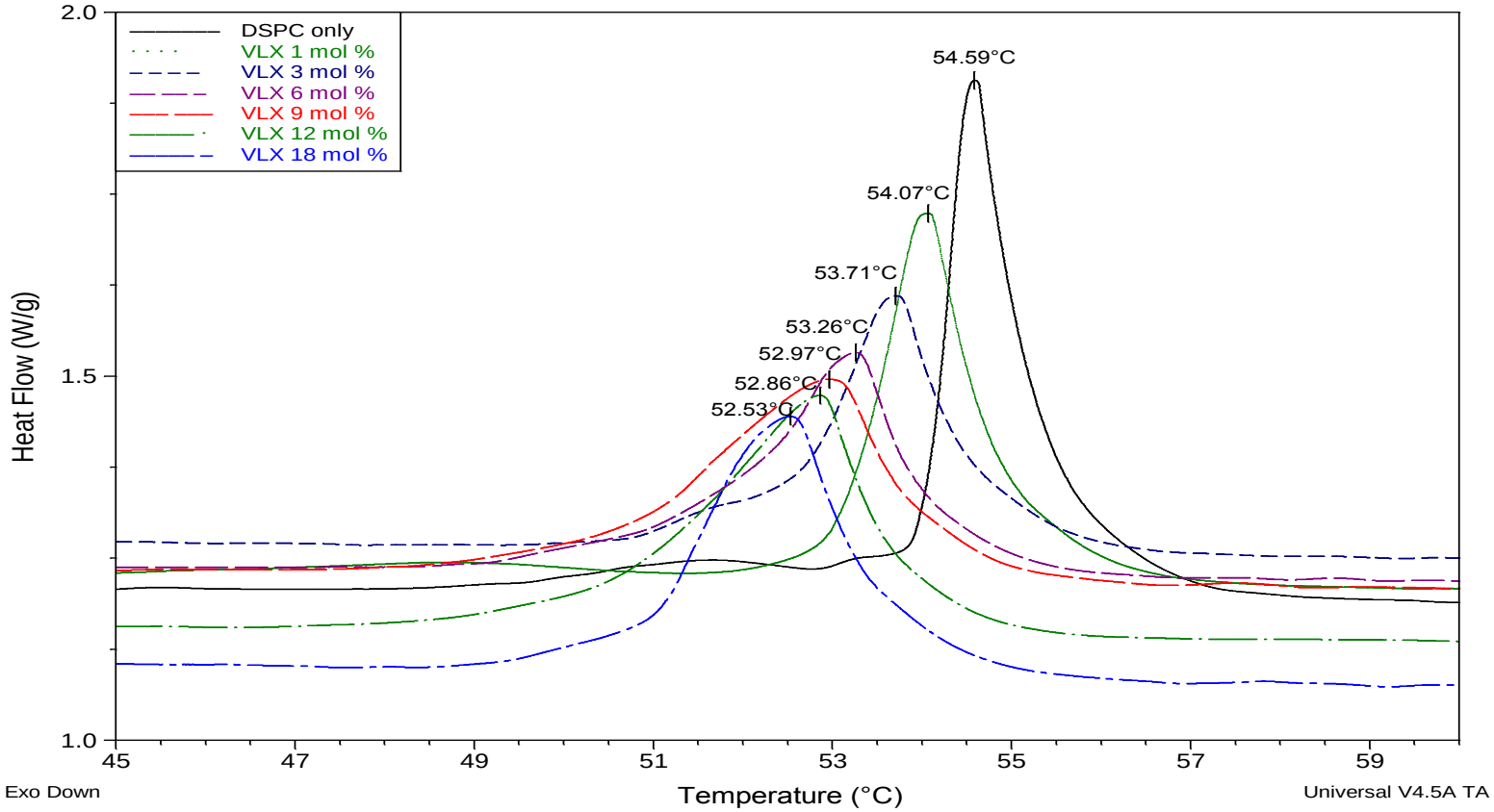

Figure 23. DSC thermogram of DSPC MLVs in the absence and presence of different concentrations of VLX.

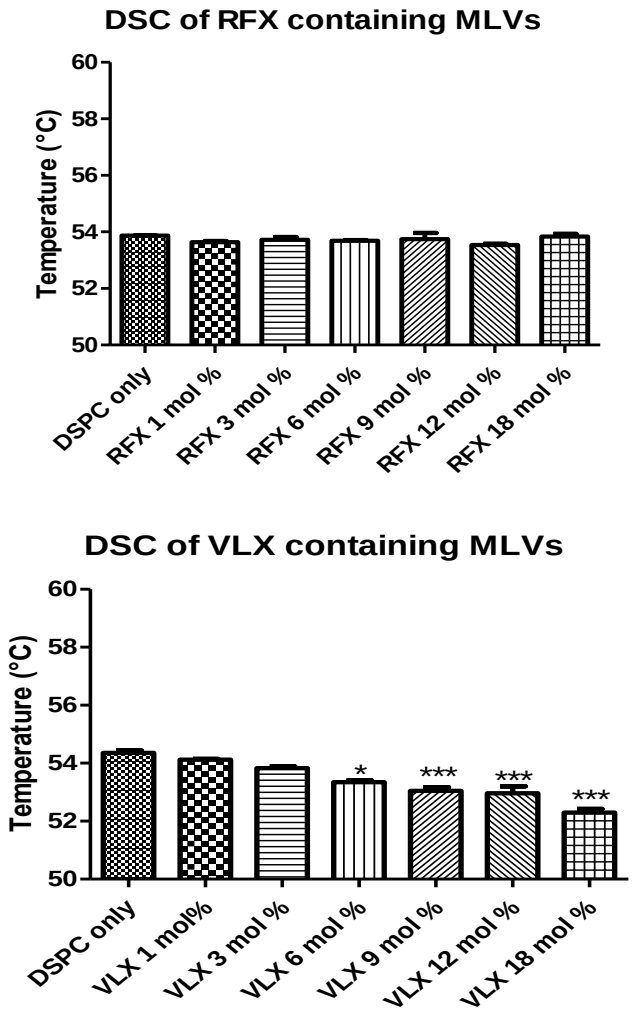

Figure 24. Bar diagrams derived from calorimetric thermograms. Each bar represents the mean ± SEM (n = 6). *P < 0.05, **P < 0.01, ***P < 0.001, compared to controls (DSPC only).

Table 3. The main phase transition temperature (Tm), and transition enthalpy (ΔH_{cal}) changes of DSPC MLVs for different concentrations of RFX (ΔH_{cal} from literature is found to be 9.8 cal/g for pure DSPC).

Drug Concentration (mol %)	**Tm (°C)**	**ΔH_{cal} (cal/g)**	**ΔH_{cal} (J/g)**
0 RFX	53.87	9.24	38.68
1 RFX	53.64	7.79	32.58
3 RFX	53.72	8.49	35.51
6 RFX	53.69	9.46	39.57
9 RFX	53.75	9.75	40.81
12 RFX	53.54	9.86	41.24
18 RFX	53.84	9.82	41.1

Table 4. The main phase transition temperature (Tm), and transition enthalpy (ΔH_{cal}) changes of DSPC MLVs for different concentrations of VLX (ΔH_{cal} from literature is found to be 9.8 cal/g for pure DSPC).

Drug Concentration (mol %)	**Tm (°C)**	**ΔH_{cal} (cal/g)**	**ΔH_{cal} (J/g)**
0 VLX	54.36	9.58	40.08
1 VLX	54.12	9.66	40.42
3 VLX	53.83	9.46	39.58
6 VLX	53.34	8.50	35.56
9 VLX	53.04	10.48	43.85
12 VLX	52.96	10.84	45.36
18 VLX	52.3	10.98	45.94

3.3. FT-IR analysis of VLX and RFX containing DSPC model membranes

3.3.1. Overview and the Representative Spectra

The effect of the drugs on the phase-transition behavior of DSPC liposomes was analyzed from the FT-IR spectra by monitoring the frequency variations of the C-H stretching bands. The representative spectra at 40°C for pure and RFX-containing liposomes are shown in Figure 25. Similar spectra were obtained for VLX containing liposomes are shown in Figure 26. These are buffer subtracted spectra which were used for analyses and relationships between band frequency and bandwidth of the selected peaks.

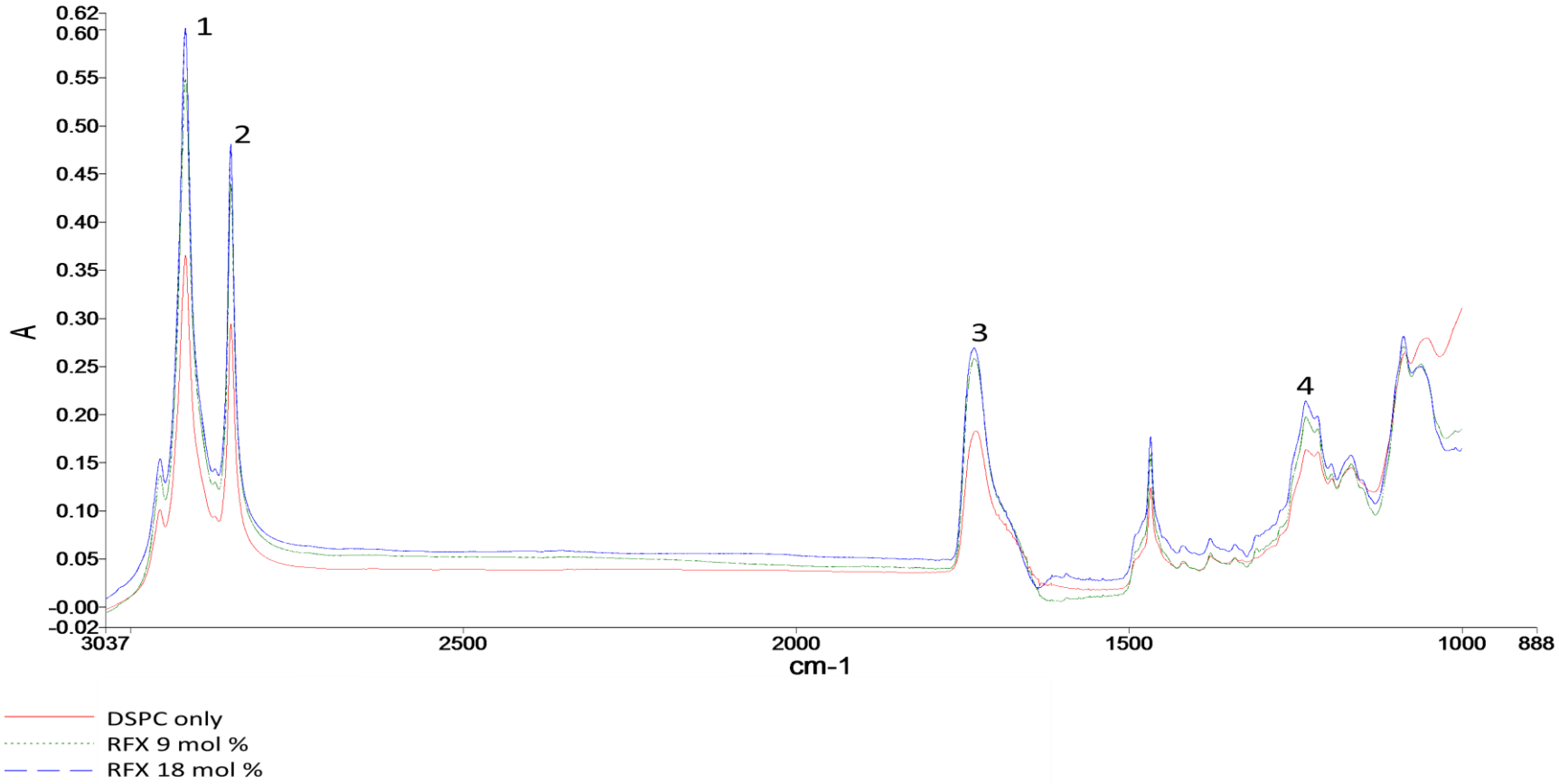

Figure 25. Representative spectra of DSPC MLVs with variable RFX concentrations at 40 °C. Labelled peaks are (numerical order): CH_2 antisymmetric stretching, CH_2 symmetric stretching, C=O stretching, PO_2^- antisymmetric stretching.

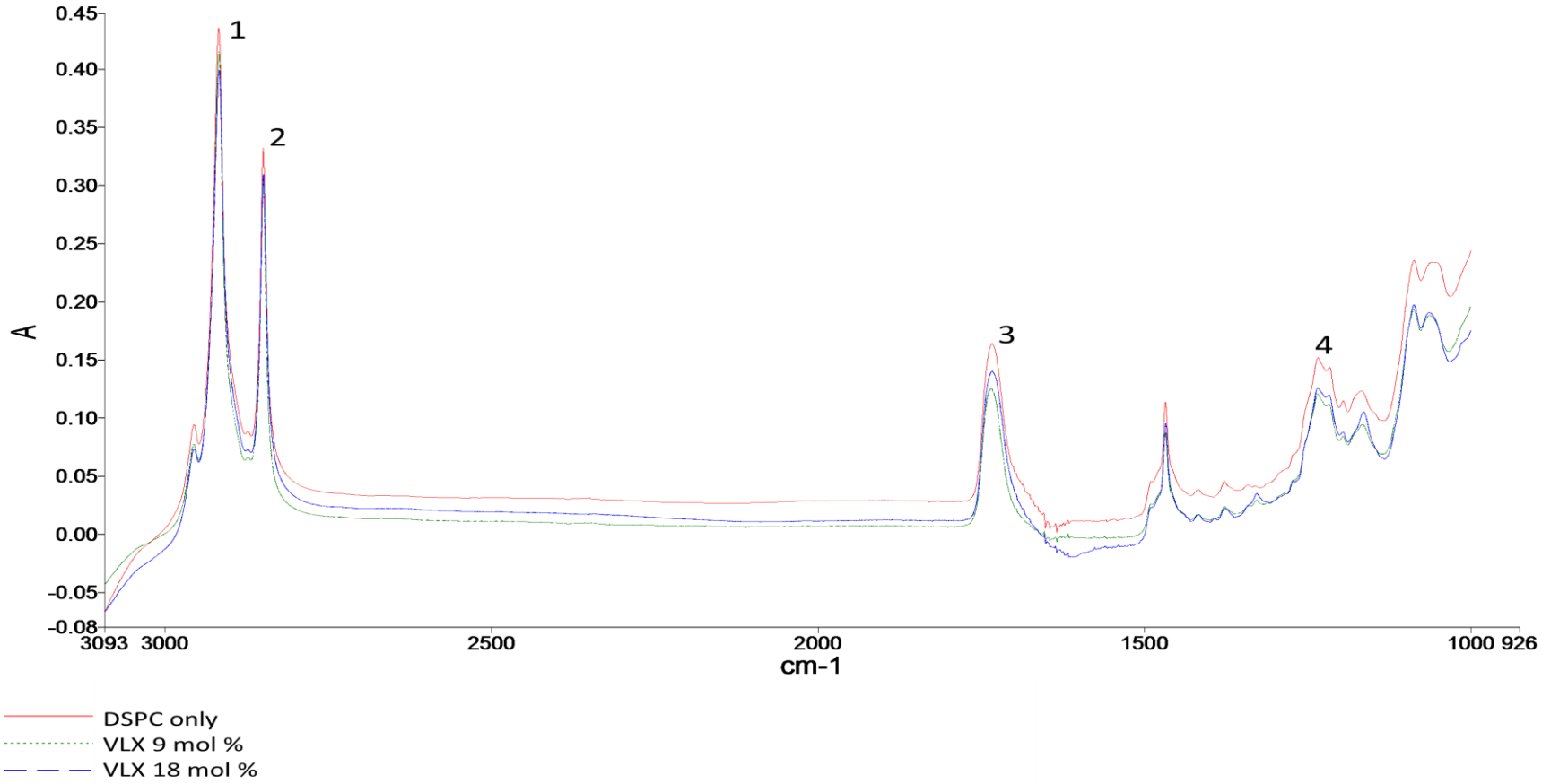

Figure 26. Representative spectra of DSPC MLVs with variable VLX concentrations at 40 °C. Labelled peaks are (numerical order): CH_2 antisymmetric stretching, CH_2 symmetric stretching, C=O stretching, PO_2^- antisymmetric stretching.

3.3.2. Effects of VLX and RFX on the CH_2 Region

In Figures 25 and 26, the bands at 2,920 and 2,850 cm^{-1} of the infrared spectrum (numbered 1 and 2) correspond to the CH_2 antisymmetric and CH_2 symmetric stretching modes of the acyl chains of the phospholipid membranes, respectively. Figures 27 and 28 display the frequency variation of the CH_2 antisymmetric stretching bands of DSPC liposomes in the absence and presence of RFX and VLX respectively as a function of temperature. As can be seen in Figures 27 and 28 the phase-transition behavior is altered with increasing concentrations of VLX, but not by RFX. The frequency increase at around 55°C represents the increase in acyl chain flexibility. This happens when the transition from gel to liquid crystalline phase occurs and monitors the well-known main cooperative endothermic phase transition of DSPC liposomes and has been associated with the change from all-trans to gauche conformers (Casal & Mantsch, 1984). These data confirm the DSC results showing a decrease in Tm with increasing VLX concentration. In addition to the Tm shift, higher concentrations of VLX also produce a broadening of the phase transition profile, though to a less extent than that produced by CLX as reported before (Sade et al., 2010). A similar effect was not seen with RFX. Acyl chain flexibility information derived from Figures 27 and 28 also give an indication of the order-disorder state of the membrane (Korkmaz & Severcan, 2005; Severcan et al., 2005). The frequency of the CH_2 stretching bands of acyl chains depend on the average trans/gauche isomerization in the system, and shifts to higher wave numbers correspond to an increase in the number of gauche conformers, which implies a more disordered state (Severcan, 1997). As seen from Figure 27, RFX has slight concentration-dependent effect on both gel and liquid crystalline phases. It shifts the frequency to lower values in both phases, but the extent of the shift does not vary depending on the concentration as much as it does with CLX (Sade et al., 2010). Curiously, in case of VLX, such effect is less apparent as seen in Figure 28.

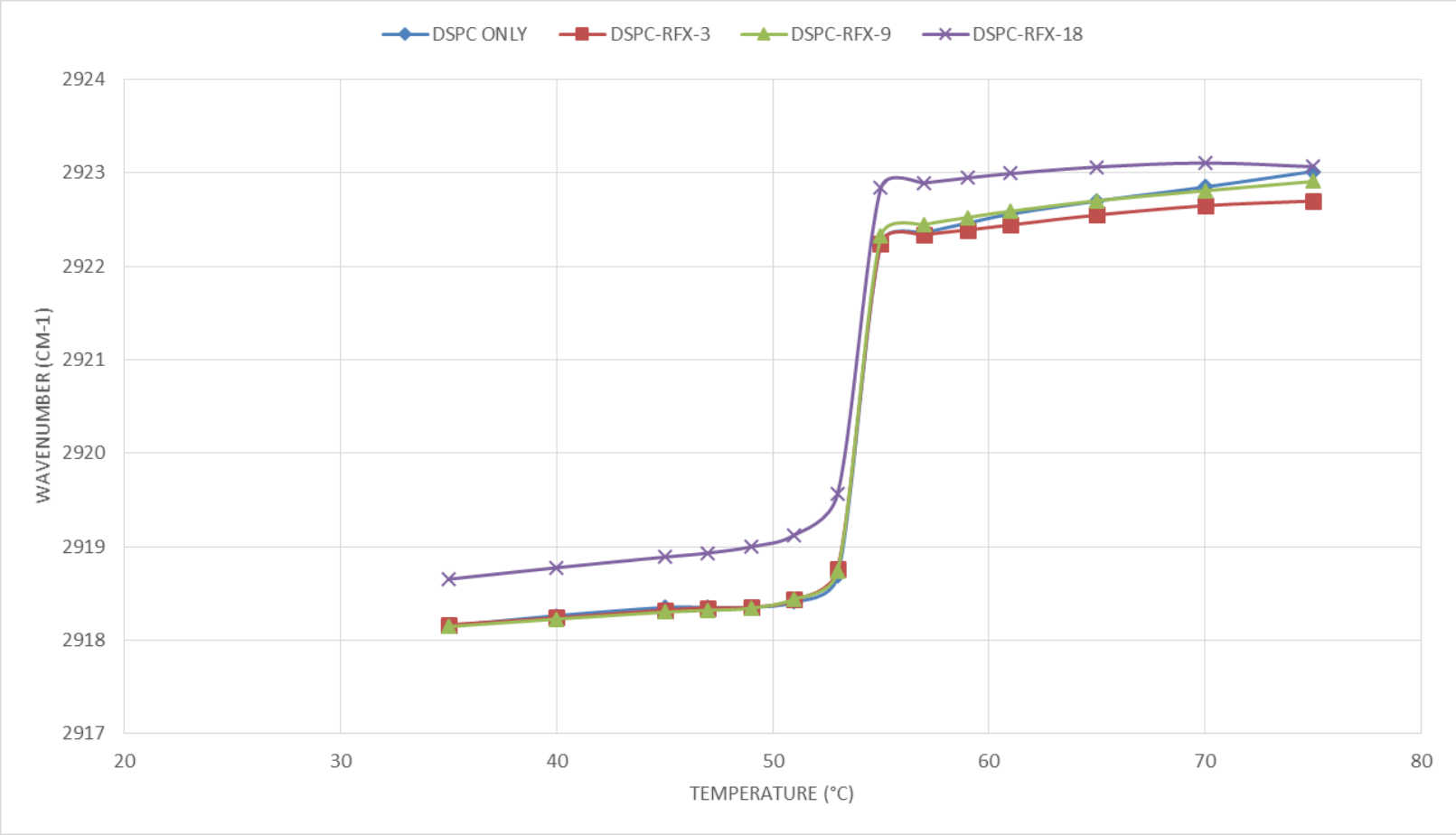

Figure 27. Variation in the frequency of the CH_2 antisymmetric stretching modes of DSPC MLVs as a function of temperature at varying concentrations of RFX (representative of three experiments).

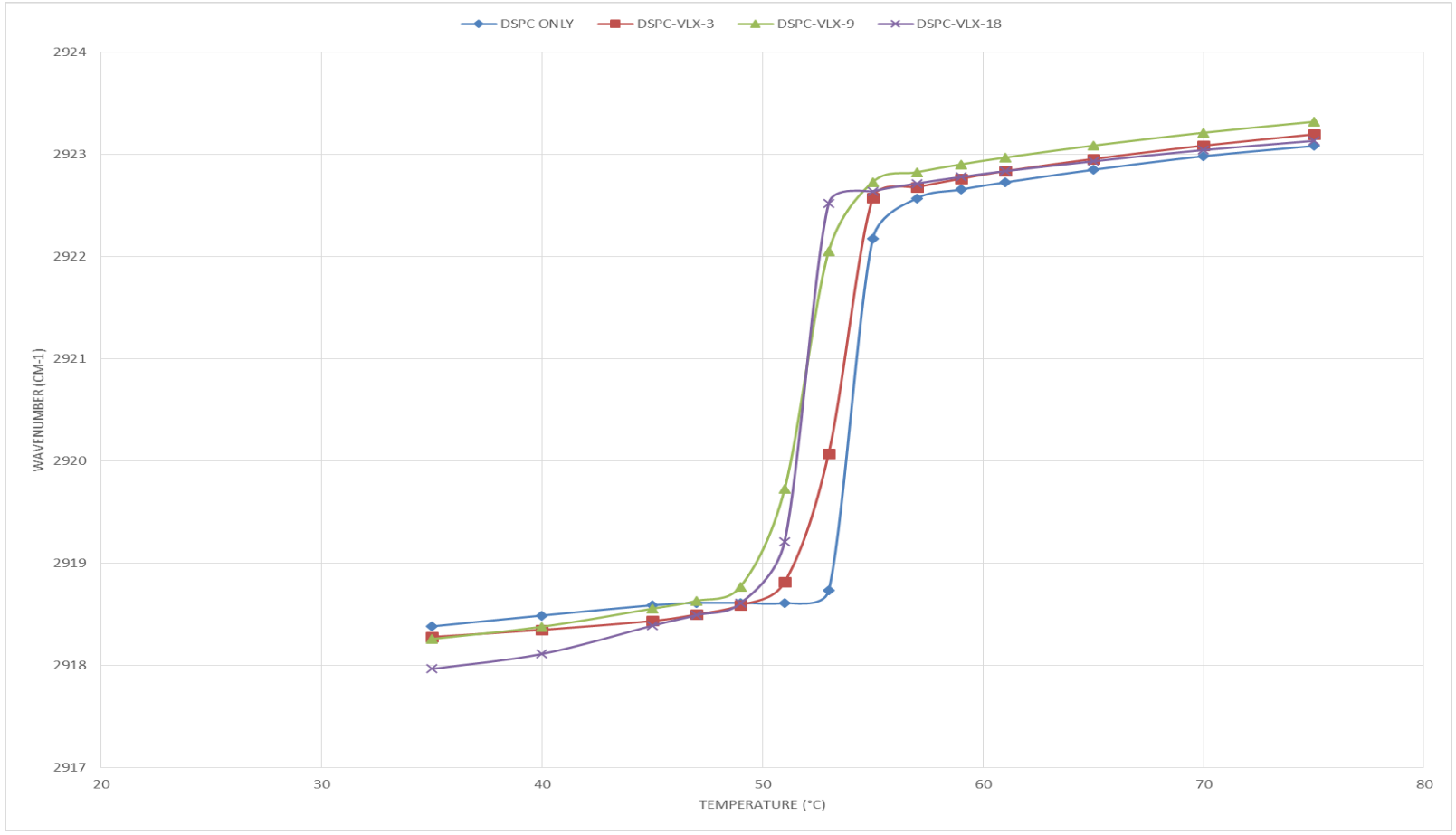

Figure 28. Variation in the frequency of the CH_2 antisymmetric stretching modes of DSPC MLVs as a function of temperature at varying concentrations of VLX (representative of three experiments).

To see the significance of the effects of the drugs on membrane order, we performed statistical analysis of the recorded spectra at two different temperatures (45 and 65 °C) corresponding to the gel and liquid crystalline phase of the DSPC membrane. The dual effect is observed here, where RFX decreases frequency in low concentrations and increases them in higher ones, as it was observed with CLX (Sade et al., 2010). The extent of this dual effect is considerably lower though, and statistical significance was not obtained for all of the data points (Figure 29). The incorporation of 3 and 9 mol% RFX into the phospholipid system slightly shifts the frequency to lower values at 45° C, which indicates an increase in the number of trans conformers in the gel phase. This effect was more significantly observed at the 65°C at 3 mol% RFX concentration. This implies a conformational ordering of the acyl chains (Severcan, 1997). In contrast, at the higher concentration of 18 mol % of RFX, a statistically significant increase in frequency at both in the gel and liquid crystalline phases can be observed. This reflects a disordering effect of RFX on DSPC MLVs as a result of an increase in the number of gauche conformers. Overall, RFX showed similar effect to CLX, though the extent of the effect appears to be lower. Curiously, VLX showed very different behavior, which showed variations depending on the phase. Figure 30 shows that VLX results in a concentration dependent significant lowering of the frequency only in the gel phase, thereby providing a stabilizing effect. In the liquid crystalline phase, however, the effect is just the opposite, showing a concentration dependent increase in frequency, with a maximum destabilizing effect at 9 mol %. The CH_2 symmetric stretching band frequencies showed similar effects with both drugs (data not shown).

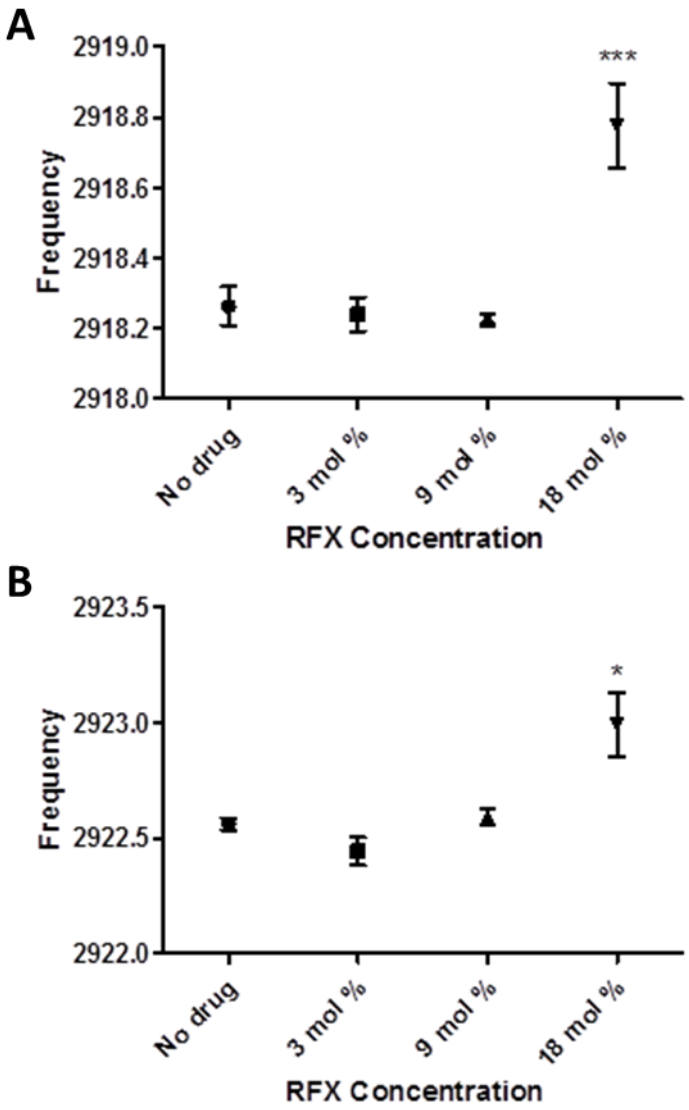

Figure 29. Variation in the frequency of the CH_2 antisymmetric stretching modes of DSPC MLVs as a function of RFX concentration at 45 (A) and 65 (B) °C. Each point represents the mean ± SEM (n = 6). *P < 0.05, **P < 0.01, ***P < 0.001, compared to controls (no drug, DSPC only).

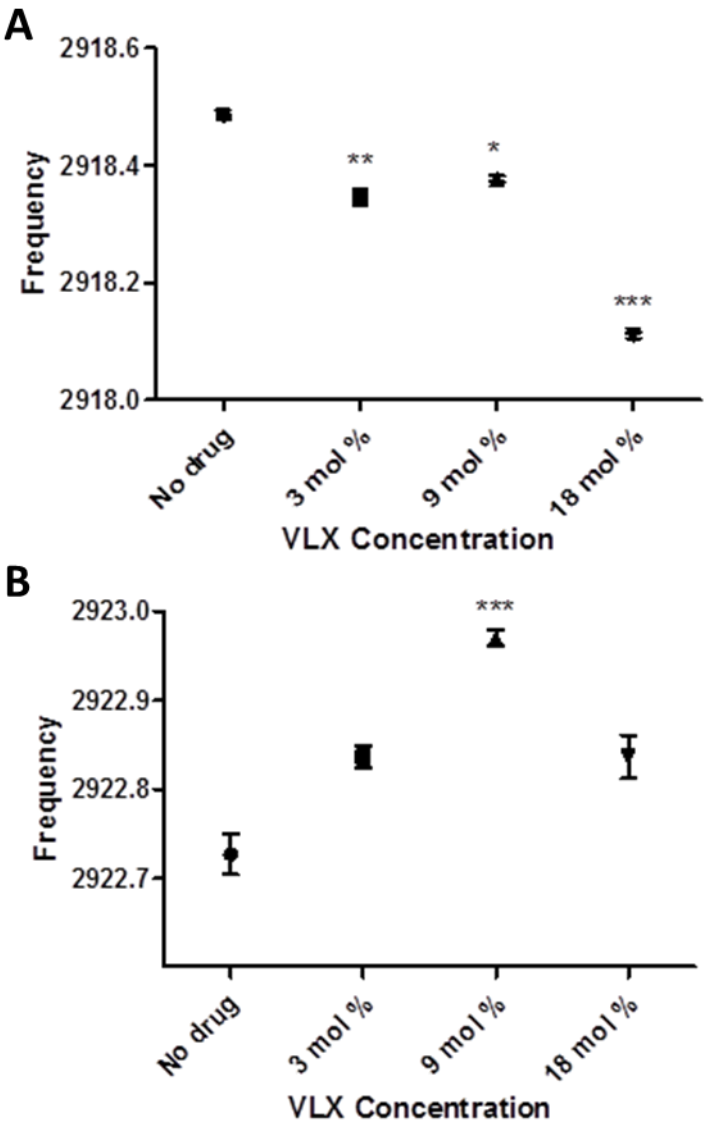

Figure 30. Variation in the frequency of the CH_2 antisymmetric stretching modes of DSPC MLVs as a function of VLX concentration at 45 (A) and 65 (B) °C. Each point represents the mean ± SEM (n = 6). *P < 0.05, **P < 0.01, ***P < 0.001, compared to controls (no drug, DSPC only).

Information about the dynamics of membrane systems can be obtained by analyzing the variations in the bandwidth of the CH_2 stretching modes, since bandwidth reflects the changes in the mobility of the acyl chains. An increase in the bandwidth is an indication of an increase in the dynamics of the membrane system (Casal, Cameron, Smith, & Mantsch, 1980; Korkmaz & Severcan, 2005; Lopez-Garcia, Micol, Villalain, & Gomez-Fernandez, 1993; Severcan, Kazanci, & Zorlu, 2000; Severcan et al., 2005). Figures 31 and 32 display the temperature dependence of the bandwidth of the CH_2 antisymmetric stretching mode of DSPC MLVs with varying concentrations of RFX and VLX respectively. It is evident that the bandwidth does not deviate significantly with the addition of RFX both in the gel and liquid crystalline phase (Figure 33). Whilst, VLX shows a significant decrease in membrane dynamics at low concentrations (just like CLX) but at 18 mol % the membrane dynamics increase (Figure 34). The bandwidth analysis of the CH_2 symmetric stretching band also showed similar results (data not shown).

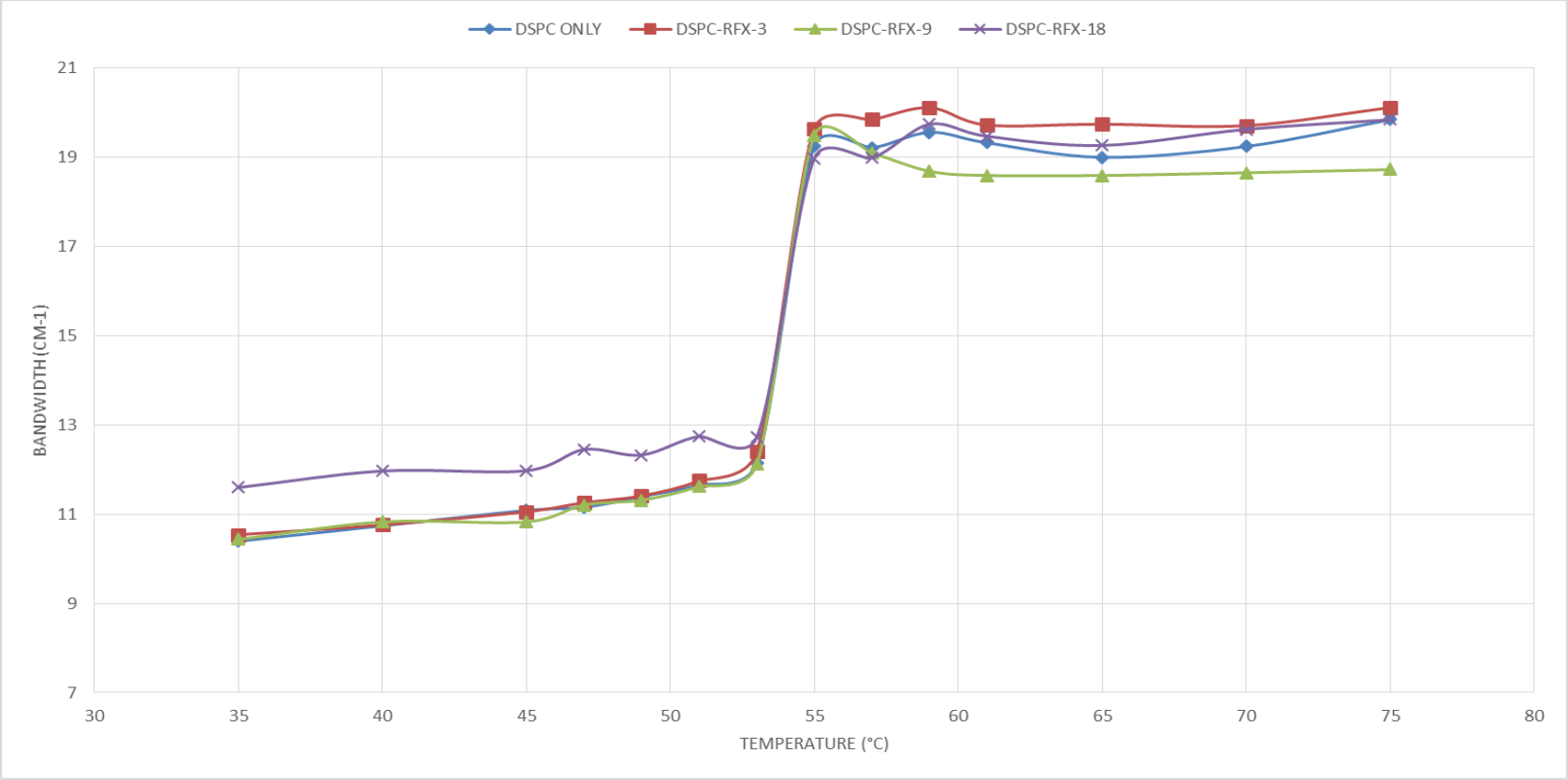

Figure 31. Variation in the bandwidth of the CH_2 antisymmetric stretching modes of DSPC MLVs as a function of temperature at varying concentrations of RFX (representative of three experiments).

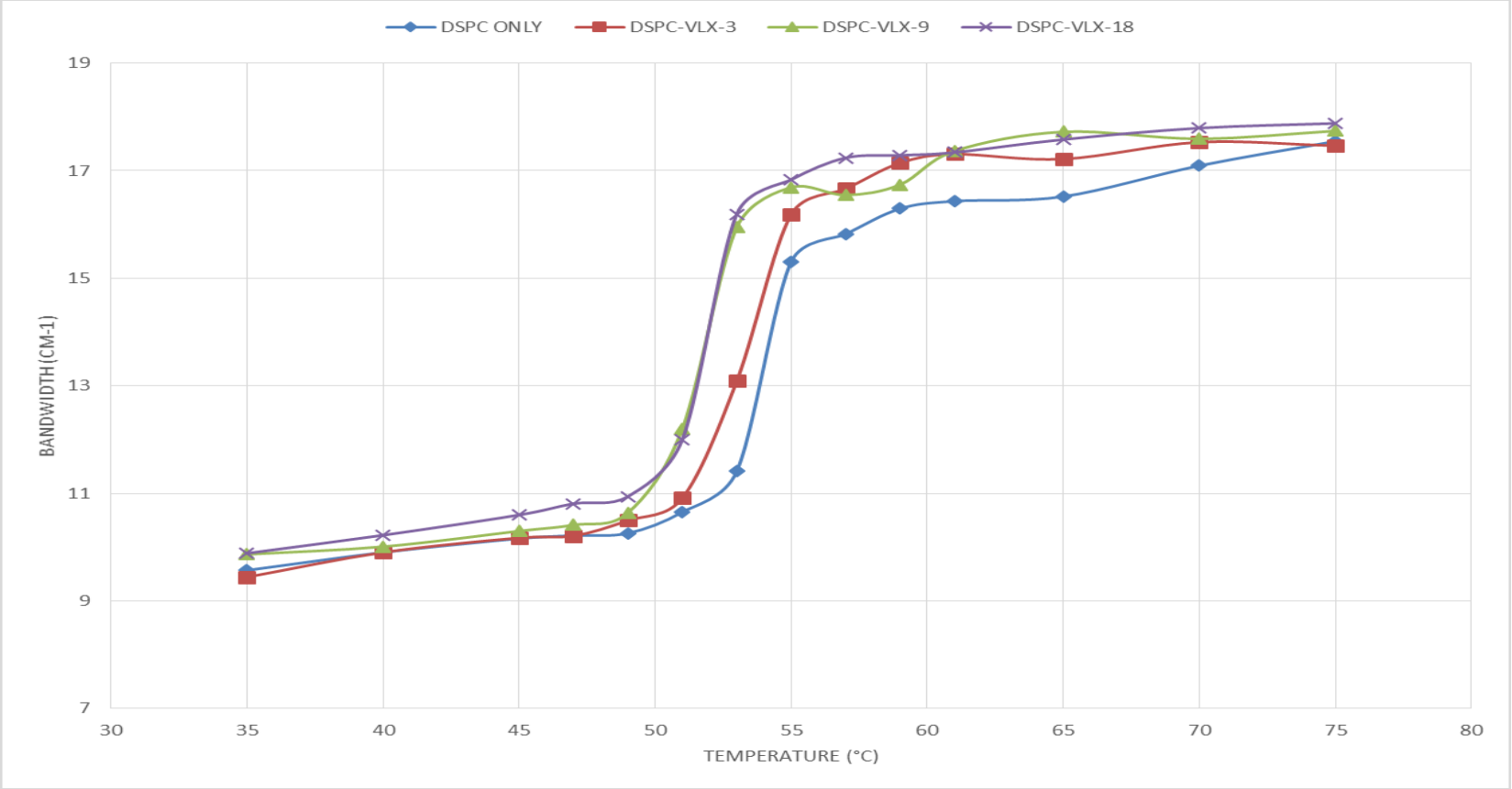

Figure 32. Variation in the bandwidth of the CH_2 antisymmetric stretching modes of DSPC MLVs as a function of temperature at varying concentrations of VLX (representative of three experiments).

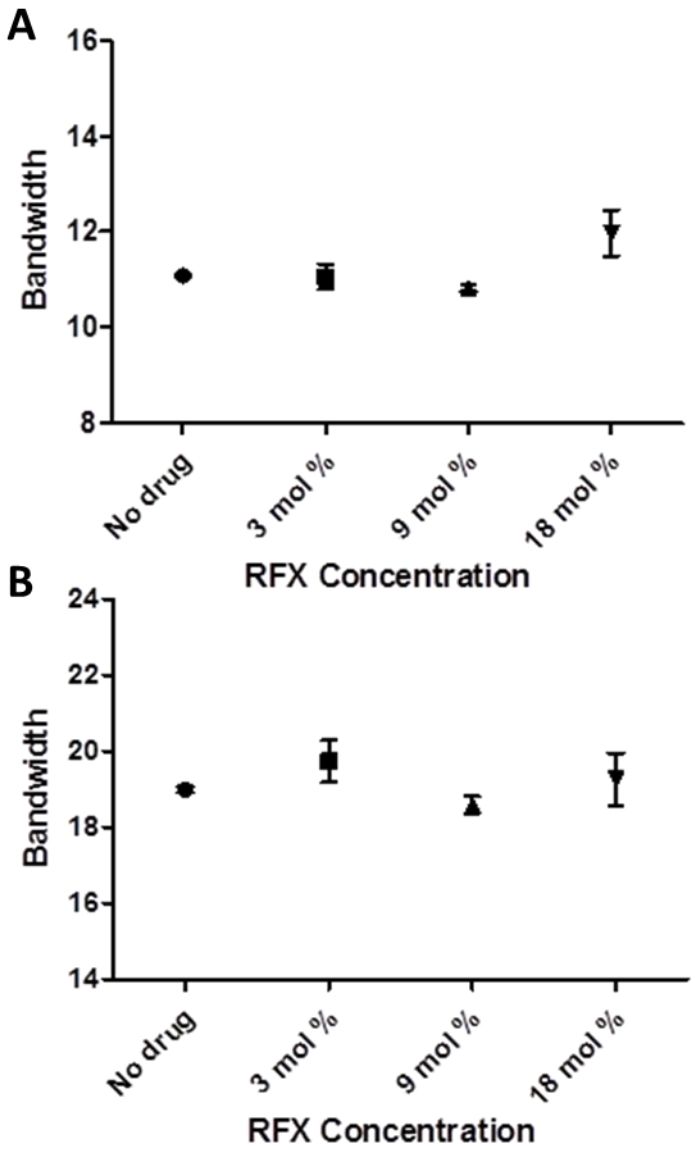

Figure 33. Variation in the bandwidth of the CH_2 antisymmetric stretching modes of DSPC MLVs as a function of RFX concentration at 45 (A) and 65 (B) °C. Each point represents the mean ± SEM (n = 6). *P < 0.05, **P < 0.01, ***P < 0.001, compared to controls (no drug, DSPC only).

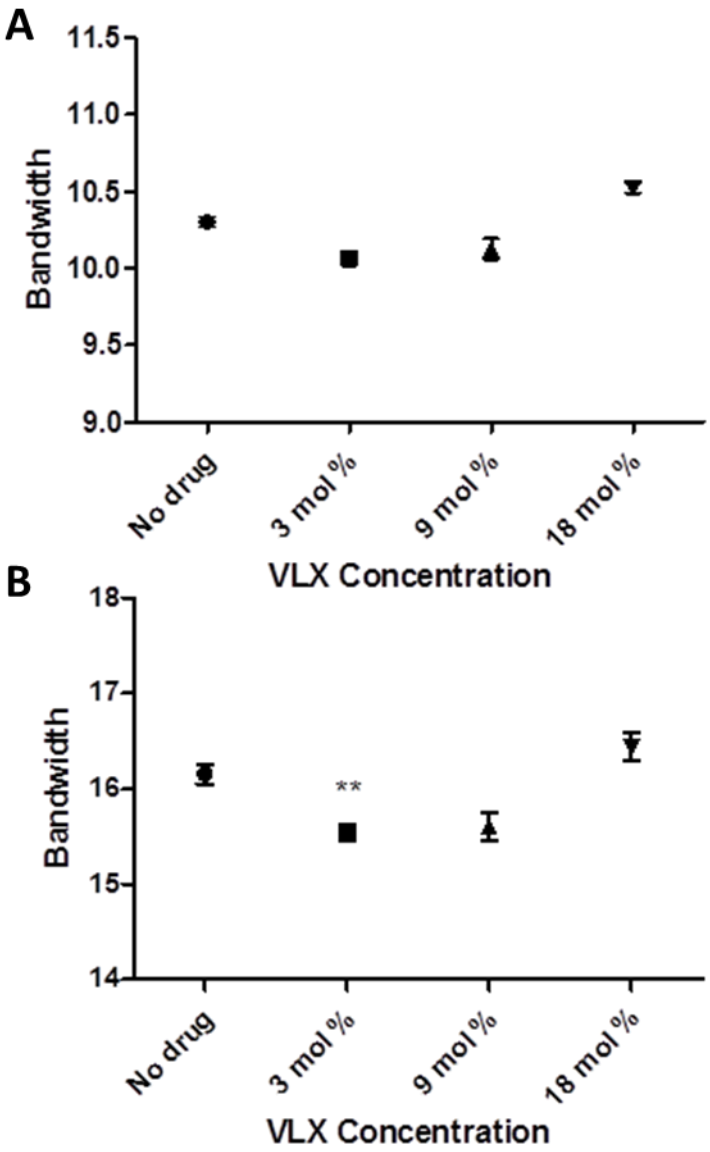

Figure 34. Variation in the bandwidth of the CH_2 antisymmetric stretching modes of DSPC MLVs as a function of VLX concentration at 45 (A) and 65 (B) °C. Each point represents the mean ± SEM (n = 6). *P < 0.05, **P < 0.01, ***P < 0.001, compared to controls (no drug, DSPC only).

3.3.3. Effects of VLX and RFX on the C=O region

To obtain information regarding the effects of VLX and RFX on the polar head groups of the membrane, the C=O stretching band of FT-IR spectra was monitored. The carbonyl absorption band at 1,735 cm^{-1} represents the stretching vibrations of ester carbonyl groups of phospholipids, which in turn varies with the level of hydration at the membrane interface and thus is affected by hydrogen bonding (Korkmaz & Severcan, 2005; Severcan et al., 2005). Therefore, any change seen in the spectra of this region can be attributed to an interaction between the drugs and the polar/apolar interfacial region of the membrane. The frequency variations in the C=O stretching band of DSPC MLVs as a function of temperature are given in Figures 35 and 36 for RFX and VLX respectively. It is clear that the addition of RFX greatly increases the C=O stretching frequency in both gel and liquid crystalline phases, with the effect being more significant at the higher RFX concentrations (Figure 37). This indicates that RFX decreases hydrogen bonding around this functional group and has a destabilizing effect, which is phase-independent. In the gel phase, at lower concentrations the addition of VLX results in an increase in the frequency, which indicates that VLX decreases hydrogen bonding around this functional group. However, at the higher concentration (18 mol %) there is a sharp decrease in frequency, indicating a sudden increase in H-bonding (Figure 38). This dual effect of VLX, when low and high concentrations of the drug produce different effects on the membrane is also seen in the liquid crystalline phase. While low concentrations of VLX increase the frequency, at a high concentration (18 mol %), VLX causes a significant decrease in the frequency of the C=O stretching mode. This implies that there is an increase in the hydrogen bonding and stabilizing effect of VLX but only at high concentration, unlike CLX, which had stabilizing effect with all concentrations, but only in liquid crystalline phase (Sade et al, 2010).

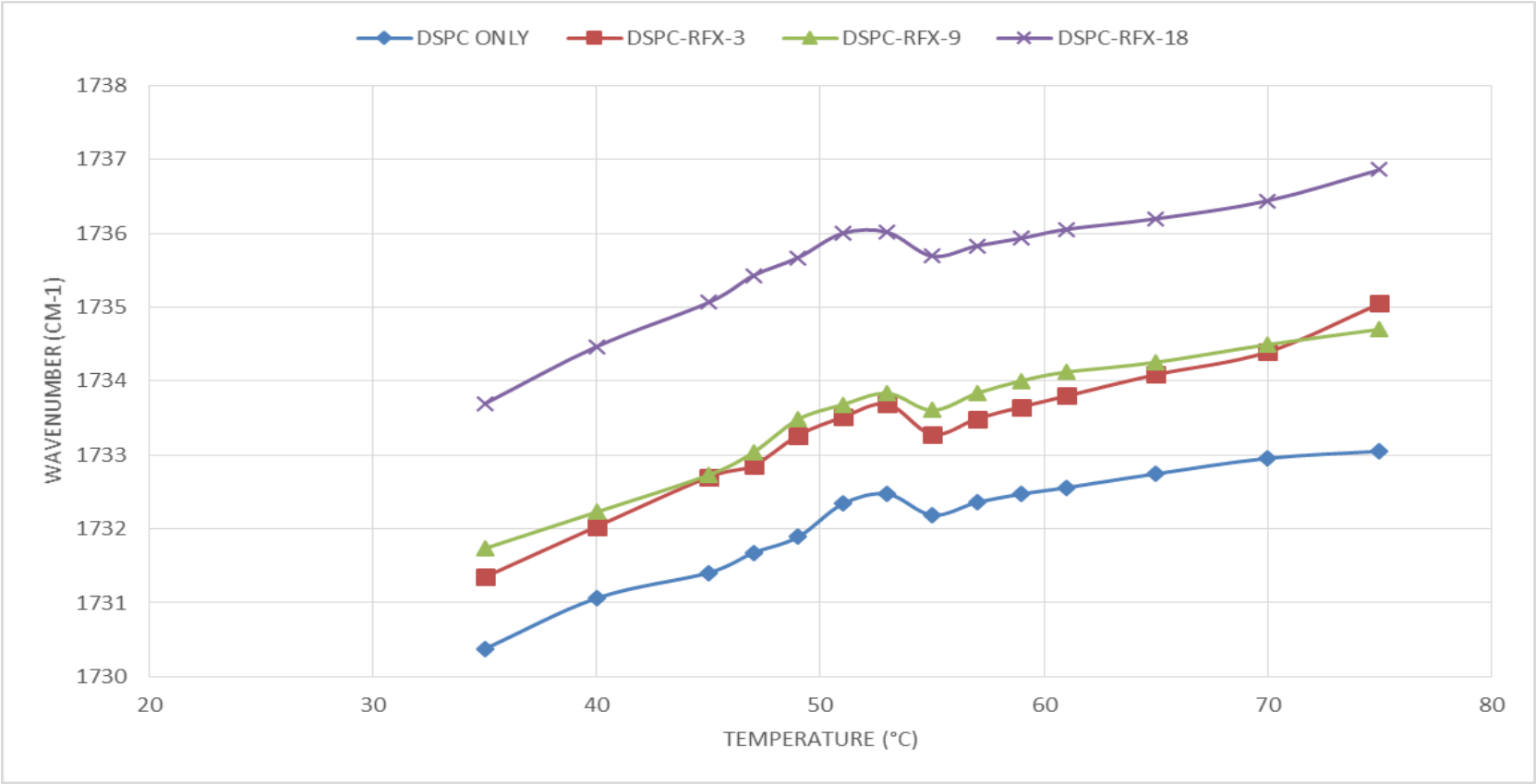

Figure 35. Variation in the frequency of the C=O stretching modes of DSPC MLVs as a function of temperature at varying concentrations of RFX (representative of three experiments).

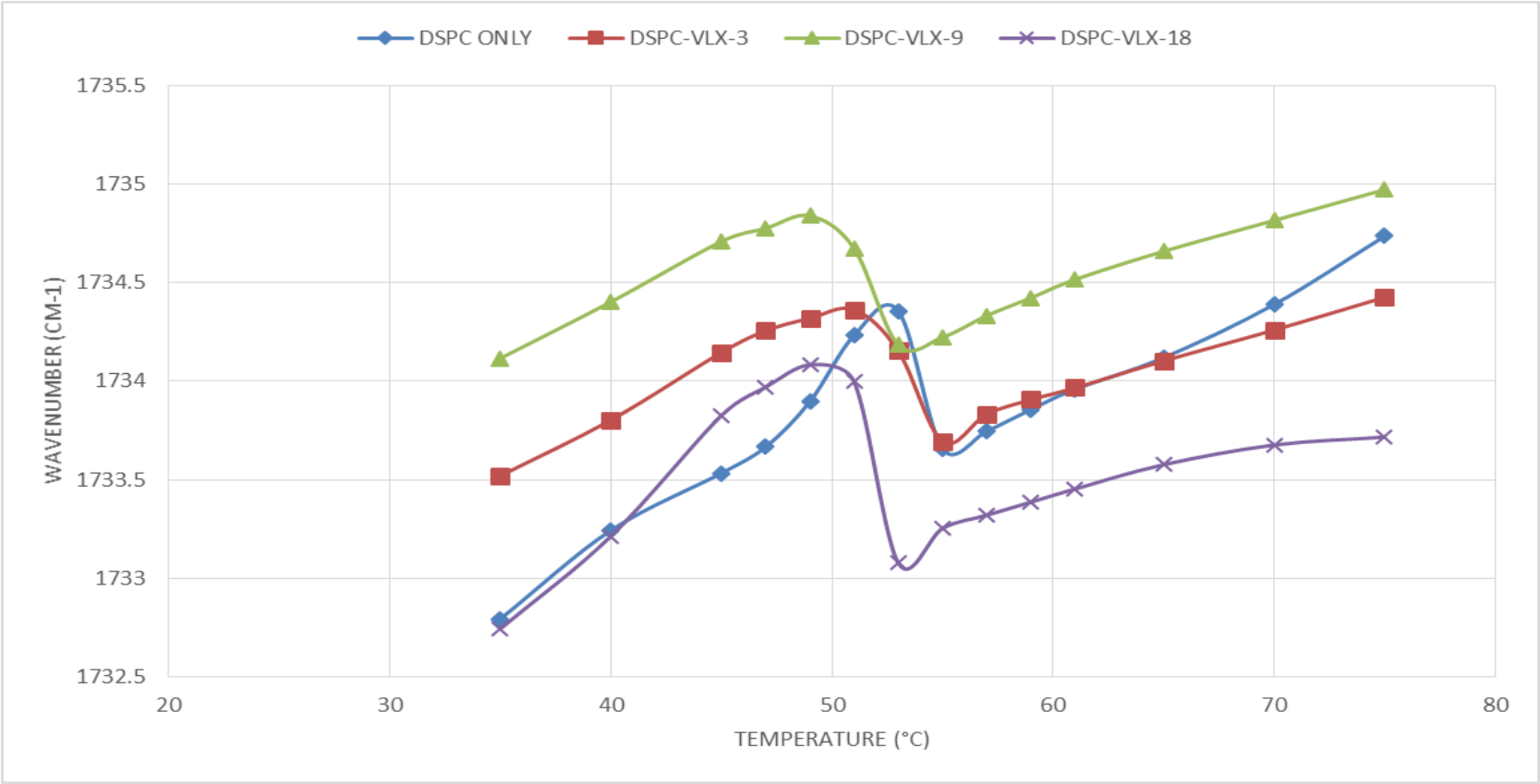

Figure 36. Variation in the frequency of the C=O stretching modes of DSPC MLVs as a function of temperature at varying concentrations of VLX (representative of three experiments).

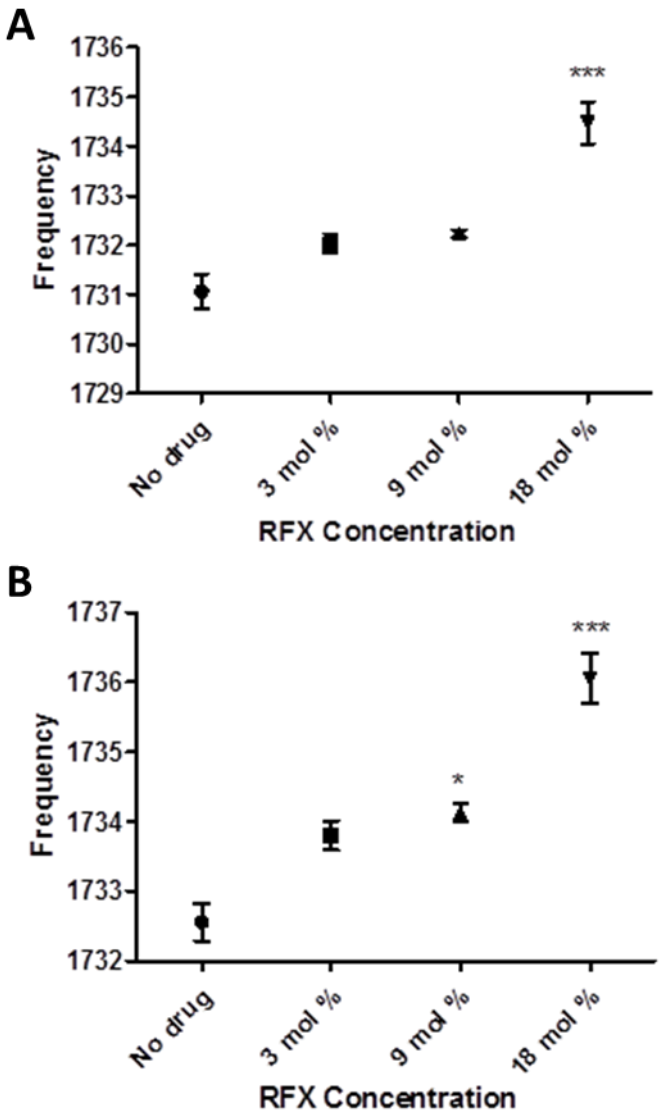

Figure 37. Variation in the frequency of the C=O stretching modes of DSPC MLVs as a function of RFX concentration at 45 (A) and 65 (B) °C. Each point represents the mean ± SEM (n = 6). *P < 0.05, **P < 0.01, ***P < 0.001, compared to controls (no drug, DSPC only).

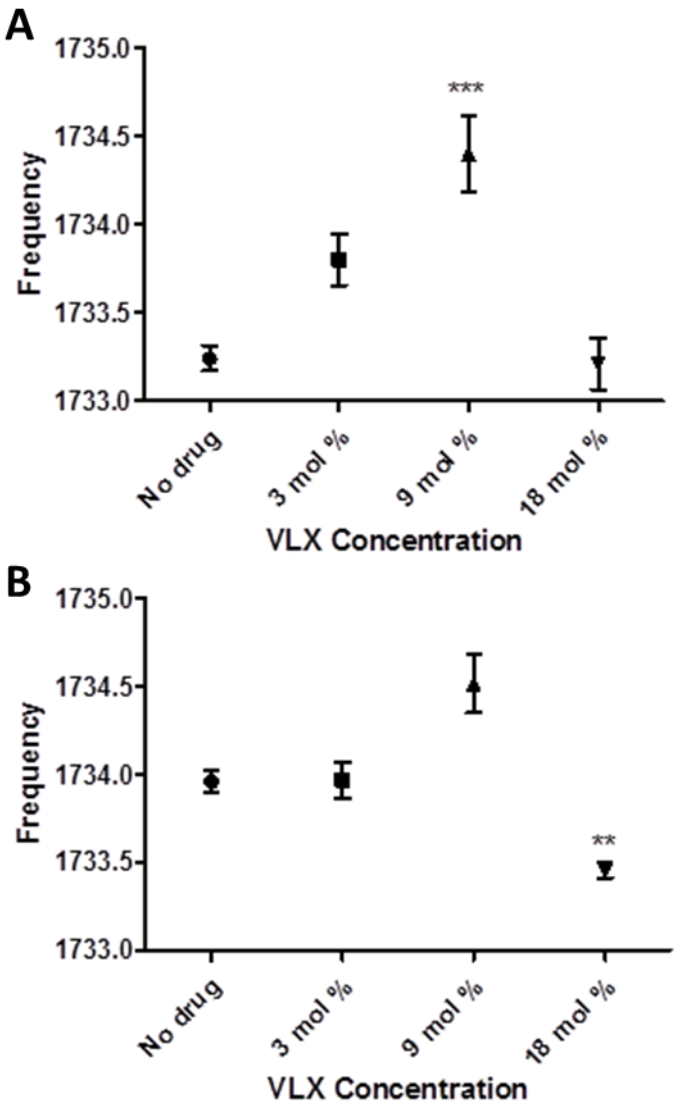

Figure 38. Variation in the frequency of the C=O stretching modes of DSPC MLVs as a function of VLX concentration at 45 (A) and 65 (B) °C. Each point represents the mean ± SEM (n = 6). *P < 0.05, **P < 0.01, ***P < 0.001, compared to controls (no drug, DSPC only).

3.3.4. Effect of RFX and VLX on the PO_2^- region

Information about the hydration state of the polar head groups of the phospholipids can be monitored by the analysis of the frequency of the PO_2^- antisymmetric double-stretching band, located at 1,220–1,240 cm^{-1} (Korkmaz & Severcan, 2005; Lopez-Garcia et al., 1993; Severcan et al., 2005). The frequency variations in the PO_2^- antisymmetric double-stretching band of DSPC liposomes as a function of temperature and different concentrations of RFX and VLX are given in Figures 39-42. Upon incorporation of both drugs into the membrane, the frequency shifted to higher values in both gel and liquid crystalline phases, indicating an increase in dehydration of the phosphate group. These variations were found to be significant and they are similar to the effect of CLX reported earlier (Sade et al., 2010). The frequency of PO_2^- antisymmetric stretching bands show that in the liquid crystalline phase, the head groups are more dehydrated. This effect is observed with both drugs studied.

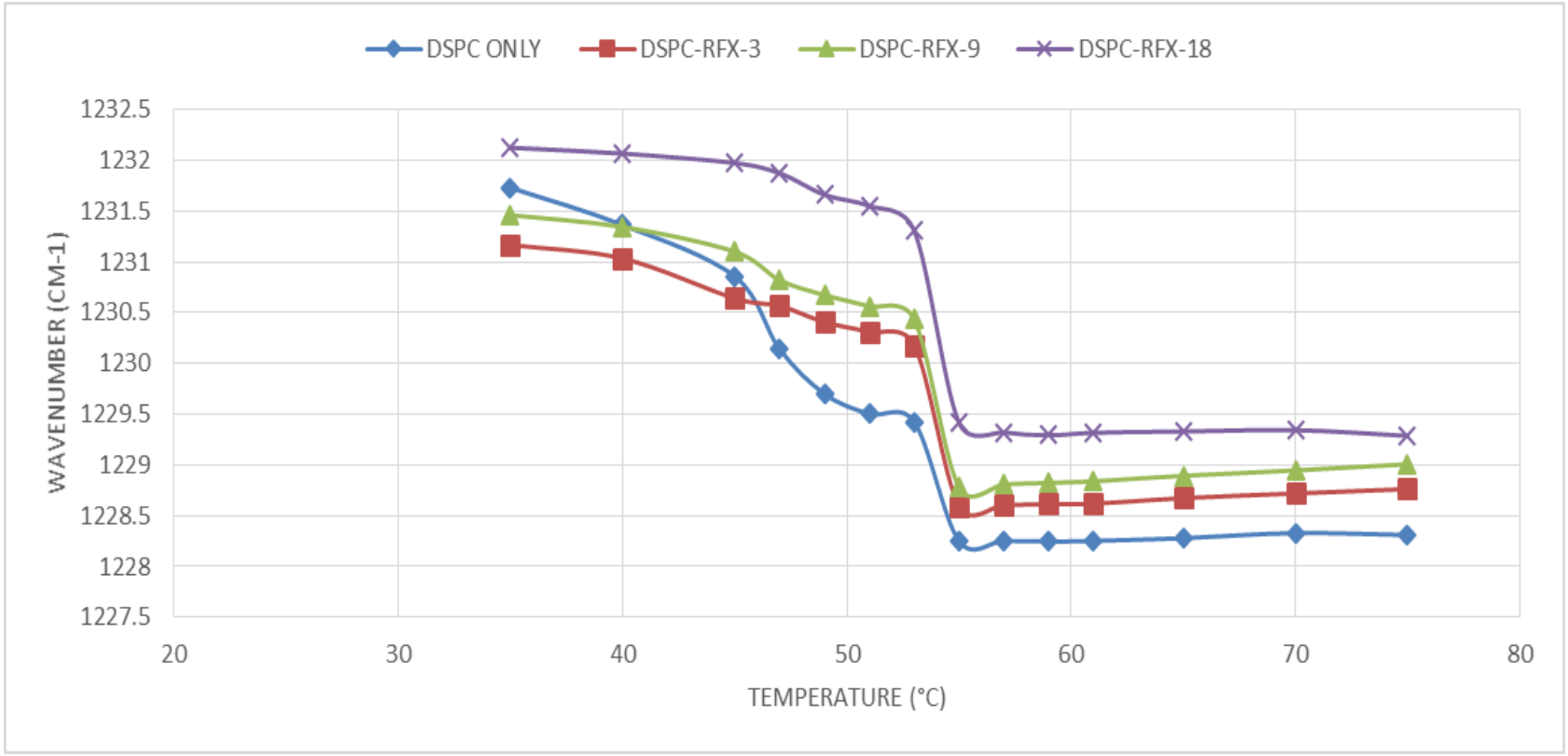

Figure 39. Variation in the frequency of the PO_2^- antisymmetric stretching modes of DSPC MLVs as a function of temperature at varying concentrations of RFX (representative of three experiments).

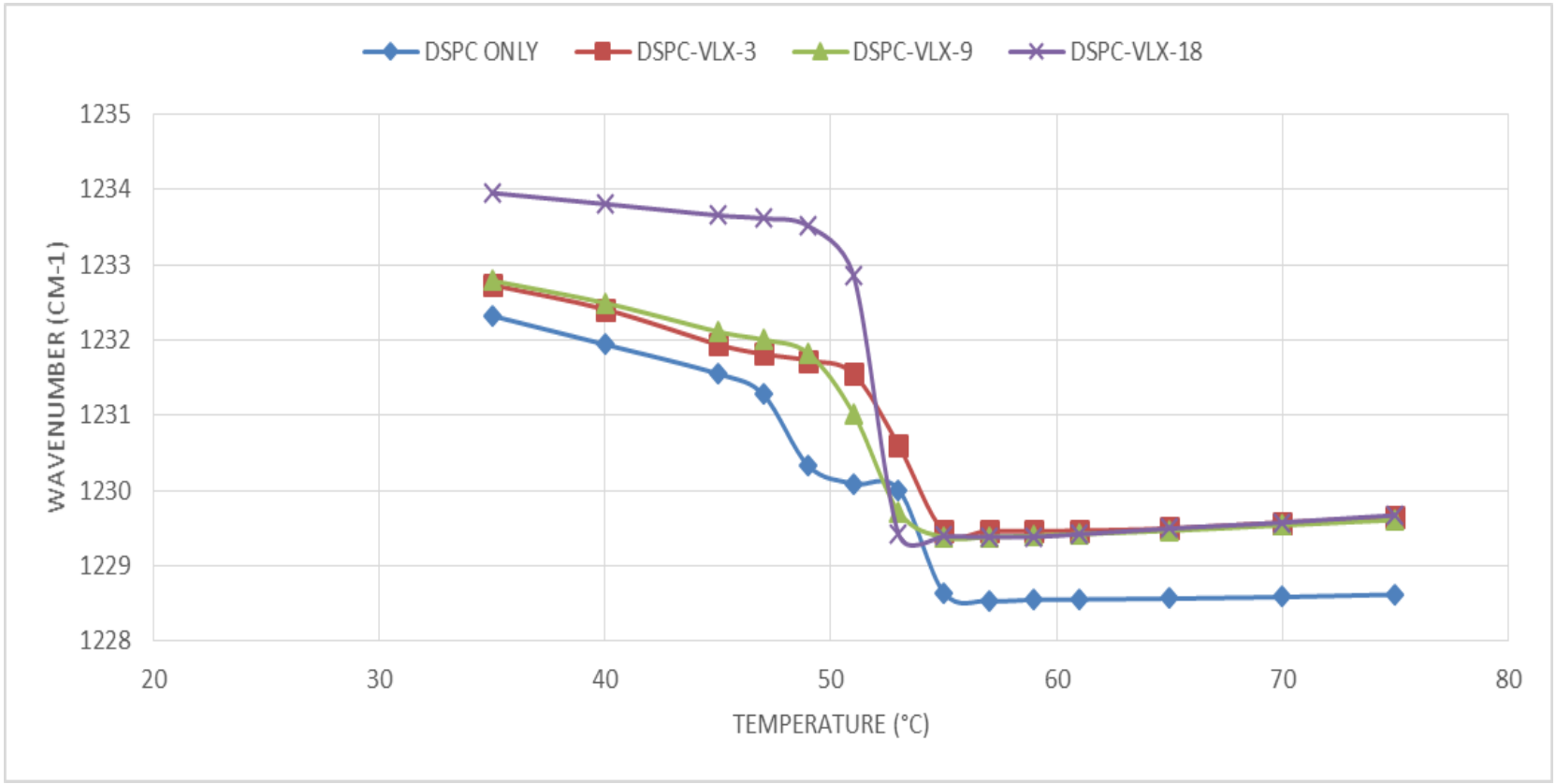

Figure 40. Variation in the frequency of the PO_2^- antisymmetric stretching modes of DSPC MLVs as a function of temperature at varying concentrations of VLX (representative of three experiments).

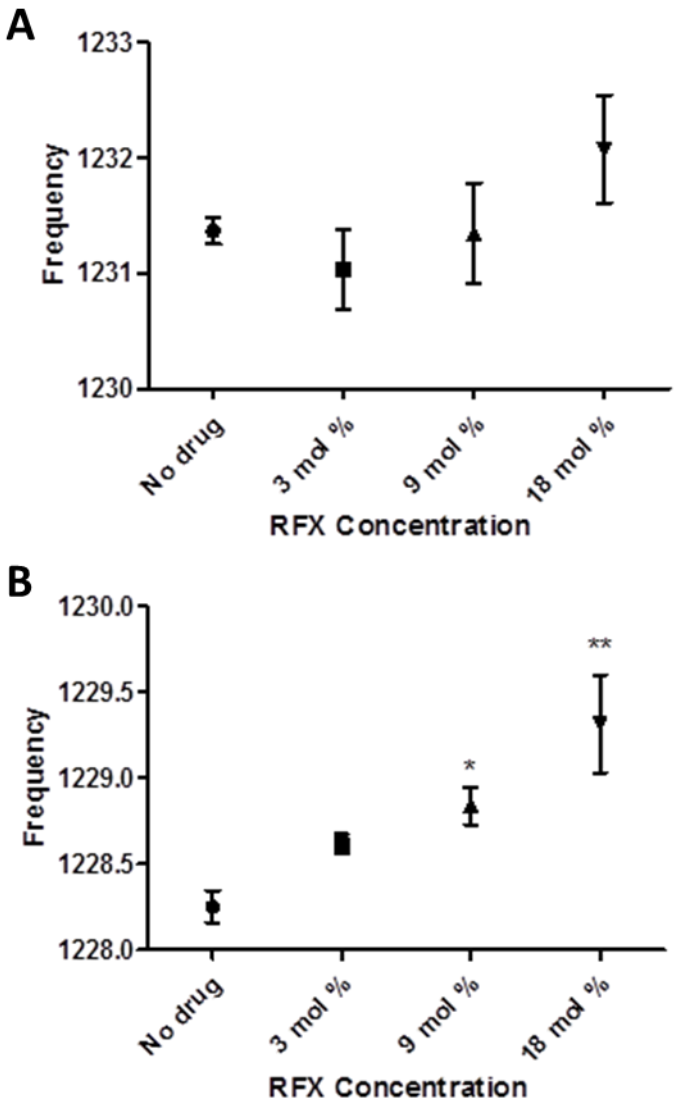

Figure 41. Variation in the frequency of the PO_2^- antisymmetric stretching modes of DSPC MLVs as a function of RFX concentration at 45 (A) and 65 (B) °C. Each point represents the mean ± SEM (n = 6). *P < 0.05, **P < 0.01, ***P < 0.001, compared to controls (no drug, DSPC only).

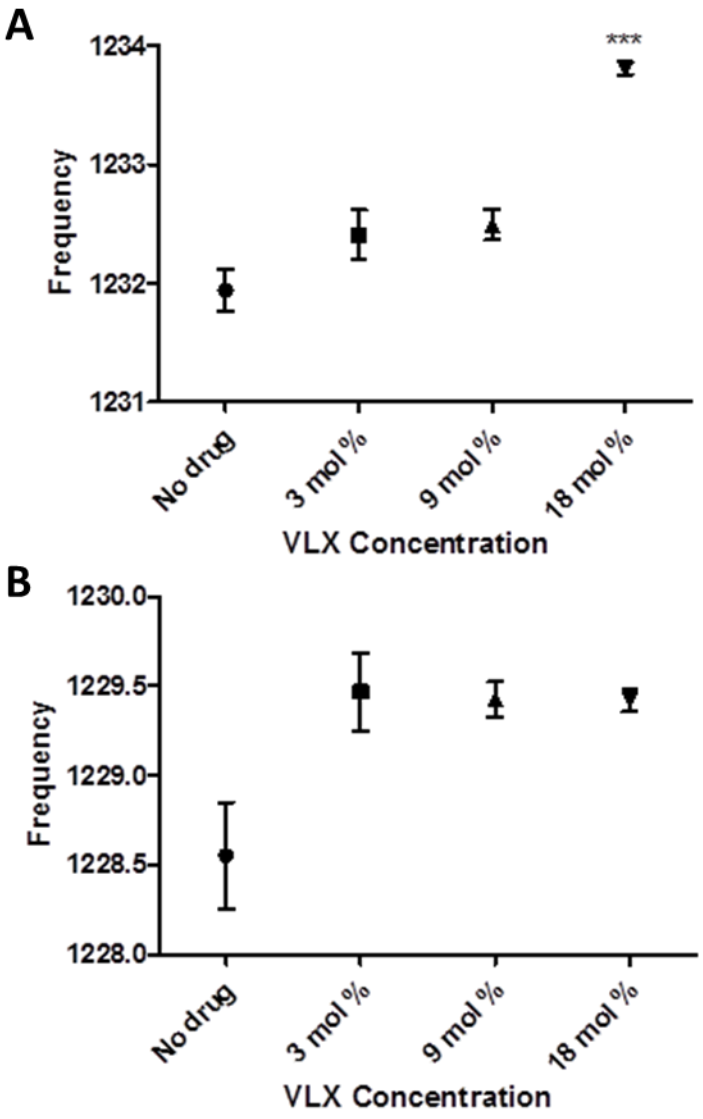

Figure 42. Variation in the frequency of the PO_2^- antisymmetric stretching modes of DSPC MLVs as a function of VLX concentration at 45 (A) and 65 (B) °C. Each point represents the mean ± SEM (n = 6). *P < 0.05, **P < 0.01, ***P < 0.001, compared to controls (no drug, DSPC only).

3.4. Effect of RFX and VLX on Turbidity

Turbidity studies were carried out in order to support the data already obtained by DSC and FT-IR for the effects of the drugs on the dynamic properties of DSPC MLVs. They were performed at 440 nm in order to minimize light scattering (Chong & Colbow, 1976; Severcan, Durmus, et al., 2000).

Figure 43 shows the temperature-dependent variations in the absorbance values of DSPC MLVs in the absence and presence of different concentrations of RFX. Figure 44 gives the same information about VLX-containing MLVs. As seen from the Figures, addition of RFX does not show significant effects on the absorbance. The same fact has been indicated by our FT-IR bandwidth data, which showed that RFX does not alter membrane dynamics significantly. On the other hand, presence of VLX results in an increase of absorbance values at low concentrations, indicating decrease in membrane dynamics, and strong decrease of absorbance at high (18 mol %) concentration, showing an increase in membrane dynamics and fluidity. This is in agreement with our FT-IR bandwidth data, which showed that VLX increases membrane dynamics in high concentrations, but decreases them in low concentrations.

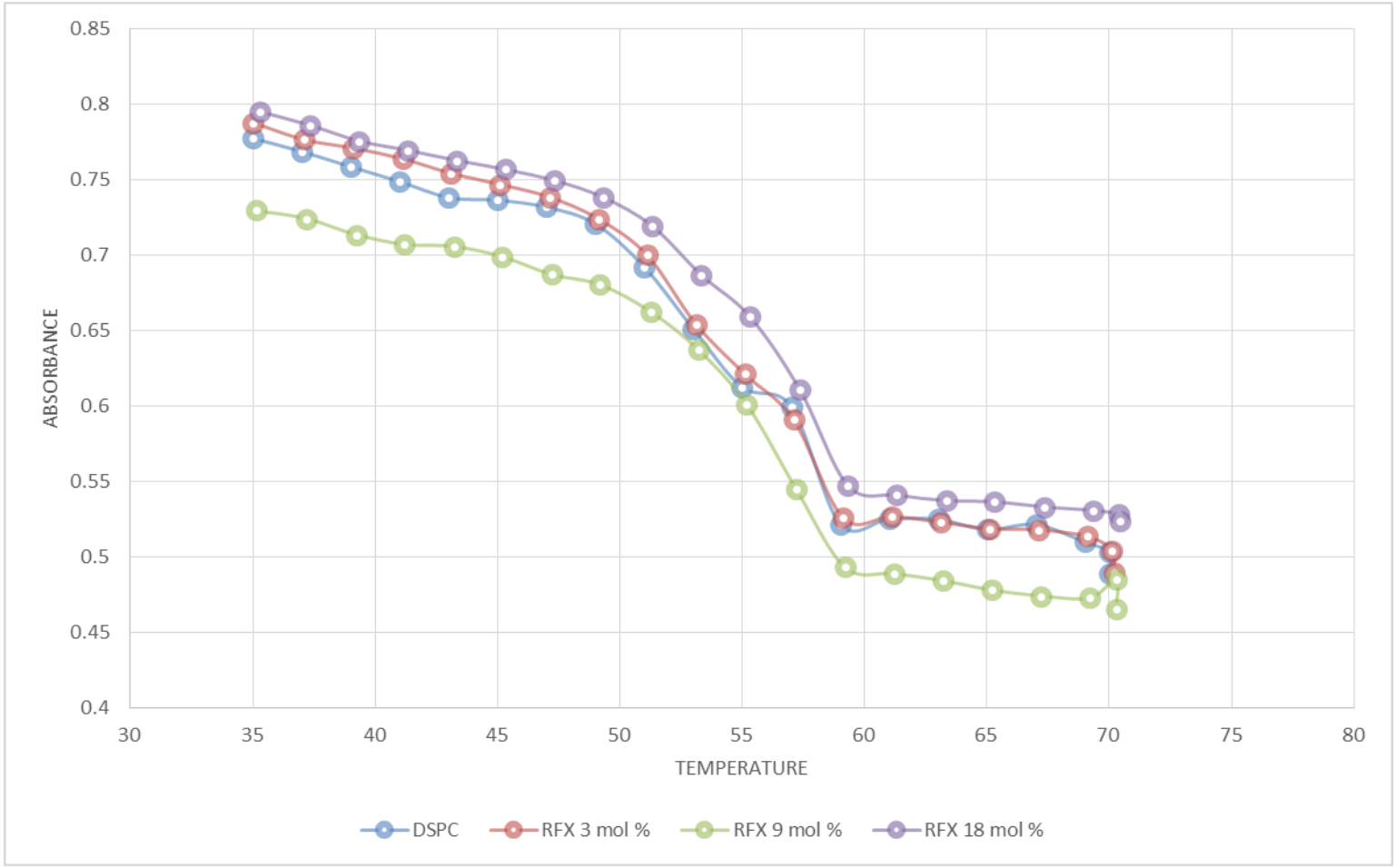

Figure 43. Temperature dependence of the absorbance at 440 nm for DSPC MLVs in the presence of different RFX concentrations.

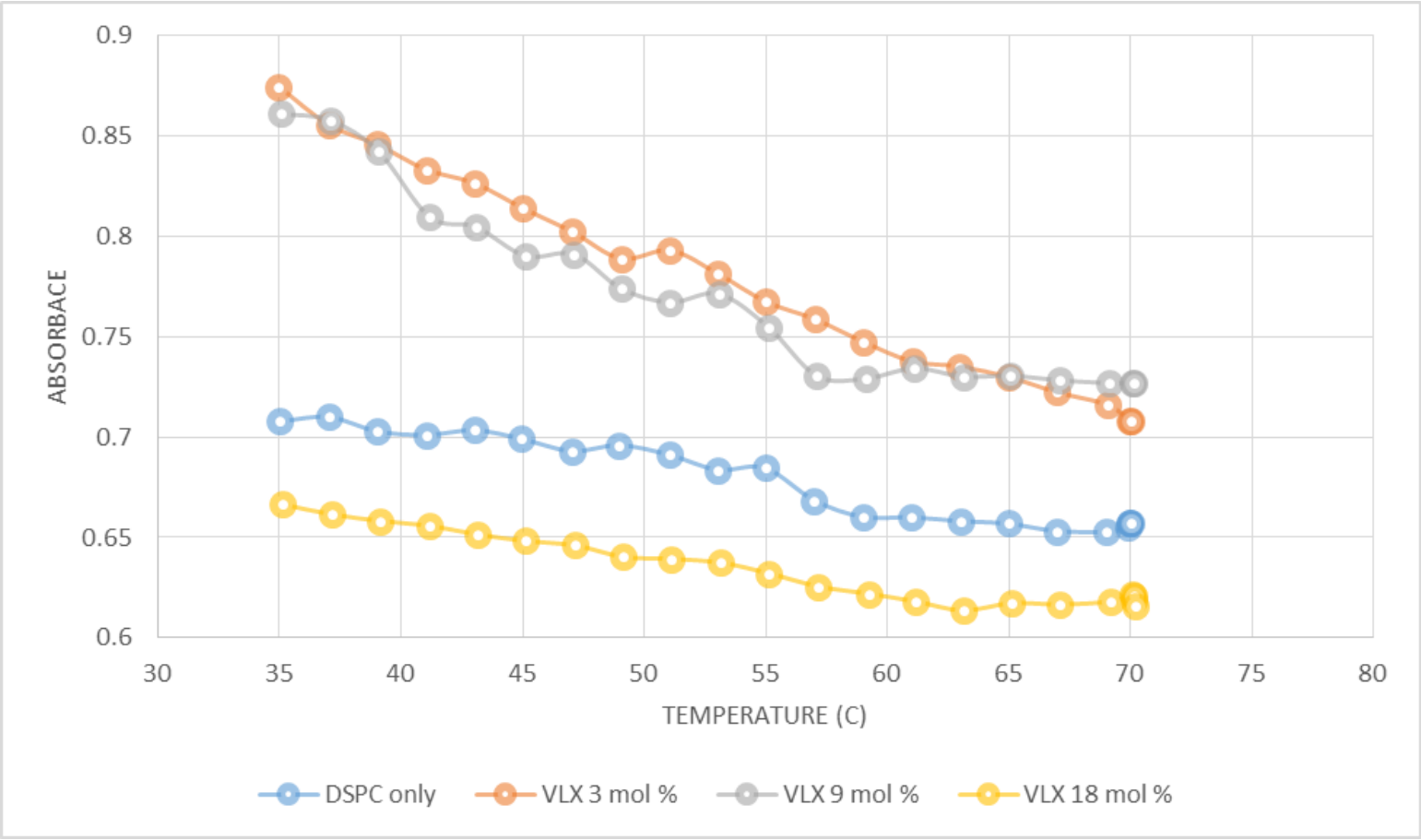

Figure 44. Temperature dependence of the absorbance at 440 nm for DSPC MLVs in the presence of different VLX concentrations.

CHAPTER 4

DISCUSSION

In this study the effects of two NSAIDs VLX and RFX on model membranes were investigated and compared with the effects of CLX. RFX has the same backbone as CLX but lacks the sulfonamide group, which is replaced by sulfone (Figure 2). VLX is slightly different from CLX but has the common sulfonamide group. CLX has F_3 moiety, which is unique to that drug among the three resulting in a bulkier molecule overall. Previous studies have shown that CLX can alter membrane fluidity and affect aggregation in model membranes (Sade et al., 2010). These properties can arise from the position of drug in the bilayer and the interaction of its chemical groups with the phospholipids.

DSC gives direct information about lipid phase transition and subdomains. Transition temperature and pretransition temperature (if present) can be determined. Additionally, the transition enthalpy reflects the acyl chain-packing properties (McElhaney, 1982) and thus is a parameter of membrane stability. On the other hand, FT-IR spectroscopy is based on monitoring the absorbed energy when molecules or functional groups of macromolecules change vibrational levels due to external factors. Therefore, it gives a spectrum unique to the system and various bands are assigned to different functional groups and thus can be monitored simultaneously. There are several band parameters of importance including frequency and bandwidth. In this study we have analyzed the frequency changes of the CH_2 stretching and C=O and PO_2^- stretching bands, which give structural information and represents order-disorder state and the strength of hydrogen bonding of the membrane, respectively. The

bandwidth of the CH_2 stretching bands, is a dynamic parameter and represents mobility. Turbidity data also confirms those parameters.

The results of RFX and VLX were compared with CLX studied before (Deniz et al., 2010; Sade et al., 2010). The comparison of the three drugs helped us make complex interpretations of the data (Table 5).

Table 5. The effects of rofecoxib, valdecoxib and celecoxib on DSPC model membrane parameters derived from analysis of FT-IR, DSC and Turbidity data.

	RFX	**VLX**	**CLX** (Sade et al., 2010)
Phase Transition Temperature (DSC)	No effect	Decreases	Decreases
ΔH_{cal} Enthalpy (DSC)	Decreases at low concentration – destabilizing effect on acyl chain packing Increases at high concentration – stabilizing effect on acyl chain packing	Decreases at low concentration – destabilizing effect on acyl chain packing Increases at high concentration – stabilizing effect on acyl chain packing	Increases at low concentration – stabilizing effect on acyl chain packing Decreases at high concentration – destabilizing effect on acyl chain packing
CH_2 frequency	Concentration dependent dual effect: decreases frequency in low concentrations (ordering effect) and increases them in higher ones (disordering effect)	Decreases frequency in gel phase (ordering effect) Increases frequency in liquid crystalline phase (disordering effect)	Concentration dependent dual effect: decreases frequency in low concentrations (ordering effect) and increases them in higher ones (disordering effect)

Table 5 (continued).

	RFX	**VLX**	**CLX** (Sade et al., 2010)
CH_2 bandwidth	No significant change	Decreases bandwidth at low concentration – decreases membrane dynamics. Increases bandwidth at high concentration – increases membrane dynamics.	Decreases bandwidth – decreases membrane dynamics.
C=O frequency	Increases the frequency – decreases hydrogen bonding around this functional group and has a destabilizing effect	Concentration dependent dual effect: at lower concentrations increase in frequency, which indicates the decrease in hydrogen bonding. At the higher concentration, decrease in frequency, indicating a sudden increase in H-bonding.	At gel phase: Concentration dependent dual effect opposite of VLX. At liquid crystalline phase: decreases the frequency – increases H bonding.
PO_2^- frequency	The frequency increases, indicating an increase in dehydration of the phosphate group.	The frequency increases, indicating an increase in dehydration of the phosphate group.	The frequency increases, indicating an increase in dehydration of the phosphate group.
Turbidity (absorbance at 440 nm)	No significant change	Increases absorbance at low concentration – decreases membrane dynamics. Decreases absorbance at high concentration – increases membrane dynamics.	Increases absorbance – decreases membrane dynamics.

According to the DSC data the Tm altering properties observed with CLX and VLX were not seen with RFX. Both CLX (Sade et al., 2010) and VLX (this study) decrease the Tm very significantly with increasing concentrations. This difference can also be corroborated with the FT-IR data plotted as a function of temperature. However, the decreasing Tm cannot be directly linked to membrane order or fluidity changes, because it results from the overall influence of the drug on the lipid bilayer. As seen from the Table 5, CLX and VLX have opposing effects to some of those parameters. However, Tm decrease may result from the domain formation in the system and will be mentioned later on.

The changes in the transition enthalpies of the DSC thermograms (Tables 3 and 4) show useful information about membrane stability. Lower ΔH_{cal} values for low concentrations of both RFX and VLX indicate a more destabilized membrane and the opposite is valid for high drug concentrations. However, those values cannot be directly linked to lipid order, but they can be linked to acyl chain packing properties and positioning of the drug. Interestingly, the opposite effect was observed with CLX (Sade et al., 2010).

FT-IR analyses have shown that RFX and VLX change hydrogen bonding and alter membrane fluidity and order parameters, some of the effects being opposite of what was observed with CLX (Sade et al., 2010).

The analysis of the frequency of the CH_2 antisymmetric stretching mode showed that low and high concentrations of RFX exert opposite effects on membrane order, similar to the observation with CLX (Sade et al., 2010). At low concentrations, RFX decreases the acyl chain flexibility, thereby increasing the lipid order, whereas at high concentrations it increases the acyl chain flexibility, introducing gauche conformers, and thus disorders the DSPC membranes. VLX did not show this effect, showing phase-dependent behavior instead: ordering in gel phase and disordering in liquid crystalline phase. This behavior is reverse of that of cholesterol. CLX has been reported to have cholesterol-like properties, but to somewhat different extent (Sade et al., 2010). CLX showed cholesterol-like effect on lipid fluidity, and VLX showed inverse cholesterol-like effect on lipid order. Effect on fluidity might be more important, in terms of drug-membrane interaction since almost any compound incorporated into the lipid bilayer would induce some sort of effect on lipid order.

The bandwidth of the CH_2 symmetric and antisymmetric stretching bands gives information about lipid dynamics and fluidity in membranes (Biruss et al., 2007; Casal et al., 1980; Korkmaz & Severcan, 2005; Lopez-Garcia et al., 1993; Severcan et al., 2005). The results of this analysis revealed that RFX does not significantly alter fluidity whereas VLX alters it on a concentration-dependent manner. At low concentration VLX decreases the fluidity of DSPC membranes and at high concentration it increases the fluidity. It is quite different from CLX, which decreases fluidity in all phases and concentrations, much like cholesterol. These results can be corroborated with turbidity data, which showed exactly the same effect of the drugs on membrane fluidity.

Lipid order and fluidity are important parameters for the proper functioning of biological membranes, which, in turn, influence cellular processes and disease states (Korkmaz & Severcan, 2005; Maxfield & Tabas, 2005). For instance, membranes of tumor cells have been found to possess higher fluidity and less-ordered acyl chains, compared to membranes of non-tumor cells (Sok, Sentjurc, & Schara, 2002), which could thus be counteracted by the ability of certain NSAIDs to decrease membrane fluidity. In case of VLX, we could control fluidity in a concentration based manner because of the dual effect of the drug. There is evidence that the modifications of physical characteristics of membrane bilayers lead to altered membrane enzyme activities, membrane-bound receptors, and the permeability of ion channels (Lee, 2004). Membrane lipid order and fluidity are essential parameters for the correct functioning of ion channels (Awayda, Shao, Guo, Zeidel, & Hill, 2004). Therefore, the membrane fluidity altering effects of VLX and CLX could be one of the COX-2 independent mechanisms contributing to their potential anticancer activity and may play a role in countering neurodegenerative diseases as well.

The changes in the frequency and bandwidth of the CH_2 stretching mode of DSPC MLVs are not concerted for VLX, since it induces a decrease in both membrane order and dynamics in gel phase in lower concentrations and increases both parameters in liquid crystalline phase at high concentrations. CLX also decreases both parameters at high concentrations regardless of the phase of the lipid (Sade et al., 2010). Only RFX does not show this effect as it does not significantly alter CH_2 dynamics, changing only the lipid order. Additionally, similar kinds of disconcerted behavior in drug-lipid

interactions has been previously reported for interactions of model membranes with melatonin (Severcan et al., 2005), progesterone (Korkmaz & Severcan, 2005), and vitamin D_2 (Kazanci et al., 2001). This controversial effect of the presence of the drug in membrane order and dynamics may reflect the presence of more than one phase in the bilayer (Villalain, Aranda, & Gómez-Fernández, 1986), which can be further confirmed by our DSC results. There is an antisymmetric broadening of the main phase-transition peak with an increase in VLX (this study) and CLX (Sade et al., 2010) concentration, which may indicate the coexistence of more than one domain in the membrane. The DSC results with RFX show no such effect, corroborating with the FT-IR data. If these multiple domains are large enough, the exchange of lipids between them cannot be resolved, and the resulting DSC curve will be a superimposition of more than one component (Kazanci et al., 2001). When considering the highest VLX concentration we can see the broadening, which reflects presence of two different domains, which may be called drug-rich and drug-poor domains, as observed with CLX (Sade et al., 2010), though exact properties of these domains may be different due to different effects of the drug on some of the membrane parameters. The dynamics of these domains are different; therefore, one of them may cause an enhanced diffusion process (Severcan & Cannistraro, 1988). Additionally, we can conclude that Tm decrease observed in case of both CLX and VLX (and cholesterol too, which is known to induce domain formation), but not in case of RFX is also a consequence of the lateral phase separation and domain formation.

The carbonyl (C=O stretching) and PO_2^- bands of the FT-IR spectrum give information about the interaction of additives with the region near the glycerol backbone and head groups of the membranes, respectively.

The analysis of C=O stretching groups revealed a significant decrease in the hydrogen bonding around this functional group with low VLX concentration, while high VLX concentration showed an increase in hydrogen bonding. The electronegative atom of the VLX molecule, just like the CLX molecule is the nitrogen of the sulfonamide group (Figure 2). The amido protons (H atoms that are covalently bonded to N), which have a partial positive charge, can make hydrogen bonds with the oxygen atoms in the C=O groups of the phospholipids. The possibility of hydrogen bonding between the carbonyl group of DSPC and nearby water molecules should also be considered (Sade

et al., 2010). In case of low VLX concentration it seems that the decreased hydrogen bonding implies that there is not enough VLX molecules and there are free carbonyl groups in the system, while with increased concentration we see that hydrogen bonding increases accordingly. This means VLX, unlike CLX positions itself mainly in the cooperativity region (C2–C8) of the acyl chains (Figure 45) and VLX molecules are located in the hydrophobic interior region of the membranes, and not at the interfacial region near the head groups, where CLX has been shown to be located (Sade et al., 2010; Severcan et al., 2005; Walter et al., 2004). As the concentration increases, excess VLX may be positioned closer to the head groups. This difference in positioning of VLX and CLX may be explained by the fact that the CLX molecule is bulkier and it has an F_3 group, which prevents its positioning near the cooperativity region in the first place, especially in the gel phase. Incorporating Fluorine has been reported as the way to prepare interdigitated lipid membranes, thus it is logical that presence of F_3 in a drug will result in its positioning near the head group (Smith et al., 2014). It is worth noting that in the liquid crystalline phase however, CLX does have similar behavior as VLX, most probably due to increased membrane dynamics and fluidity and its fluorine induced positioning effect being less important. RFX on the other hand lacks the sulfonamide group and thus is unable to make substantial hydrogen bonds. Indeed our FT-IR data has shown RFX to decrease hydrogen bonding in all phases. It is implied from other data that RFX is also positioned between the acyl chains farther from the head groups. This VLX and RFX drug positioning happens not because of their hydrogen bonding properties but rather because this is more favorable position in terms of thermodynamics, since both drugs are hydrophobic in nature (Figure 45).

It may be deduced that the default positioning of the hydrophobic NSAIDs is indeed between the acyl chains, and is not dependent primarily on hydrogen bonding properties, while the different position of CLX is because of unique interactions of the F_3 moiety and the head groups. The reduction in the enthalpy changes starting at low concentrations of both VLX and RFX supports this idea, since a decrease in ΔH_{cal} is explained by the presence of a molecule in the cooperativity region (Zhao et al., 2007). The subsequent increase of the enthalpy and stabilizing effect of high concentrations of VLX and RFX can be explained by saturation of the system with excess drug molecules, increasing density between acyl chains and their positioning closer to the head groups. Increasing the CLX concentration did not have such effect due to the

tendency of F_3 to interact with head groups and thus having a destabilizing effect, and this can be seen from CLX ΔH_{cal} data reported before (Sade et al., 2010). As seen from the frequency analysis of CH_2 antisymmetric mode, RFX have some ordering effect at low concentration even though it is unable to form as many hydrogen bonds as CLX. It is an interesting property considering that RFX did not alter the membrane dynamics significantly. Both drugs show disordering effect at high concentrations. It is implied that packing interactions between the hydrocarbon chains are now less important and result in a decrease in the order of DSPC membranes for high concentrations of both CLX (Sade et al., 2010) and RFX (this study). Both drugs have little hydrogen bonds in gel phase at high concentrations (though the reasons behind it are unique for each of these drugs), and while CLX has high hydrogen bonding in liquid phase, it also decreases membrane dynamics (Sade et al., 2010). Moreover, combined with the destabilizing effect of the F_3 group this still results in decrease of the membrane order. VLX, which can form hydrogen bonds, but is not as bulky as CLX and lacks the F_3 group, on the other hand show opposite effect: ordering in gel phase and disordering in liquid crystalline phase, mirroring the hydrogen bonding behavior.

Finally, phosphate group band frequency showed similar data in both drugs studied. Both drugs showed a decrease in hydrogen bonding around the PO_2^- group, which indicates an increase in the dehydration of the head groups, which is similar to the observation with CLX (Sade et al., 2010). This may indicate that no matter where drug is positioned, it still exerts the dehydration effect on the phosphate head groups, possibly by the help of oxygen molecules bound to sulfur (and possibly, presence of fluorine group in case of CLX) pulling the water molecules away from the lipid head groups. The size analysis data, which shows the decreased MLV size when RFX or VLX is added confirms this, since less hydrated phosphate head groups decrease vesicle-to-vesicle and vesicle-to-water interactions, which results in decreased lipid vesicle aggregation (Table 1).

As a summary, Figure 45 shows the putative localization of the three drugs as well as cholesterol in the lipid bilayer. We can conclude that, the ability of the drugs to form hydrogen bonds with the ester carbonyl moiety in the interfacial region is important for the domain formation and phase transition properties of the system but it is not the critical factor for the drug localization within the lipid bilayer.

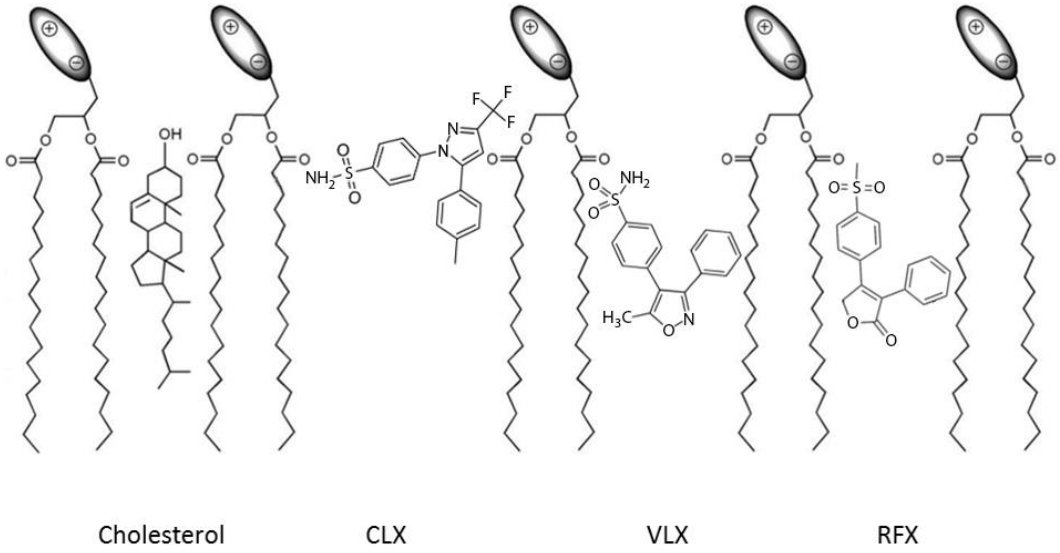

Figure 45. Putative localization of cholesterol (Chen & Tripp, 2008), CLX (Sade et al., 2010), VLX (this study) and RFX (this study) in the lipid bilayer.

CHAPTER 5

CONCLUSION

This study investigated the effects of two drugs of the NSAID family, RFX and VLX on DSPC liposomes, which served as model membranes. Using thermoanalytical and spectroscopic techniques, namely DSC and FT-IR, it was shown that these two drugs can alter certain properties of the membrane, such as fluidity, order and phase transition temperature.

VLX has been shown to mimic certain properties of the previously studied drug CLX, namely decreasing the phase transition temperature (Tm) of the membrane. The structural similarities between these drugs, such as presence of the same sulfonamide moiety and the resulting similar interactions of these drugs with certain parts of the membrane, namely ester carbonyl moiety of phospholipids were suggested to be responsible for this fact. It was also shown that both drugs induce phase separation in the bilayer, resulting in drug-poor and drug-rich domain formation in the lipid vesicles. However, VLX did not show all of CLX effects, and it has been hypothesized that the unique F_3 moiety of CLX gives it a unique positioning in the lipid bilayer and thus some unique interaction profile with the lipids. On the other hand, RFX lacking sulfonamide moiety and thus being more hydrophobic has shown different interaction profile, but the drug's positioning inside the lipid bilayer and thus certain effects it exerted on the membrane properties were found to be close to VLX. It has been deduced that the default drug positioning is within the bilayer, near the cooperativity region, and only CLX is positioned differently, in the interfacial region, presumably due to the F_3 group interacting with the DSPC head groups of the lipids.

Considering possible roles of NSAIDs in various diseases this study may prove useful for the understanding of the mechanisms of drug-membrane interaction, which lead to new ways of increasing drug efficacy for both their traditional use and other pleiotropic effects, developing new modified versions of the drugs, and even better understanding lipid based targeted drug delivery systems. If we are able to predict the altered membrane parameters by knowing what effects certain chemical groups and compounds which are part of the drugs have on either lipid bilayers in the cells or in the delivery vesicles composed of model membranes we can make the potential optimization studies more efficient.

REFERENCES

Al-Saidan, S. M., Krishnaiah, Y. S. R., Satyanarayana, V., & Rao, G. S. (2005). In vitro and in vivo evaluation of guar gum-based matrix tablets of rofecoxib for colonic drug delivery. *Current Drug Delivery*, *2*(2), 155–63. Retrieved from http://www.ncbi.nlm.nih.gov/pubmed/16305416

Arsov, Z., & Quaroni, L. (2007). Direct interaction between cholesterol and phosphatidylcholines in hydrated membranes revealed by ATR-FTIR spectroscopy. *Chemistry and Physics of Lipids*, *150*(1), 35–48. doi:10.1016/j.chemphyslip.2007.06.215

Awayda, M. S., Shao, W., Guo, F., Zeidel, M., & Hill, W. G. (2004). ENaC-membrane interactions: regulation of channel activity by membrane order. *The Journal of General Physiology*, *123*(6), 709–727.

Bangham, A. D. (1972). Model membranes. *Chemistry and Physics of Lipids*, *8*(4), 386–92. Retrieved from http://www.ncbi.nlm.nih.gov/pubmed/5041948

Bangham, A. D., Standish, M. M., & Watkins, J. C. (1965). Diffusion Of Univalent Ions Across Lamellae Of Swollen Phospholipids. *Journal of Molecular Biology*, *13*, 238.

Bertagnolli, M. M., Eagle, C. J., Zauber, A. G., Redston, M., Solomon, S. D., Kim, K., … Hawk, E. T. (2006). Celecoxib for the prevention of sporadic colorectal adenomas. *The New England Journal of Medicine*, *355*(9), 873–884. doi:10.1056/NEJMoa061355

Biruss, B., Dietl, R., & Valenta, C. (2007). The influence of selected steroid hormones on the physicochemical behaviour of DPPC liposomes. *Chemistry and Physics of Lipids*, *148*(2), 84–90.

Campbell, I. D., & Dwek, R. A. (1984). *Biological spectroscopy*.

Casal, H. L., Cameron, D. G., Smith, I. C., & Mantsch, H. H. (1980). Acholeplasma laidlawii membranes: a Fourier transform infrared study of the influence of protein on lipid organization and dynamics. *Biochemistry*, *19*(3), 444–451.

Casal, H. L., & Mantsch, H. H. (1984). Polymorphic phase behaviour of phospholipid membranes studied by infrared spectroscopy. *Biochimica et Biophysica Acta*, *779*(4), 381–401. Retrieved from http://www.ncbi.nlm.nih.gov/pubmed/6391546

Chapman, D., & Hayward, J. A. (1985). New biophysical techniques and their application to the study of membranes. *The Biochemical Journal*, *228*(2), 281–95. Retrieved from http://www.pubmedcentral.nih.gov/articlerender.fcgi?artid=1144986&tool=pmcentrez&rendertype=abstract

Chen, C., & Tripp, C. P. (2008). An infrared spectroscopic based method to measure membrane permeance in liposomes. *Biochimica et Biophysica Acta*, *1778*(10), 2266–72. doi:10.1016/j.bbamem.2008.05.010

Chen, S. C., Sturtevant, J. M., & Gaffney, B. J. (1980). Scanning calorimetric evidence for a third phase transition in phosphatidylcholine bilayers. *Proceedings of the National Academy of Sciences*, *77*(9), 5060–5063. doi:10.1073/pnas.77.9.5060

Chong, C. S., & Colbow, K. (1976). Light scattering and turbidity measurements on lipid vesicles. *Biochimica et Biophysica Acta*, *436*(2), 260–282.

Danese, S., & Mantovani, A. (2010). Inflammatory bowel disease and intestinal cancer: a paradigm of the Yin-Yang interplay between inflammation and cancer. *Oncogene*, *29*(23), 3313–3323. Retrieved from http://dx.doi.org/10.1038/onc.2010.109

De Vries, E. F. J. (2006). Imaging of cyclooxygenase-2 (COX-2) expression: potential use in diagnosis and drug evaluation. *Current Pharmaceutical Design*, *12*(30), 3847–56. Retrieved from http://www.ncbi.nlm.nih.gov/pubmed/17073683

Demel, R. A., & De Kruyff, B. (1976). The function of sterols in membranes. *Biochimica et Biophysica Acta (BBA) - Reviews on Biomembranes*, *457*(2), 109–132. doi:10.1016/0304-4157(76)90008-3

Deniz, A., Sade, A., Severcan, F., Keskin, D., Tezcaner, A., & Banerjee, S. (2010). Celecoxib-loaded liposomes : effect of cholesterol on encapsulation and in vitro release characteristics. *Bioscience Reports*, *30*(5), 365–373. doi:10.1042/BSR20090104

Drummond, D. C., Meyer, O., Hong, K., Kirpotin, D. B., & Papahadjopoulos, D. (1999). Optimizing liposomes for delivery of chemotherapeutic agents to solid tumors. *Pharmacological Reviews*, *51*(4), 691–743. Retrieved from http://www.ncbi.nlm.nih.gov/pubmed/10581328

Edidin, M. (2003). The state of lipid rafts: from model membranes to cells. *Annual Review of Biophysics and Biomolecular Structure*, *32*, 257–83. doi:10.1146/annurev.biophys.32.110601.142439

Eker, F., Durmus, H. O., Akinoglu, B. G., & Severcan, F. (1999). Application of turbidity technique on peptide-lipid and drug-lipid interactions. *Journal of Molecular Structure*, *482-483*, 693–697. doi:10.1016/S0022-2860(98)00690-5

FitzGerald, G. a. (2003). COX-2 and beyond: Approaches to prostaglandin inhibition in human disease. *Nature Reviews. Drug Discovery*, *2*(11), 879–90. doi:10.1038/nrd1225

Freifelder, D. (1983). *Physical biochemistry, applications to biochemistry and molecular biology* (2nd ed., Vol. 60, p. A321). American Chemical Society. doi:10.1021/ed060pA321.3

Funk, C. D. (2001). Prostaglandins and leukotrienes: advances in eicosanoid biology. *Science (New York, N.Y.)*, *294*(5548), 1871–5. doi:10.1126/science.294.5548.1871

Gamerdinger, M., Clement, A. B., & Behl, C. (2007). Cholesterol-like effects of selective cyclooxygenase inhibitors and fibrates on cellular membranes and amyloid-beta production. *Molecular Pharmacology*, *72*(1), 141–51. doi:10.1124/mol.107.034009

Ghosh, R. (1988). Phosphorus-31 and deuterium NMR studies of structure and motion in bilayers of phosphatidylcholine and phosphatidylethanolamine. *Biochemistry*, *27*(20), 7750–7758. doi:10.1021/bi00420a025

Goldenberg, M. M. (1999). Celecoxib, a selective cyclooxygenase-2 inhibitor for the treatment of rheumatoid arthritis and osteoarthritis. *Clinical Therapeutics*, *21*(9), 1497–1513. doi:S0149291800800053 [pii]

Grösch, S., Maier, T. J., Schiffmann, S., Geisslinger, G., & Grosch, S. (2006). Cyclooxygenase-2 (COX-2)-independent anticarcinogenic effects of selective COX-2 inhibitors. *Journal of the National Cancer Institute*, *98*(11), 736–47. doi:10.1093/jnci/djj206

Hauser, H., & Poupart, G. (2004). *Lipid Structure* (2nd ed.). CRC Press.

Hinz, B., Renner, B., & Brune, K. (2007). Drug insight: cyclo-oxygenase-2 inhibitors--a critical appraisal. *Nature Clinical Practice. Rheumatology*, *3*(10), 552–560; quiz 1 p following 589. doi:10.1038/ncprheum0619

Hui, S. W., & Huang, C. H. (1986). X-ray diffraction evidence for fully interdigitated bilayers of 1-stearoyllysophosphatidylcholine. *Biochemistry*, *25*(6), 1330–5. Retrieved from http://www.ncbi.nlm.nih.gov/pubmed/3964679

Hung, W.-C., Lee, M.-T., Chen, F.-Y., & Huang, H. W. (2007). The condensing effect of cholesterol in lipid bilayers. *Biophysical Journal*, *92*(11), 3960–7. doi:10.1529/biophysj.106.099234

Illya, G., Lipowsky, R., & Shillcock, J. C. (2006). Two-component membrane material properties and domain formation from dissipative particle dynamics. *The Journal of Chemical Physics*, *125*(11), 114710. doi:10.1063/1.2353114

Jain, M. K. (1979). Molecular Motions in Biomembranes. *Proc. INSA*, *45*, 558–566.

Jain, M. K. (1988). *Introduction to Biological Membranes* (2nd ed.). John Wiley & Sons.

Johnson, A. J., Hsu, A.-L., Lin, H.-P., Song, X., & Chen, C.-S. (2002). The cyclo-oxygenase-2 inhibitor celecoxib perturbs intracellular calcium by inhibiting endoplasmic reticulum Ca2+-ATPases: a plausible link with its anti-tumour effect and cardiovascular risks. *The Biochemical Journal*, *366*(Pt 3), 831–7. doi:10.1042/BJ20020279

Kazanci, N., Toyran, N., Haris, P. I., & Severcan, F. (2001). Vitamin D2 at high and low concentrations exert opposing effects on molecular order and dynamics of dipalmitoyl phosphatidylcholine membranes. *Spectroscopy*, *15*(2), 47–55. doi:10.1155/2001/890975

Korkmaz, F., & Severcan, F. (2005). Effect of progesterone on DPPC membrane: evidence for lateral phase separation and inverse action in lipid dynamics. *Archives of Biochemistry and Biophysics*, *440*(2), 141–147.

Kukar, T., Murphy, M. P., Eriksen, J. L., Sagi, S. A., Weggen, S., Smith, T. E., … Golde, T. E. (2005). Diverse compounds mimic Alzheimer disease-causing mutations by augmenting Abeta42 production. *Nature Medicine*, *11*(5), 545–50. doi:10.1038/nm1235

Kutchai, H., Chandler, L. H., & Zavoico, G. B. (1983). Effects of cholesterol on acyl chain dynamics in multilamellar vesicles of various phosphatidylcholines. *Biochimica et Biophysica Acta (BBA) - Biomembranes*, *736*(2), 137–149. doi:10.1016/0005-2736(83)90277-8

Lee, A. G. (2004). How lipids affect the activities of integral membrane proteins. *Biochimica et Biophysica Acta - Biomembranes*.

Levine, Y. K., & Wilkins, M. H. F. (1971). Structure of Oriented Lipid Bilayers. *Nature*, *230*(11), 69–72. doi:10.1038/10.1038/newbio230069a0

Lewis, R. A. H., & McElhaney, R. (2011). The Mesomorphic Phase Behavior of Lipid Bilayers. In P. L. Yeagle (Ed.), *The Structure of Biological Membranes, Third Edition* (pp. 19–89). CRC Press. doi:doi:10.1201/b11018-5

Li, Y., Ge, M., Ciani, L., Kuriakose, G., Westover, E. J., Dura, M., … Tabas, I. (2004). Enrichment of endoplasmic reticulum with cholesterol inhibits sarcoplasmic-endoplasmic reticulum calcium ATPase-2b activity in parallel with increased order of membrane lipids: implications for depletion of endoplasmic reticulum calcium stores and apoptos. *The Journal of Biological Chemistry*, *279*(35), 37030–9. doi:10.1074/jbc.M405195200

Lindblom, G., Johansson, L. B., & Arvidson, G. (1981). Effect of cholesterol in membranes. Pulsed nuclear magnetic resonance measurements of lipid lateral diffusion. *Biochemistry*, *20*(8), 2204–2207.

Liu, J., & Conboy, J. C. (2009). Phase Behavior of Planar Supported Lipid Membranes Composed of Cholesterol and 1,2-Distearoyl-sn-Glycerol-3-Phosphocholine Examined by Sum-Frequency Vibrational Spectroscopy. *Vibrational Spectroscopy*, *50*(1), 106–115. doi:10.1016/j.vibspec.2008.09.004

London, E. (2005). How principles of domain formation in model membranes may explain ambiguities concerning lipid raft formation in cells. *Biochimica et Biophysica Acta*, *1746*(3), 203–20. doi:10.1016/j.bbamcr.2005.09.002

Lopez-Garcia, F., Micol, V., Villalain, J., & Gomez-Fernandez, J. C. (1993). Infrared spectroscopic study of the interaction of diacylglycerol with phosphatidylserine in the presence of calcium. *Biochimica et Biophysica Acta - Lipids and Lipid Metabolism*, *1169*(3), 264–272.

Mabrey, S., & Sturtevant, J. M. (1976). Investigation of phase transitions of lipids and lipid mixtures by sensitivity differential scanning calorimetry. *Proceedings of the National Academy of Sciences of the United States of America*, *73*(11), 3862–3866.

Madden, T. D. (1997). *Membranes and Cell Signaling*. *Principles of Medical Biology* (Vol. 7, pp. 1–17). Elsevier. doi:10.1016/S1569-2582(97)80082-7

Mannock, D. A., Lee, M. Y. T., Lewis, R. N. A. H., & McElhaney, R. N. (2008). Comparative calorimetric and spectroscopic studies of the effects of cholesterol and epicholesterol on the thermotropic phase behaviour of dipalmitoylphosphatidylcholine bilayer membranes. *Biochimica et Biophysica Acta*, *1778*(10), 2191–202. doi:10.1016/j.bbamem.2008.05.004

Mantovani, A., Allavena, P., Sica, A., & Balkwill, F. (2008). Cancer-related inflammation. *Nature*, *454*(7203), 436–44. doi:10.1038/nature07205

Marcelli, A., Cricenti, A., Kwiatek, W. M., & Petibois, C. (2012). Biological applications of synchrotron radiation infrared spectromicroscopy. *Biotechnology Advances*, *30*(6), 1390–404. doi:10.1016/j.biotechadv.2012.02.012

Maxfield, F. R., & Tabas, I. (2005). Role of cholesterol and lipid organization in disease. *Nature*, *438*(7068), 612–621. doi:10.1038/nature04399

McElhaney, R. N. (1982). The use of differential scanning calorimetry and differential thermal analysis in studies of model and biological membranes. *Chemistry and Physics of Lipids*, *30*(2-3), 229–259. doi:10.1016/0009-3084(82)90053-6

McIntosh, T. J. (1978). The effect of cholesterol on the structure of phosphatidylcholine bilayers. *Biochimica et Biophysica Acta*, *513*(1), 43–58. Retrieved from http://www.ncbi.nlm.nih.gov/pubmed/718889

McMullen, T. P. W., Lewis, R. N. A. H., & McElhaney, R. N. (1993). Differential scanning calorimetric study of the effect of cholesterol on the thermotropic phase behavior of a homologous series of linear saturated phosphatidylcholines. *Biochemistry*, *32*(2), 516–522. doi:10.1021/bi00053a016

McMullen, T. P. W., & McElhaney, R. N. (1997). Differential scanning calorimetric studies of the interaction of cholesterol with distearoyl and dielaidoyl molecular species of phosphatidylcholine, phosphatidylethanolamine, and phosphatidylserine. *Biochemistry*, *36*(16), 4979–4986.

Melchior, D. L., & Steim, J. M. (1976). Thermotropic transitions in biomembranes. *Annual Review of Biophysics and Bioengineering*, *5*, 205–38. doi:10.1146/annurev.bb.05.060176.001225

Nakazawa, I., & Iwaizumi, M. (1989). A role of the cancer cell membrane fluidity in the cancer metastases: an ESR study. *The Tohoku Journal of Experimental Medicine*, *157*(3), 193. Retrieved from http://www.ncbi.nlm.nih.gov/pubmed/2543101

Penning, T. D., Talley, J. J., Bertenshaw, S. R., Carter, J. S., Collins, P. W., Docter, S., … Isakson, P. C. (1997). Synthesis and biological evaluation of the 1,5-diarylpyrazole class of cyclooxygenase-2 inhibitors: Identification of 4-[5-(4-methylphenyl)-3-(trifluoromethyl)-1H-pyrazol-1-yl]benzenesulfona mide (SC-58635, Celecoxib). *Journal of Medicinal Chemistry*, *40*, 1347–1365 ST – Synthesis and biological evaluatio.

Sade, A., Banerjee, S., & Severcan, F. (2010). Concentration-dependent differing actions of the nonsteroidal anti-inflammatory drug, celecoxib, in distearoyl phosphatidylcholine multilamellar vesicles. *Journal of Liposome Research*, *20*(2), 168–77. doi:10.3109/08982100903244492

Santangelo, R., Paderu, P., Delmas, G., Chen, Z.-W., Mannino, R., Zarif, L., & Perlin, D. S. (2000). Efficacy of Oral Cochleate-Amphotericin B in a Mouse Model of Systemic Candidiasis. *Antimicrobial Agents and Chemotherapy*, *44*(9), 2356–2360. doi:10.1128/AAC.44.9.2356-2360.2000

Severcan, F. (1997). Vitamin e decreases the order of the phospholipid model membranes in the gel phase: An FTIR study. *Bioscience Reports*, *17*(2), 231–235.

Severcan, F., & Cannistraro, S. (1988). Direct electron spin resonance evidence for alpha-tocopherol-induced phase separation in model membranes. *Chemistry and Physics of Lipids*, *47*(2), 129–133.

Severcan, F., Kazanci, N., & Zorlu, F. (2000). Tamoxifen increases membrane fluidity at high concentrations. *Bioscience Reports*, *20*(3), 177–184.

Severcan, F., Okan Durmus, H., Eker, F., Akinoglu, B. G., & Haris, P. I. (2000). Vitamin D(2) modulates melittin-membrane interactions. *Talanta*, *53*(1), 205–211.

Severcan, F., Sahin, I., & Kazanci, N. (2005). Melatonin strongly interacts with zwitterionic model membranes-evidence from Fourier transform infrared spectroscopy and differential scanning calorimetry. *Biochimica et Biophysica Acta - Biomembranes*, *1668*(2), 215–222. Retrieved from http://www.ncbi.nlm.nih.gov/pubmed/15737332

Shiff, S. J., & Rigas, B. (1999). The role of cyclooxygenase inhibition in the antineoplastic effects of nonsteroidal antiinflammatory drugs (NSAIDs). *The Journal of Experimental Medicine*, *190*(4), 445–50. Retrieved from http://www.pubmedcentral.nih.gov/articlerender.fcgi?artid=2195605&tool=pmcentrez&rendertype=abstract

Slater, J. L., & Huang, C. H. (1988). Interdigitated bilayer membranes. *Progress in Lipid Research*, *27*(4), 325–59. Retrieved from http://www.ncbi.nlm.nih.gov/pubmed/3076241

Smith, E. A., & Dea, P. K. (2013). Differential scanning calorimetry studies of phospholipid membranes: the interdigitated gel phase. In A. A. Elkordy (Ed.), *Applications of Calorimetry in a Wide Context – Differential Scanning Calorimetry, Isothermal Titration Calorimetry and Microcalorimetry* (pp. 407–444). doi:10.5772/2898

Smith, E. A., Smith, C., Tanksley, B., & Dea, P. K. (2014). Effects of cis- and trans-unsaturated lipids on an interdigitated membrane. *Biophysical Chemistry*, *190-191*, 1–7. doi:10.1016/j.bpc.2014.03.004

Sok, M., Sentjurc, M., & Schara, M. (2002). Cell membrane fluidity and prognosis of lung cancer. *The Annals of Thoracic Surgery*. Retrieved from http://ats.ctsnetjournals.org/cgi/content/abstract/73/5/1567\npapers://3e321f02-60bb-4759-8bba-12fdbb489c83/Paper/p7187

Somerharju, P., Virtanen, J. A., & Cheng, K. H. (1999). Lateral organisation of membrane lipids. *Biochimica et Biophysica Acta (BBA) - Molecular and Cell Biology of Lipids*, *1440*(1), 32–48. doi:10.1016/S1388-1981(99)00106-7

Srinivasan, C., & Burgess, D. J. (2009). Optimization and characterization of anionic lipoplexes for gene delivery. *Journal of Controlled Release : Official Journal of the Controlled Release Society*, *136*(1), 62–70. doi:10.1016/j.jconrel.2009.01.022

Stuart, B. H., & Ando, D. J. (1997). *Biological Applications of Infrared Spectroscopy*. Retrieved from http://books.google.com.tr/books/about/Biological_Applications_of_Infrared_Spec.html?id=EX-Sy7dvA_EC&pgis=1

Szoka, F., & Papahadjopoulos, D. (1980). Comparative properties and methods of preparation of lipid vesicles (liposomes). *Annual Review of Biophysics and Bioengineering*, *9*(1), 467–508. doi:10.1146/annurev.bb.09.060180.002343

Tamai, N., Uemura, M., Takeichi, T., Goto, M., Matsuki, H., & Kaneshina, S. (2008). A new interpretation of eutectic behavior for distearoylphosphatidylcholine-cholesterol binary bilayer membrane. *Biophysical Chemistry*, *135*(1-3), 95–101.

Thakral, N. K., Ray, A. R., Bar-Shalom, D., Eriksson, A. H., & Majumdar, D. K. (2011). The quest for targeted delivery in colon cancer: mucoadhesive valdecoxib microspheres. *International Journal of Nanomedicine*, *6*, 1057–68. doi:10.2147/IJN.S19561

Tomisato, W., Tanaka, K., Katsu, T., Kakuta, H., Sasaki, K., Tsutsumi, S., … Mizushima, T. (2004). Membrane permeabilization by non-steroidal anti-inflammatory drugs. In *Biochem Biophys Res Commun* (Vol. 323, pp. 1032–9 ST – Membrane permeabilization by non–ster). Graduate School of Medical and Pharmaceutical Sciences, Kumamoto University, Kumamoto 862-0973, Japan. doi:10.1016/j.bbrc.2004.08.205

Toyran, N., & Severcan, F. (2003). Competitive effect of vitamin D2 and Ca2+ on phospholipid model membranes: An FTIR study. *Chemistry and Physics of Lipids*, *123*(2), 165–176.

Van Ginkel, G., van Langen, H., & Levine, Y. K. (1989). The membrane fluidity concept revisited by polarized fluorescence spectroscopy on different model membranes containing unsaturated lipids and sterols. *Biochimie*, *71*(1), 23–32. doi:10.1016/0300-9084(89)90127-2

Vane, J. R. (1971). Inhibition of prostaglandin synthesis as a mechanism of action for aspirin-like drugs. *Nature: New Biology*, *231*(25), 232–5. Retrieved from http://www.ncbi.nlm.nih.gov/pubmed/5284360

Vane, J. R., Bakhle, Y. S., & Botting, R. M. (1998). Cyclooxygenases 1 and 2. *Annual Review of Pharmacology and Toxicology*, *38*, 97–120. doi:10.1146/annurev.pharmtox.38.1.97

Villalain, J., Aranda, F. J., & Gómez-Fernández, J. C. (1986). Calorimetric and infrared spectroscopic studies of the interaction of alpha-tocopherol and alpha-tocopheryl acetate with phospholipid vesicles. *European Journal of Biochemistry / FEBS*, *158*(1), 141–147. doi:10.1111/j.1432-1033.1986.tb09731.x

Vist, M. R., & Davis, J. H. (1990). Phase equilibria of cholesterol/dipalmitoylphosphatidylcholine mixtures: deuterium nuclear magnetic resonance and differential scanning calorimetry. *Biochemistry*, *29*(2), 451–464. doi:10.1021/bi00454a021

Voskuhl, J., & Ravoo, B. J. (2009). Molecular recognition of bilayer vesicles. *Chemical Society Reviews*, *38*(2), 495–505. doi:10.1039/b803782p

Walter, M. F., Jacob, R. F., Day, C. A., Dahlborg, R., Weng, Y., & Mason, R. P. (2004). Sulfone COX-2 inhibitors increase susceptibility of human LDL and plasma to oxidative modification: comparison to sulfonamide COX-2 inhibitors and NSAIDs. *Atherosclerosis*, *177*(2), 235–243. doi:10.1016/j.atherosclerosis.2004.10.001

Yeagle, P. L. (1985). Cholesterol and the cell membrane. *Biochimica et Biophysica Acta*, *822*(3-4), 267–87. Retrieved from http://www.ncbi.nlm.nih.gov/pubmed/3904832

Yeagle, P. L., Hutton, W. C., Huang, C. H., & Martin, R. B. (1975). Headgroup conformation and lipid--cholesterol association in phosphatidylcholine vesicles: a 31P(1H) nuclear Overhauser effect study. *Proceedings of the National Academy of Sciences of the United States of America*, *72*(9), 3477–81. Retrieved from http://www.pubmedcentral.nih.gov/articlerender.fcgi?artid=433017&tool=pmcentrez&rendertype=abstract

Zhang, J., Ding, E. L., & Song, Y. (2006). Adverse effects of cyclooxygenase 2 inhibitors on renal and arrhythmia events: meta-analysis of randomized trials. *JAMA : The Journal of the American Medical Association*, *296*(13), 1619–1632. doi:10.1097/01.sa.0000296335.58935.52

Zhao, L., Feng, S. S., Kocherginsky, N., & Kostetski, I. (2007). DSC and EPR investigations on effects of cholesterol component on molecular interactions between paclitaxel and phospholipid within lipid bilayer membrane. *International Journal of Pharmaceutics*, *338*(1-2), 258–266.

APPENDIX A

CALIBRATION CURVES

The calibration curves of RFX dissolved in methanol measured at 282 nm and VLX dissolved in ethanol measured at 203 nm are shown in Figures 46 and 47 respectively. Statistically reliable equations were obtained and were used to determine drug concentration in the MLVs using Beer-Lambert's law. The R^2 values and the calibration equations are shown in the Figures as well.

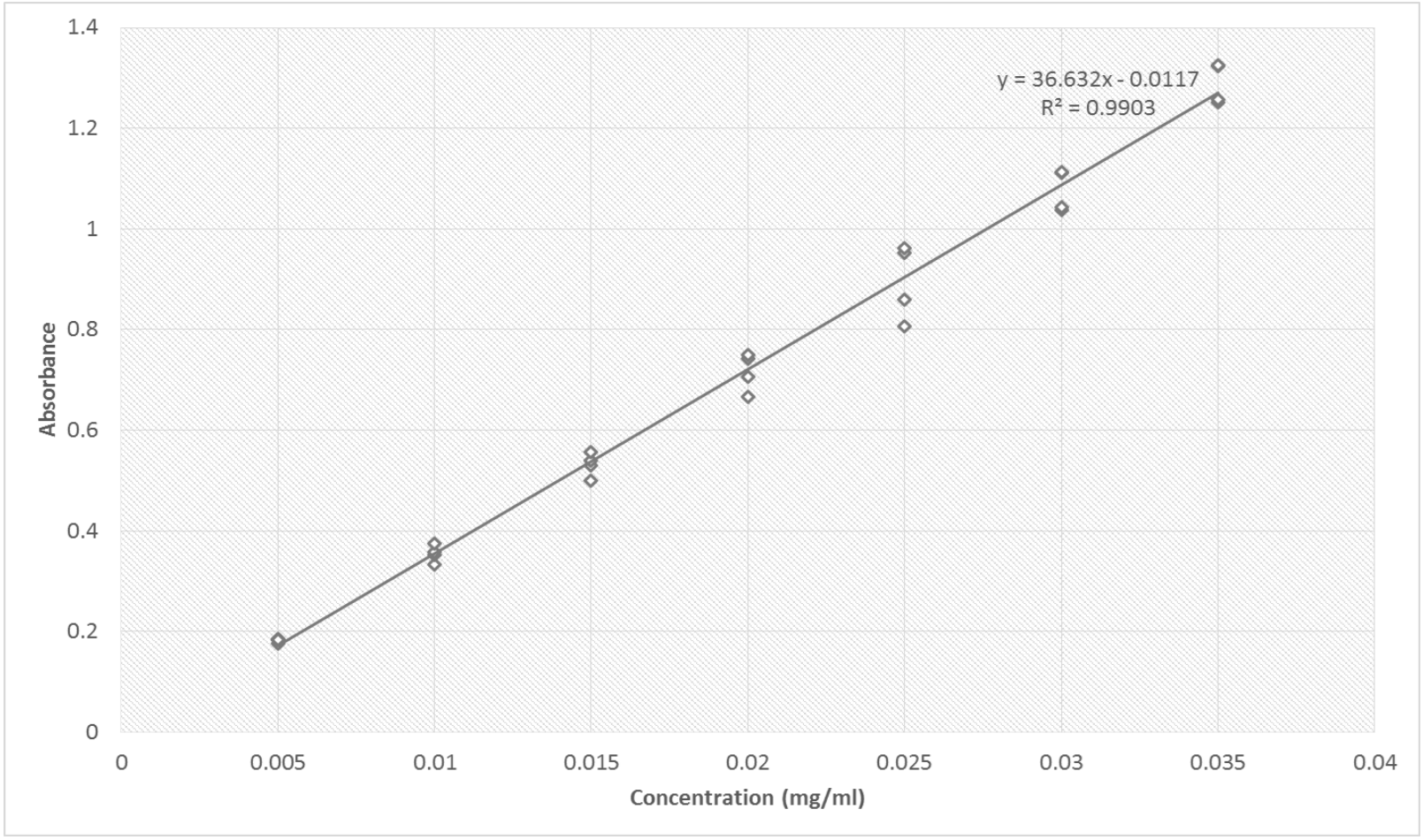

Figure 46. Absorbance calibration curve of RFX dissolved in methanol and measured at 282 nm.

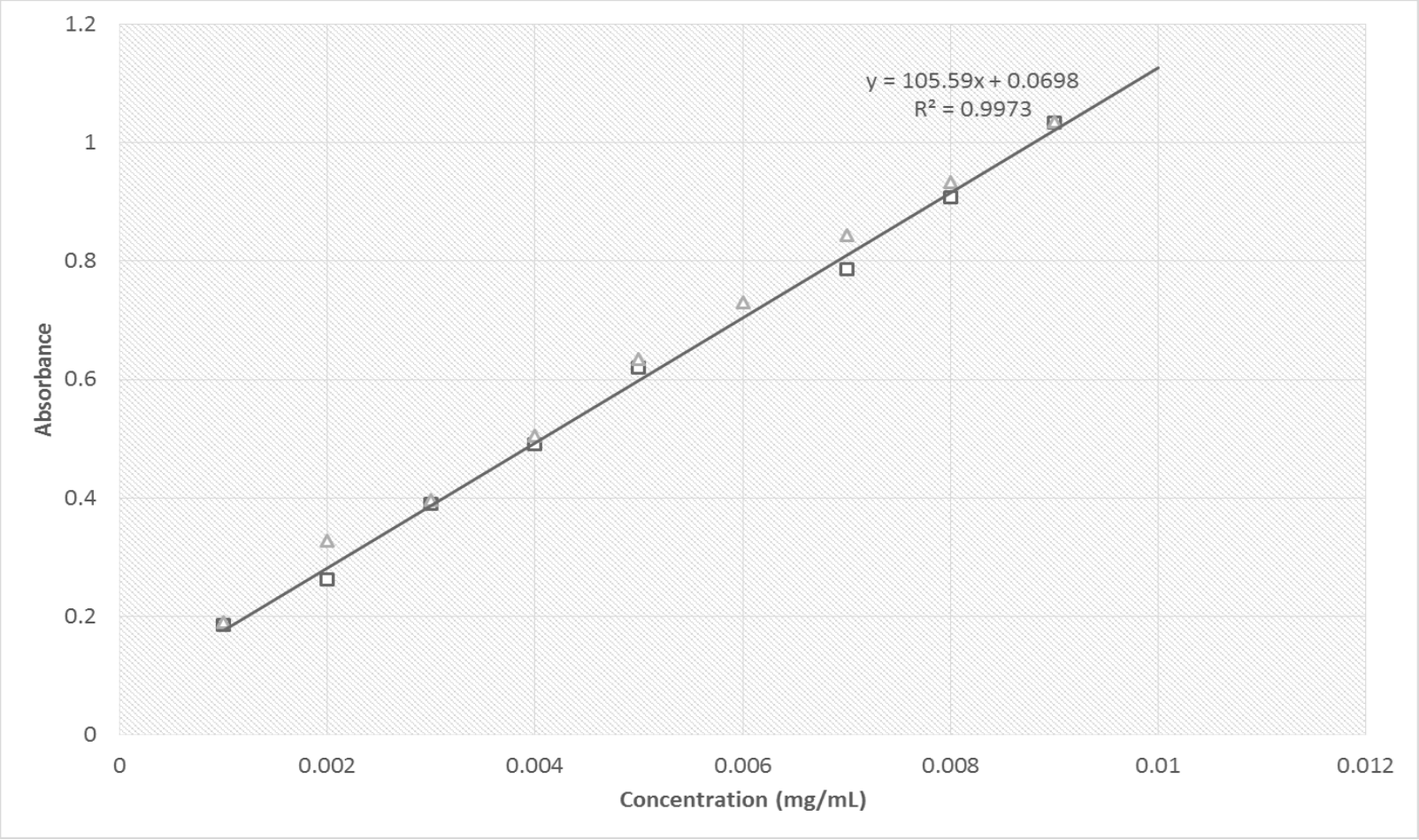

Figure 47. Absorbance calibration curve of VLX dissolved in ethanol and measured at 203 nm.